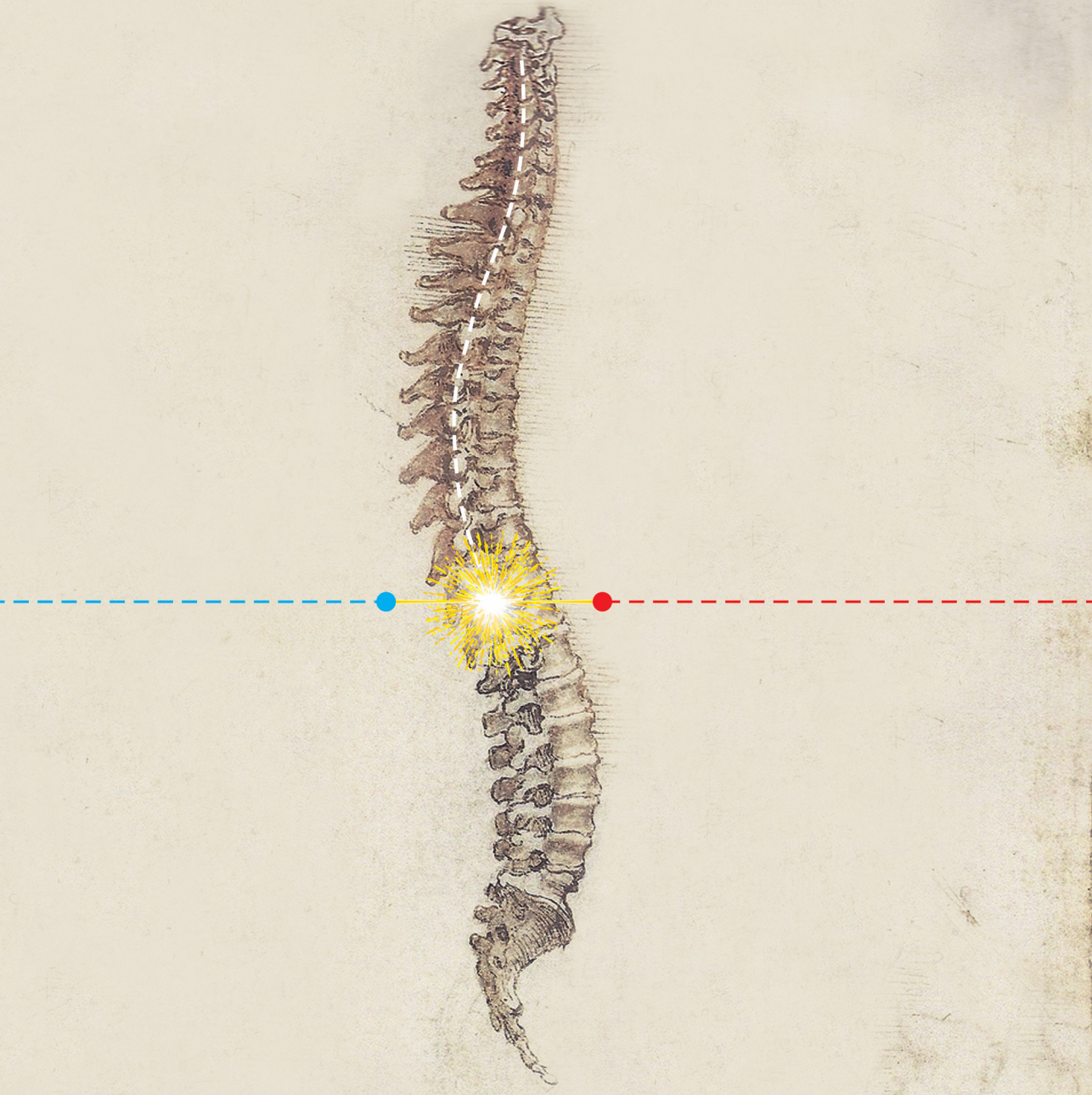

Trans-Spinal Direct Current Stimulation for the Modulation of the Lumbar Spinal Motor Networks

Alexander Kuck

Trans-Spinal Direct Current Stimulation for the Modulation of the Lumbar Spinal Motor Networks

Alexander Kuck

Graduation Committee:

Chairman:	Prof. dr. G.P.M.R. Dewulf	University of Twente
Promotors:	Prof. dr. ir. D.F. Stegeman	Vrije Universiteit Amsterdam
	Prof. dr. ir. H. van der Kooij	University of Twente
		TU Delft
Co-Promotor:	Dr. E.H.F. van Asseldonk	University of Twente
Members:	Prof. dr.ir. P.H. Veltink	University of Twente
	Prof. dr.ir. M.J.A.M. van Putten	University of Twente
	Prof. dr. T.W.J. Janssen	Vrije Universiteit Amsterdam
	Prof. dr. rer. nat. C. Wolters	University of Münster
	Dr. T.F. Oostendorp	Radboud University Medical Center

Trans-Spinal Direct Current Stimulation for the Modulation of the Lumbar Spinal Motor Networks

Alexander Kuck

Dissertation, University of Twente, Enschede, The Netherlands

ISBN:
978-90-365-4474-0

DOI:
10.3990/1.9789036544740

Cover Design:
A. Kuck, based on artwork by Leonardo da Vinci

Printed by:
Gildeprint Drukkerijen
Javastraat 123
7512 ZE Enschede

TRANS-SPINAL DIRECT CURRENT STIMULATION FOR THE MODULATION OF THE LUMBAR SPINAL MOTOR NETWORKS

Dissertation

to obtain
the degree of doctor at the University of Twente,
on the authority of the rector magnificus
Prof. dr. T.T.M. Palstra
on account of the decision of the graduation committee,
to be publicly defended
on Wednesday the 24th of January 2018 at 14:45

by

Alexander Kuck
Born on December 23rd, 1985
in Kirchheim unter Teck, Germany

This dissertation has been approved by:

Supervisors:	Prof. dr. ir. D.F. Stegeman	Vrije Universiteit Amsterdam
	Prof. dr. ir. H. van der Kooij	University of Twente TU Delft
Co-supervisor:	Dr. E.H.F. van Asseldonk	University of Twente

ISBN: 978-90-365-4474-0

The work in this dissertation was supported by ZonMw (Grand Nr. 10-10400-98-008) as part of the NeuroControl - Assessment and Stimulation (NeurAS) consortium.

This work has also benefited from the collaboration and financial support of the following companies and organizations. Their support is thankfully acknowledged.

Table of Contents

Summary

Trans-spinal Direct Current Stimulation (tsDCS) is a noninvasive neuromodulatory tool for the modulation of the spinal neurocircuitry. Initial studies have shown that tsDCS is able to induce a significant and lasting change in spinal-reflex- and corticospinal information processing. It is therefore hypothesized that tsDCS may be a useful tool in the rehabilitation of spinal cord dysfunctions or injuries. However, to efficiently utilize tsDCS as a tool in neurorehabilitation, more knowledge is necessary about its mechanisms of action, as well as how tsDCS needs to be applied to ensure the desired outcome. This dissertation therefore focuses on the use of tsDCS for the modulation of the lumbar spinal motor circuitry, aiming at a possible application in spinal cord injury rehabilitation. This is investigated using theoretical as well as experimental techniques.

To increase the theoretical understanding of tsDCS, chapter 2 focusses on simulating the electric field (EF) generated during tsDCS and its interaction with the targeted neural structures. This includes visualization and analysis of the generated EF as well as the identification of neural structures, likely to be most targeted by the intervention. Furthermore, a comparison with existing human tsDCS studies as well as the possible effects of electrode misplacement during application are discussed. Methodologically, the EF is calculated via the Finite Element Method and subsequently combined with a multicompartmental model of an alpha-motoneuron and its main incoming axon connections. The resulting neural membrane polarization is used to identify the primary neural target of tsDCS. Additional analyses investigated the expected acute network responses via an existing lumbar spinal network model, which are then compared to in-vivo measurements from literature. The primary results, give an insight into the distribution and strength of the generated EF in the spinal cord for several electrode configurations. Furthermore, axon terminals were identified as the primary cellular target of tsDCS. The simulated acute network effects were in opposite direction when related to the electrophysiological long-term changes observed in human tsDCS studies.

After having established a theoretical basis of some of the underlying mechanisms of action, the following two chapters deal with experimentally assessing the effects of tsDCS for different protocol variations. The main motivation of these studies, was the optimization of tsDCS for a more targeted use in a clinical setting.

Chapter 3 deals with experimentally assessing the effects of tsDCS applied with different EF directions, as well as the repeatability of results previously obtained by others. The central question hereby was to assess whether the tsDCS outcome is dependent on EF direction. This question was addressed in a randomized, double-blind placebo controlled study, whereby 10 healthy subjects received lumbar spinal tsDCS in three different electrode configurations, plus a placebo stimulation. The H-reflex recruitment curve was utilized as a probe for the induced neural changes. The primary outcome confirms, that the effects of tsDCS are dependent on EF direction. Furthermore, results previously reported by others could not be replicated. This highlights current challenges, with regards to repeatability, in the field of neuromodulation research.

Chapter 4 compares the effects of tsDCS during active movement and rest, to investigate during which of the two conditions the application of tsDCS leads to larger modulatory effects. The underlying hypothesis is, that the modulatory effect of tsDCS can be significantly increased when paired with ongoing neural activity. As in the previous study, this question was investigated in a randomized, double-blind placebo controlled study, which included 10 healthy subjects. In four different experiments, subjects received real- or placebo tsDCS during either lying and walking. The resulting neural changes were measured using the H-reflex. The results confirm, that the outcome of tsDCS is dependent on neural activity during stimulation. Thereby, tsDCS in combination with walking had a significantly larger modulatory effect compared to placebo stimulation during walking. No modulatory effect was detected for tsDCS during rest.

Lastly, chapter 5 investigates important safety aspects, when tsDCS is applied in the presence of metallic spinal implants. The presence of metallic implants in the body is still a safety concern, in connection with electrical stimulation procedures. Since spinal implants are expected to be present in at least part of the targeted population with spinal cord injury, it is necessary to explore the safety and application specific consequences of tsDCS with the presence of a spinal metallic implant. This was investigated by simulating the tsDCS induced electric field and current density in the presence of a metallic spinal implant. Calculations were performed via Finite Element Analysis. The results show that implant presence was able to substantially affect peak current density, compared to the no-implant condition. Nonetheless, the highest calculated current density levels were a factor six lower than the most conservative estimate of what is thought to lead to tissue damaging effects. Additionally, implant presence did not considerably affect the average electric field inside the spinal cord. The findings do therefore not indicate potentially unsafe current density levels, or significant alterations to stimulation intensity inside the spinal cord, caused by a spinal implant during tsDCS.

Samenvatting

Trans-spinal Direct Current Stimulation (tsDCS) is een niet-invasieve methode om het gedrag van spinale neurale circuits te moduleren. Eerdere studies hebben aangetoond dat tsDSC een significante en langdurige verandering in ruggenmergreflexen en corticospinale informatieverwerking teweeg kan brengen. Daarom zou tsDCS een gunstig effect kunnen hebben op de revalidatie van mensen met een dwarslaesie. Echter om tsDCS efficiënt te gebruiken als hulpmiddel bij neurorevalidatie, is meer kennis nodig over de werkingsmechanismen van tsDCS, en over de manier waarop tsDCS moet worden toegepast om de gewenste uitkomst te verkrijgen. Dit proefschrift richt zich daarom op het gebruik van tsDCS voor de modulatie van het lumbale spinale motorcircuit, met focus op een mogelijke toepassing bij revalidatie na letsel aan het ruggenmerg. Dit wordt onderzocht met behulp van simulaties en experimenten.

Voor een beter theoretisch begrip van tsDCS wordt in hoofdstuk 2 het elektrisch veld (EV) tijdens tsDCS, en de interactie van dit veld met de neurale structuren, gesimuleerd. Dit geeft een visualisatie en analyse van het gegenereerde EV, en worden de neurale structuren geïdentificeerd die het meest beinvloed worden door de interventie. Bovendien wordt een vergelijking met bestaande tsDCS-onderzoeken op mensen gemaakt, en worden de mogelijke effecten van elektrode-misplaatsing tijdens de toepassing besproken. Het EV wordt berekend via de eindige-elementenmethode en vervolgens gecombineerd met een mult-icompartimentaal model van een alfa-motoneuron en diens belangrijkste inkomende axonverbindingen. De resulterende neurale membraanpolarisatie wordt gebruikt om het primaire neurale doelwit van tsDCS te identificeren. Aanvullende simulaties tonen de verwachte acute respons van het neurale netwerk via een bestaand lumbale spinale netwerkmodel, die vervolgens worden vergeleken met de in vivo bevindingen uit de literatuur. De primaire resultaten geven inzicht in de verdeling en sterkte van het opgewekte EV in het ruggenmerg voor verschillende elektrodeconfiguraties. Bovendien werden axonterminals geïdentificeerd als het primaire cellulaire doelwit van tsDCS. Vergeleken met langetermijnveranderingen door tsDCS op mensen, zijn de gesimuleerde acute netwerkeffecten in tegenovergestelde richting.

Na een theoretische basis te hebben gelegd voor enkele van de onderliggende werkingsmechanismen, de volgende twee hoofdstukken op het experimenteel bepalen van de effecten van tsDCS voor verschillende protocolvariaties. De belangrijkste motivatie van deze studies was de optimalisatie van tsDCS voor een meer gericht gebruik in een klinische omgeving.

Hoofdstuk 3 gaat over het experimenteel bepalen van de effecten van tsDCS toegepast met verschillende richtingen van het EV, evenals het testen van de herhaalbaarheid van eerder verkregen resultaten door anderen. Het doel was om te beoordelen of het tsDCS-resultaat afhankelijk is van de richting van het EV. Dit werd onderzocht in een gerandomiseerde, dubbelblinde, placebo-gecontroleerde studie, waarbij 10 gezonde proefpersonen tsDCS van de lumbale wervelkolom kregen in drie verschillende elektrodeconfiguraties, plus een placebostimulatie. De H-reflex rekruteringscurve werd gebruikt als een maat voor de geïnduceerde neurale veranderingen. De primaire uitkomst bevestigt dat de effecten van tsDCS afhankelijk zijn van de richting van het EV. Bovendien konden resultaten die eerder door anderen

werden gerapporteerd niet worden gerepliceerd. Dit benadrukt de huidige uitdagingen op het gebied van neuromodulatie-onderzoek met betrekking tot herhaalbaarheid.

Hoofdstuk 4 vergelijkt de effecten van tsDCS tijdens actieve beweging en rust, om te onderzoeken tijdens welke van de twee condities de toepassing van tsDCS leidt tot grotere modulerende effecten. De onderliggende hypothese is dat het modulerende effect van tsDCS aanzienlijk kan worden verhoogd wanneer het gepaard gaat met aanhoudende neurale activiteit. Net als in de vorige studie, werd dit onderzocht in een gerandomiseerde, dubbelblinde, placebo-gecontroleerde studie met 10 gezonde personen. In vier verschillende experimenten ontvingen proefpersonen tsDCS of een placebo-stimulatie tijdens zowel rust (liggen) als lopen. De resulterende neurale veranderingen werden gemeten met behulp van de H-reflex. De resultaten bevestigen dat de uitkomst van tsDCS afhankelijk is van neurale activiteit tijdens stimulatie. Daarbij had tsDCS in combinatie met lopen een significant groter modulerend effect, vergeleken met placebo-stimulatie tijdens het lopen. Er werd geen modulerend effect gedetecteerd van tsDCS tijdens rust.

Ten slotte gaat hoofdstuk 5 over belangrijke veiligheidsaspecten wanneer tsDCS wordt toegepast in aanwezigheid van metalen implantaten die de wervelkolom stabiliseren. De aanwezigheid van metalen implantaten in het lichaam vormen nog steeds een veiligheidsrisico bij elektrische stimulatie. Omdat verwacht wordt dat ruggengraatimplantaten aanwezig zijn in een aanzienlijk deel van mensen met een dwarslaesie, moeten de veiligheids- en toepassingsspecifieke gevolgen van tsDCS met de aanwezigheid van een spinaal metalen implantaat worden onderzocht. Het door tsDCS geïnduceerde EV en de elektrische stroomdichtheid werden gesimuleerd in de aanwezigheid van een metalen ruggengraatimplantaat. Berekeningen werden uitgevoerd via de eindige-elementenmethode. De resultaten tonen aan dat de aanwezigheid van een implantaat in staat is om de piekstroomdichtheid aanzienlijk te beïnvloeden, vergeleken met de toestand zonder implantaat. Niettemin was de hoogst berekende stroomdichtheid een factor zes lager dan de meest conservatieve schatting van de stroomdichtheid die wordt verondersteld te leiden tot weefselbeschadiging. Bovendien had de implantaataanwezigheid geen substantiële invloed op het gemiddelde EV in het ruggenmerg. De bevindingen wijzen daarom niet op potentieel onveilige stroomdichtheidsniveaus of significante veranderingen in de stimulatie-intensiteit in het ruggenmerg tijdens tsDCS wanneer een implantaat het ruggenmerg stabiliseert.

Chapter I – Introduction

Trans-spinal Direct Current Stimulation (tsDCS) belongs to the group of electro-neuromodulatory techniques, which aim to influence nervous system function via the application of electrical stimulation. Due to the multidisciplinary nature of electrotherapeutic interventions, the analysis and development of electrotherapeutic techniques is complex. It therefore requires the understanding of a wide range of disciplines within the medical and engineering domains. To make the reader familiar with the multifaceted subject of direct current (DC) stimulation intervention design, the following section contains a brief introduction to the most relevant topics.

After a short overview of tsDCS and its context within the neurostimulation field in section 1.1, the reader will be introduced to the basic anatomy of the spinal cord on a macroscopic scale (sect. 1.2), as well as the concept of electrostimulation for the rehabilitation of spinal cord injury (sect. 1.3). Section 1.4 will subsequently give an overview of the neuroanatomy and neural working mechanisms on a microscopic level, with a focus on the neural interaction with electrostimulation.

For understanding and designing electrotherapeutic interventions, experimental and theoretical techniques can be utilized. To measure the effects of an electrical stimulation experimentally, neurological tests can give an insight on the resulting changes in the nervous system. Section 1.5 will therefore introduce the most relevant concepts and clinical tools to evaluate changes in the corticospinal and spinal pathways. Thereafter, theoretical and computational techniques for the analysis of neuro-electrical stimulation will be covered in section 1.6. These techniques comprise the computational modeling of the generated electric field and the associated effects on neural structures.

1.1 General Introduction

Trans-spinal direct current stimulation, is a non-invasive electrostimulation technique, which aims to modulate the neural circuits in the spinal cord. During tsDCS, the spinal cord is stimulated with a direct current, generating an electric field, with the final goal of inducing a lasting functional change in the targeted neural pathways. A well-designed use of tsDCS may therefore be able to facilitate the regeneration of neural connections and thus benefit in the rehabilitation of injuries or dysfunctions to the spinal cord.

TsDCS belongs to the group of non-invasive electrical neuromodulation procedures, which can be applied throughout the central nervous system (CNS) such as the cortex, the cerebellum or the spinal cord. Noninvasive electrical neuromodulation is applied to the human body via electrodes placed on the skin, which are connected to an electrical stimulator (fig. 1A). The body thus becomes part of an electrical circuit. During electrical stimulation, an electric field is generated in the body, driven by the potential difference between the attached electrodes (fig. 1B). The electric field subsequently influences the functioning of neurons and other neural elements in the CNS. Since neurons are connected, forming a functional neural circuit, the electric field may have the potential to change the underlying neural function as a whole.

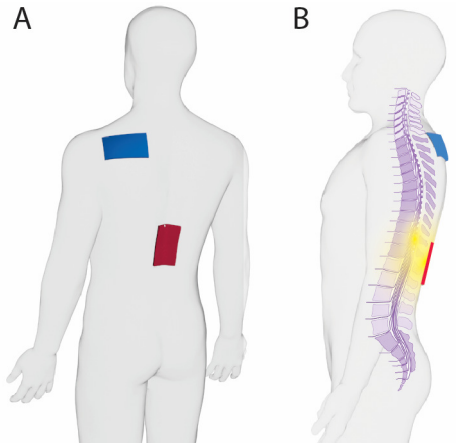

Figure 1: A) A typical electrode placement configuration, used in tsDCS studies. (red: anode, blue: cathode) B) The generated electric field penetrates the body, where it is meant to influence the neural signaling in the spinal cord.

By altering stimulation parameters, such as electrode position, stimulation intensity and stimulus waveform, as well as ongoing neural activity, it is possible to influence the intervention outcome. For example, controlling the shape and orientation of the generated electric field has an effect on how neural structures are affected. This is based on the fact, that the stimulation effect depends on neural morphology and its orientation with respect to the electric field. Furthermore, by scaling stimulation intensity, the resulting effect magnitude can be regulated. At higher stimulation intensities, it is possible to evoke direct neural activation in the form of action potentials (APs), building blocks of the neural communication. Lower intensities merely influence neural function without leading to APs directly.

When applying tsDCS, electrodes are positioned to target the spinal cord via the generated electric field and a constant, current controlled waveform is used to stimulate the spinal cord for a period of typically 10-20 minutes. The applied current generates a weak electric field, which does, as indicated above, not directly evoke neural activity, but interacts with and modulates the targeted neural structures. In addition to tsDCS, there are several other representatives of non-invasive nervous brain stimulation, such as the more commonly known transcranial Direct Current Stimulation (tDCS), transcranial Alternating Current Stimulation (tACS) or transcutaneous Spinal Cord Stimulation (tSCS). In terms of effects on a network level, all of the mentioned stimulation protocols have been utilized to influence specific parts of CNS circuitry, including the facilitation of learning or the modulation of connections among brain regions. Specifically for tsDCS, studies have shown significant modulatory effects on lumbar spinal reflexes as well as for corticospinal afferent and efferent pathways [1–7].

1.2 Anatomy of the Spinal Cord

As part of the CNS, the spinal cord is a direct extension of the brainstem and descends through the spinal canal (fig. 2A), enclosed and protected by the bony structures of the vertebral column, as well as three protective membranes and the corticospinal fluid (fig. 2B). The vertebrae of the surrounding spine are formally separated into the cervical, thoracic and lumbar sections, whereby individual vertebrae within each section are numbered in descending order (e.g. T3, meaning:

third thoracic vertebra). The spinal cord tissue consists of white and grey matter, with the grey matter located in the center, surrounded by the white matter. The grey matter mostly consists of neuronal cell bodies, whereas the white matter is made of nerve fiber bundles carrying information to and from other CNS regions (fig. 2C).

Central functions of the spinal cord encompass the exchange of information with peripheral body parts, such as movement commands and somatosensory information, as well as controlling internal organ functions. It further receives and conveys information from or to the higher order control centers of the brain. The information exchange within the CNS is achieved via longitudinally ascending or descending bundled axons, called spinal tracts. Furthermore, connection with the periphery is accomplished via axons that enter and exit though large nerve bundles, called the dorsal and ventral roots. Whereas the dorsal root transmits sensory information, motor information is sent to the muscles via the ventral roots.

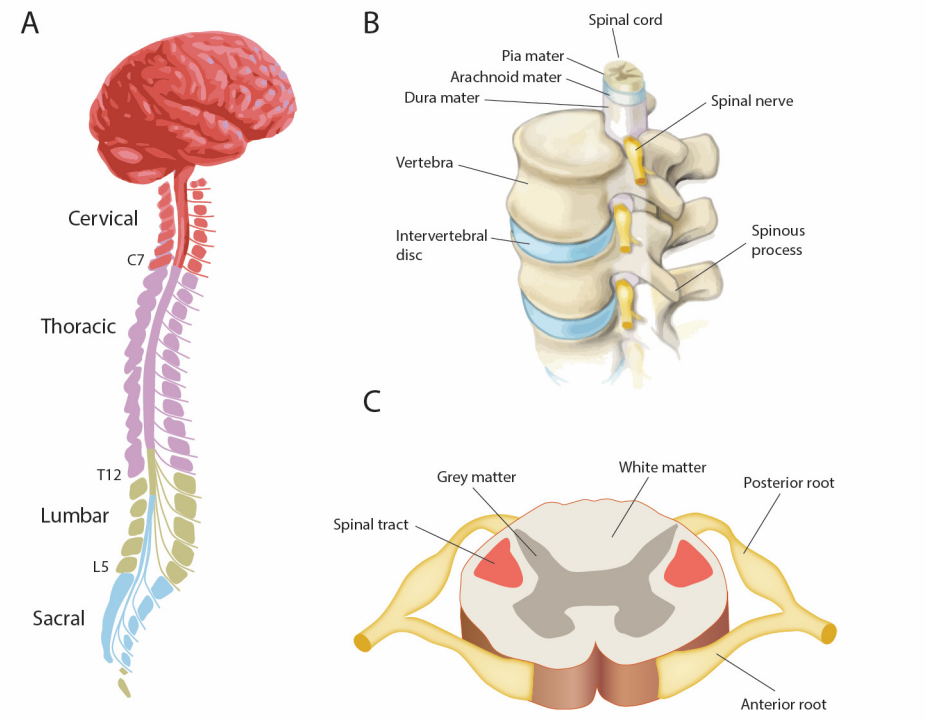

Figure 2: Overview of spinal anatomy. A) The spinal cord is an extension of the brainstem and is sub-divided into cervical, thoracic, lumbar and sacral regions. B) It is enclosed by the spinal column, as well as three protective skin layers. C) The neuroanatomy of the spinal cord consists of the grey and white matter, which harbor spinal neurons and axons respectively. Signal exchange with the periphery is relayed by thick axon bundles called the spinal roots. Hereby, the posterior and anterior sensory roots, convey afferent (incoming) and efferent (outgoing) signals respectively.

Sub-figures adapted from Alexander & Turner Inc. (Santa Rosa Beach, USA) (A) and http://www.edoctoronline.com (B)

The lumbar spinal cord contains circuits for locomotion generation and control of the lower limbs [8]. Lumbar spinal circuitry has a versatile architecture which allows the execution of dexterous, voluntary movements, the feedback of state information as well as the autonomous generation and correction of locomotion patterns. A central part of these functions is executed by alpha motoneurons and interneurons. Alpha motoneurons receive motor-signals from higher brain centers and convey them to the leg-muscles, which respond in the form of muscle contractions. Each muscle has a dedicated motoneuron pool, in which each single motoneuron serves many muscle fibers (a motor unit). A muscle typically consists of tens to several hundreds of motor units. Alpha motoneurons also receive sensory feedback from muscles at the spinal level, which includes information about muscle stretch and force, used for corrective behavior of posture or movement. Interneurons are present in the circuit, when more complex signal operations are necessary, such as signal inversion or integration. When applied to the lumbar spinal cord, the central goal of tsDCS is to modulate the behavior of the lumbar spinal circuitry, which will subsequently be visible in changes to the resulting motor output or signal transmission.

1.3 Spinal Stimulation for the Rehabilitation of Spinal Cord Injury

Spinal cord injury (SCI) is typically defined as a damage to the neural structures of the spinal cord. SCI can have various causes, such as a traumatic injury, cancer or spinal cord vascular disease [9,10]. The resulting symptoms vary based on the type of injury, but may include the dysfunctions or loss of motor control as well as the control over bladder, bowel and sexual function [11].

Recovery after spinal injury is often met with challenges and patients do not- or only partly regain the lost neural function [9,11]. For this reason, increasing scientific effort is made in finding techniques that may help to improve the quality of life after acute initial care and rehabilitation. To find a possible treatment for SCI, current research primarily focusses on pharmacological, biotechnological and electrophysiological approaches [12]. Whereas pharmacology and biotechnology research aim to induce tissue recovery via genetic modification, stem cells or other biomedical techniques, the goal of electromodulatory methods is to guide neural plasticity to functionally reconnect existing neurons and support the sprouting of novel axonal connections. Previous research has successfully demonstrated, that spinal electrostimulation may be particularly useful in the rehabilitation of SCI. The utilized protocols hereby consisted of either transcutaneous [13,14] or epidural [15–18] supra- or sub-threshold pulsed electrical stimulation protocols, combined with intensive manual therapy. In animal studies, a pharmacological cocktail of neuro-facilitatory drugs was administered in addition to training and stimulation [17]. Due to these observations, the question arises whether the sub-threshold tsDCS could lead to similar results. The hypotheses for using sub-threshold over supra-threshold methods are a resulting decrease in patient comfort, possibly higher control over protocol outcomes and the non-invasive nature of the technique.

1.4 Neural Basis of Direct Current Stimulation

A principal way of signal processing in the brain is the inter-neural-exchange of electrical neural signals, in the form of APs (fig. 3A). In a neuron, this electrical signal is generated due to a potential difference between intracellular and extracellular space, which are separated by a cellular

membrane (fig. 3B). The transmembrane voltage is caused by ionic electrochemical gradients across the semi-permeable neural membrane. During rest, this potential difference is approximately -70mV and is referred to as the "resting membrane potential" (fig. 3C).

The cellular membrane is equipped with ion channels that allow the influx or outflow of ions. While some ion channels are open permanently, others open and close in response to, for example, changes in trans-membrane potential or the presence of specific chemical messengers (ligands). When ion channels open, specific ions flow in or out of the cell which changes (polarizes) the membrane potential in positive (depolarizing) or negative (hyperpolarizing) direction. Polarization thus refers to an in- or decrease in membrane potential compared to its resting state. In most neurons, the depolarization above a certain threshold leads to the opening of several voltage gated ion channels, which results in the generation of an action potential.

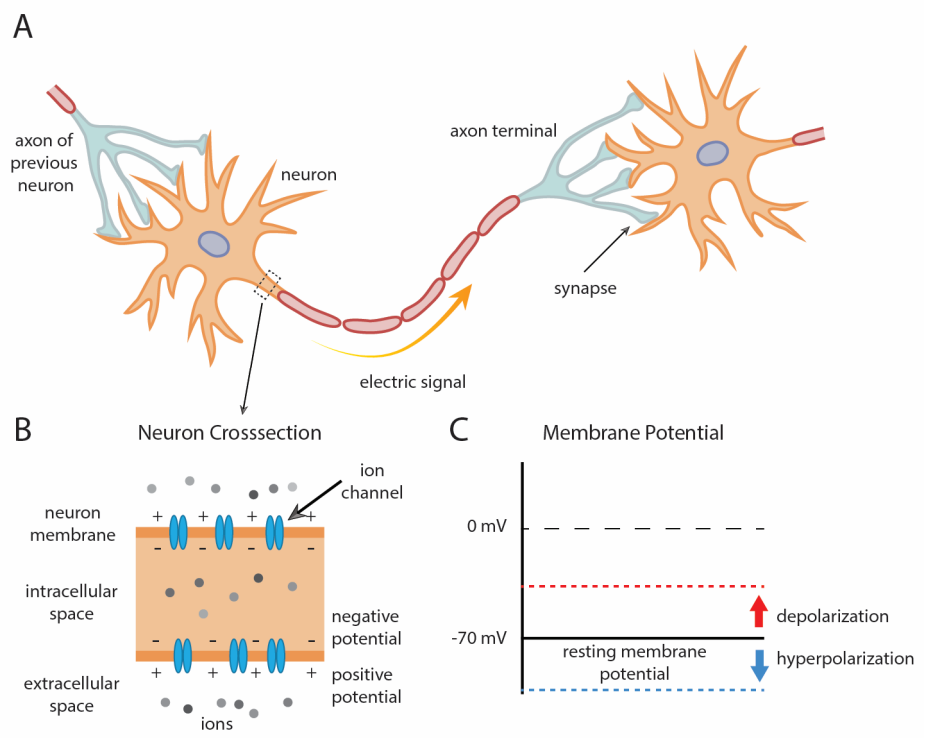

Figure 3: A) Neurons exchange information via electrical signals, which are often transmitted to other neurons by means of axons. Before interfacing with other neurons via synapses, axons branch out multiple times, which is refered to as the axon terminal. B) The voltage difference between the inside and the outside of the neuron is generated by ionic electrochemical gradients. C) Neural signals are computed and generated by changes in transmembrane voltage, by adjusting the ionic transmemrane electrochemical gradients. At rest, the voltage gradient is approximately -70 millivolts, referred to as the “resting membrane potential”. Changes in transmembrane potential in either direction are called polarization (depolarization = less negative inside, hyperpolarization = more negative inside).

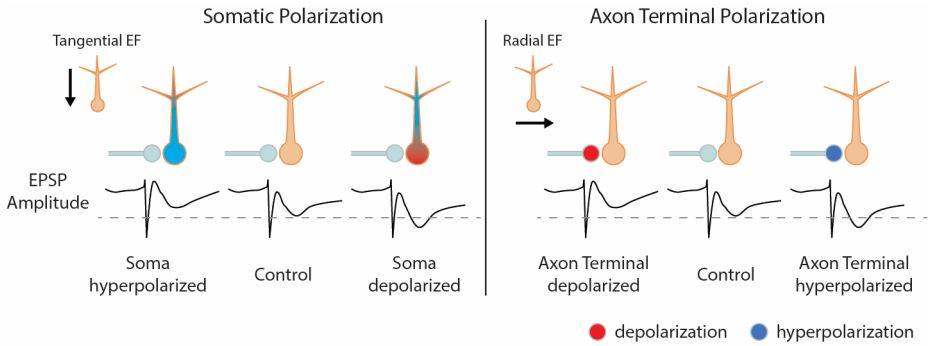

Figure 4: Effects of somatic and axon terminal polarization on the excitatory postsynaptic – potential (EPSP), which is the signal measured on the neuron side, due to an arriving action potential on the corresponding synapse. Both, somatic and axon terminal polarization are able to substantially modify the signal strength of the neural response to synaptic input.

Data reproduced from [21].

When a neuron is exposed to an external electric field, this can also lead to polarization. Polarization in the neuron varies locally depending on neural morphology, the biophysical parameters of the neuron, orientation with respect to electric field and electric field strength. Subsequently the acute functioning of the neuron can be affected depending on the polarization profile and the present membrane functionality. For example, experiments in vivo have shown that the polarization of incoming axon terminals leads to direct changes in the amplitude of the transmitted signal on the side of the neuron (excitatory postsynaptic potential or EPSP), proportional to the polarization [19] (fig. 4). Similar effects have been described for somatic polarization [19], whereby it has to be pointed out that in a realistic situation these scenarios are certainly nonexclusive.

After a finite amount of time, in the order of several minutes, these acute effects can lead to alterations in the function of the neuron or neural circuit, which can be measured long after the offset of the stimulation. This implies, that the stimulation resulted in neuroanatomical changes in the structure of the neuron, known as long term plasticity. The exact mechanism at which this occurs is not fully understood. However, research has shown that these changes are highly dependent on factors such as ongoing neural activity during stimulation, the local neuromechanics or genetic predisposition [20].

1.5 Physiological Assessment of Corticospinal Functionality

To investigate the neural effects generated by tsDCS, electrophysiological tests can be performed which give information about neural connection strength, reliability and speed of the pathway of interest. These tests typically involve inducing a form of stimulation at the beginning, and measuring the electrophysiological response at the end of the targeted pathway. Elapsed time and response characteristics, allow conclusions about the underlying pathologies or mechanisms of action. While many such techniques exist, the following sections will introduce two common clinical assessments of corticospinal and spinal pathway connectivity: Motor evoked potentials (MEPs) and the Hoffman (H)- reflex.

1.5.1 Motor Evoked Potentials

A motor evoked potential (MEP) is an electrophysiological signal, artificially induced in the motocortex and measured in a muscle. Most often the cortex is stimulated by a short and strong magnetic impulse. In a typical example, the pulse is applied to the neurons of the primary motocortex. The rapid change in magnetic field generates an electric field which subsequently activates neurons in close proximity (fig. 5A[1]). The generated signal travels through the corticospinal tract and activates a certain number of spinal motoneurons, which further convey the signal to the alpha motoneurons of an associated muscle (fig. 5A[2,3+4]). The resulting muscle activation (fig. 5A[5]) can then be detected as an electric potential, measured over the muscle (electromyogram or EMG) (fig. 5B). Since the generated corticospinal signal is conveyed to the muscle via spinal motoneurons, measuring MEPs leads to information about motoneuron function in response to a corticospinal input. For example, a change in MEP area or amplitude after tsDCS may be related to an altered signal strength leading to changes in muscle activation. In case of an increase, this may originate from the recruitment of more spinal motoneurons and/or an increase in motoneuron activation frequency.

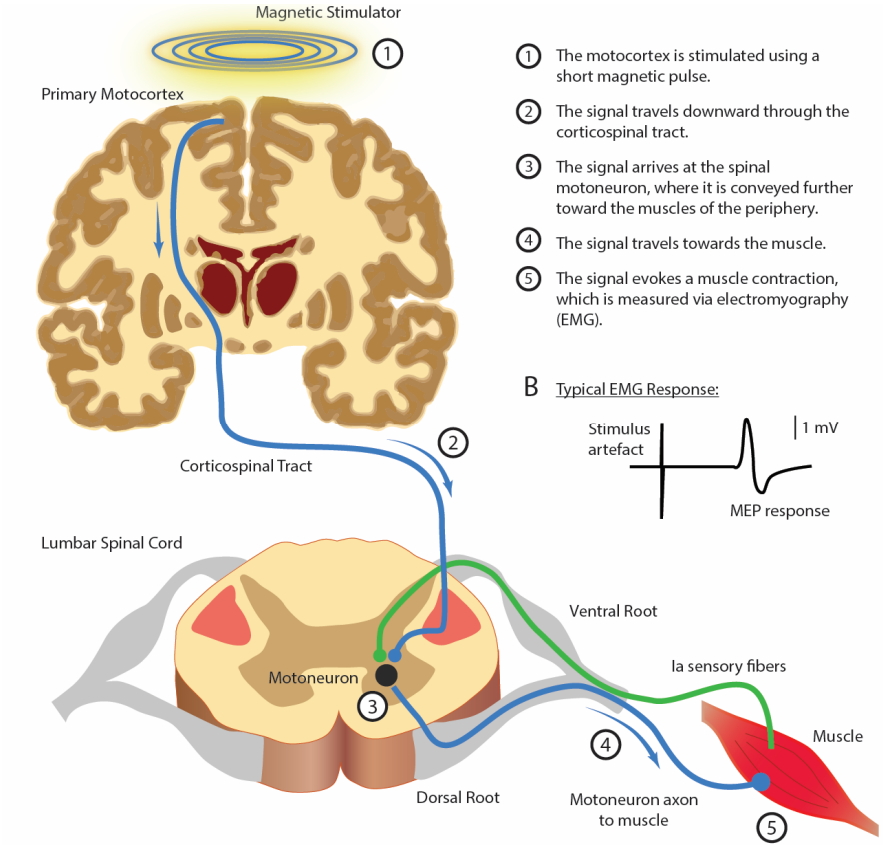

Figure 5: A) Simplified illustration of the motor evoked potential pathway. B) The muscle activation is visible as a prominent positive - negative deflection in the electromyographic (EMG) signal.
Figure redrawn and adapted from original by John Wiley and Sons, Inc.

1.5.2 The Hoffman Reflex

The Hoffman (H)-Reflex, is the electrophysiological equivalent of the stretch (or tendon tap) reflex. The H-reflex is induced by stimulating a motor-nerve bundle with a short (e.g. 1 ms) electrical pulse (fig. 6A[1]), which generates an AP in both, sensory and motor axons (fig. 6A[2]). While the AP in the motor axon reaches the muscle over a short trajectory, evoking a first muscle twitch (M-Wave), the AP in the sensory axon travels to the spinal cord and activates alpha-motoneurons, where it is conveyed further to the muscle (fig. 6A[3]). The forwarded signal then travels along the motoneuron axon towards the associated muscle (fig. 6A[4]), where it evokes a second contraction (H-Wave) (fig. 6A[5]). Figure 6B shows a typical EMG recording in response to a single stimulation pulse. Following the initial stimulation artefact, are the M- and H-wave which are both characterized by a positive -negative EMG deflection.

For varying stimulation amplitudes, the amplitude of the M- and H-Wave vary in a nonlinear fashion (fig. 6C). The resulting graphs are known as, the H- and M-Wave recruitment curves. At lower stimulation amplitudes, only the (thicker) sensory axons are stimulated. This happens after

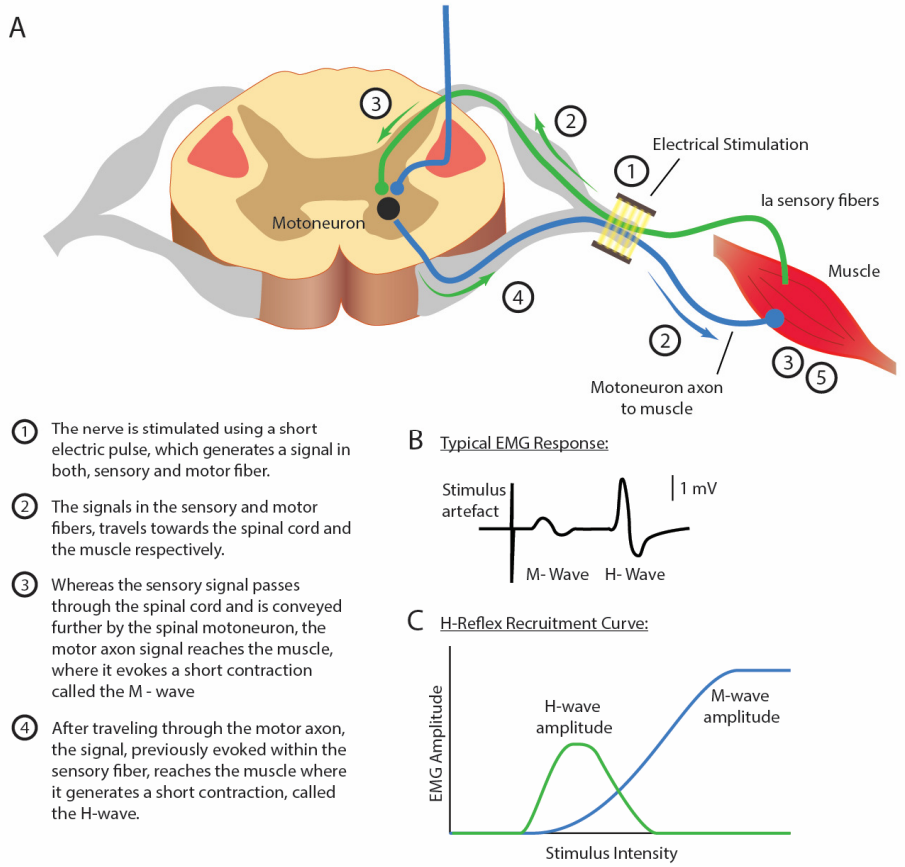

Figure 6: A) Simplified illustration of the H-Reflex pathway. B) A typical EMG response of the H-reflex a medium stimulation intensity. C) The H- and M-Wave recruitment curves, which reflect the amplitudes of both H- and M- Wave as a function of stimulation intensity.

Figure redrawn and adapted from original by John Wiley and Sons, Inc

the stimulus amplitude surpasses a certain level, called the recruitment threshold. When the stimulus is increased further, more sensory axons are recruited, which leads to a rise of the H-Wave recruitment curve. Furthermore, motor axons start to be recruited, which leads to a rise of the M-wave recruitment curve. At a certain stimulus intensity, all sensory axons are recruited, which is why the H-Wave does not increase further from this point. However, when the stimulus intensity is increased further, the H-Wave amplitude starts to decrease whereas the M-wave will increase until all motor axons are recruited, after which the M-wave recruitment curve settles. The H-wave decreases at higher stimulation amplitudes, since not one, but two separate action potentials are generated by the stimulus applied to the nerve. These travel in opposite directions, away from the site of stimulation. Therefore, whereas the descending motor-AP activates the muscle (M-wave), the ascending motor- AP collides with the now descending reflex signal, which leads to its cancelation.

1.6 Computational Modeling of Direct Current Stimulation

The goal of noninvasive neurostimulation, is to induce lasting, functionally distinct and meaningful changes to the nervous system. Optimally, it should be possible to precisely control stimulation outcome and apply the intervention with surgical precision.

Direct Current Stimulation (DCS) interventions seem straightforward, due to the relative ease of application, involving two or more electrodes, placed on the skin and connected to an electrical stimulator. This ease of application is in contrast to an underlying highly complex, non-linear, state dependent, dynamic system. The DC generated electric field is distributed throughout the body, dependent on subject anatomy and biophysical tissue properties (fig. 7A). Subsequently, the electric field interacts with the targeted neural architecture, causing the de- or hyper-polarization of any neural structure exposed to the electric field (fig. 7B). This is dependent on neural morphology, electric field orientation and magnitude as well as the bioelectric properties of the neurons.

Especially due to the noninvasive nature, it is experimentally challenging to gain a proper understanding of the systems complexity. Therefore, computational techniques can be a valuable addition as they allow further insights into such complex systems. For the effects of neural direct current stimulation, a number of different theoretical methods have been utilized, which mainly include the calculation of the generated electric field in the CNS [22–24] , and the resulting polarization effects on individual neurons [19,20,25]. The following sections will therefore briefly introduce the methods for simulation the electric field, as well as its interaction with an exposed neural structure.

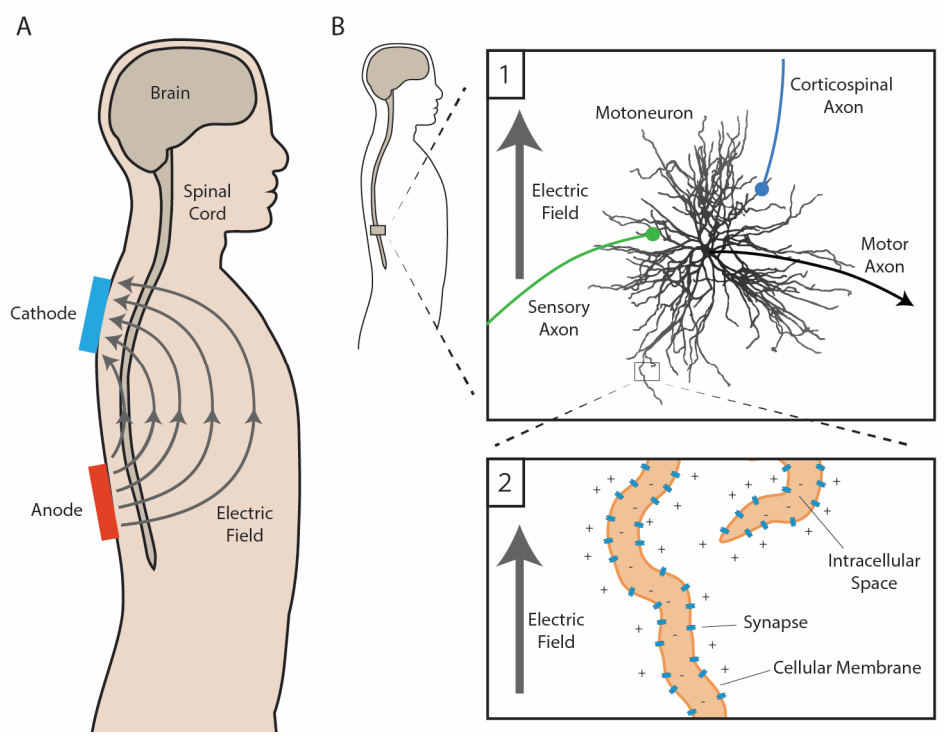

Figure 7: Macro- to microscopic overview of electrical spinal stimulation. A) The applied electrical stimulation generates an electric field in the human body, between the attached transcutaneous electrodes. B) The electric field interacts with the neural circuits of highly complex geometry (1), which microscopically consist of cable-like structures (2).

1.6.1 Simulation of Electric Fields in the Human Body

1.6.1.1 Electrostatics

The electric field generated by tsDCS can be understood and analyzed, by using the concepts of electrostatics. Electrostatics describes the behavior of electric fields in space under static conditions, meaning constant in time.

In a battery, a potential gradient exists between both poles, due to differences in voltage between anode and cathode. When both poles are connected by an electrical conductor, the poles turn into current sources and charged particles flow through the conductor, moving along the potential gradient. This gradient, also known as the electric field, is thus the force that is exerted on a particle of unit charge. Since a spatially changing electric potential V_E exists at any given point around the two charges (battery dipole),

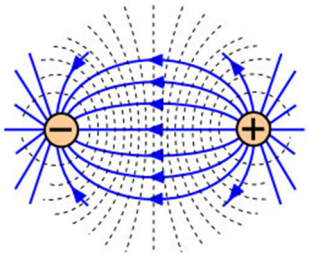

Figure 8: Equipotential and electric field lines, generated by a dipole arrangement of current sources.

Source: Electric Field Lines. Brilliant.org. Retrieved 16:13, August 22.

decreasing in proportion to the distance from either pole, the static electric field vector E can then be expressed via

$$E = -\nabla V_E \quad (1)$$

with ∇ the spatial gradient.

To analyze the tsDCS generated electric field in the body, it is thus necessary to calculate the potential distribution caused by the connected stimulation electrodes. These calculations are often complex, involving detailed anatomical models of the body with inhomogeneous electrical properties. They are therefore often executed via computational methods, such as the finite element method.

1.6.1.2 Finite Element Method for the Simulation of Electric Fields

The Finite Element Method (FEM) is a numerical procedure of solving large scale mathematical problems in physics and engineering. Typical areas of application include structural analysis, fluid flow or electromagnetics. These problems generally involve the solution of partial differential equations with boundary value constraints. A relevant example, is the description of an electric field as it spreads through the human body. The equation in this case solves the three-dimensional electric potential, based on electrode position, subject anatomy and the electrical parameters of the tissue. The FEM solves these problems by subdividing them into smaller "finite elements". This results in a system of "simpler" equations, for which the solution can be approximated using numerical methods. An advantage of FEM over other methods, is the ability to easily extend the model in complexity by including more complex geometry, material properties, or increasing the resolution at points of interest within the model.

1.6.2 Modeling Neurons

When investigating the effect of an electric field on neural circuitry, one needs to have a model of the targeted neural morphology. This model must be capable of describing neuron morphology, voltage dependency and other biophysical characteristic, as well as the interaction with an external electric field.

Most of a neural cell, including axons and dendrites, can geometrically be described as a pipe structure and the neuron's electrical properties can be divided into passive and active components.

A good approximation of the passive neural properties comes from cable theory, which was originally developed by Professor William Thomson to describe the signal decay in underwater telegraphic cables [26]. Due to the analogies with neural signal transduction, cable theory can also be used to simulate the electric current and voltage along neurons [27]. The resulting mathematical formulation is a partial differential equation that describes the transmembrane and axial currents as well as the associated voltage differences throughout the cell.

The neuron is thereby approximated with connected segments, containing capacitances and resistances combined in parallel (fig. 9). The capacitance c_m is a property of the neuronal membrane and is caused by electrostatic forces that are acting on both sides of the membrane. The resistances r_l and r_m are caused by the membranes and axoplasm's resistance to movement

of electric charge. The formulation can further be extended to incorporate more sophisticated mechanisms, such as active and voltage dependent ion channels as well as externally applied electric fields.

Since solving the resulting partial differential equation is challenging, especially for more complex geometries and transmembrane mechanisms, a common approach is again to refer to numerical approximations. The cable equation is thereby discretized in time and space, which replaces the partial differential equation by a coupled system of ordinary differential equations. This is referred to as "compartmental neural modeling" and is the basis of most computational implementations in common neural modeling software such as Neuron [28] or GENESIS [29]. The resulting framework allows for the simulation of neurons with a high degree of morphological and mechanistic complexity. It is thus also possible to simulate the neural effects of electrical stimulation, by calculating the tsDCS generated electric field (see section 1.6.1.2) and combining the results with a compartmental neuron model. This computational pipeline can therefore be a valuable tool for the understanding and development of electrotherapeutic protocols.

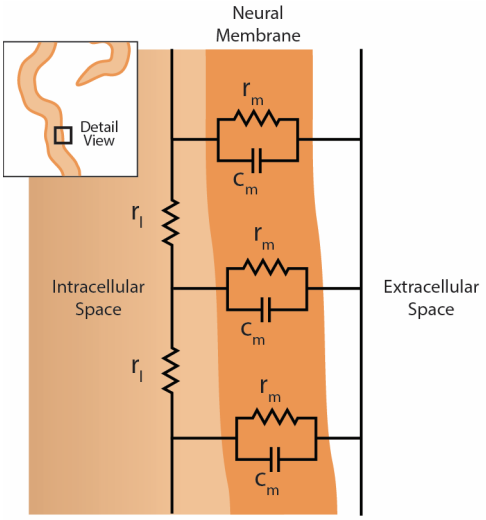

Figure 9: Simplified view of the electrical properties of a neuronal fiber as described by the cable theory. C_m: membrane capacitance, r_m: membrane resistance, r_l: longitudinal resistance.

1.7 Outline of this Thesis

TsDCS, as well as other neurostimulation modalities, have received increasing interest as a possible intervention option for the rehabilitation of spinal cord dysfunction or injury. However, little is known about how tsDCS needs to be applied to lead to the desired stimulation outcome. The goal of this dissertation is therefore to increase the mechanistic understanding of tsDCS to aid a hypothesis driven intervention design of tsDCS, aiming at a possible application in spinal cord injury rehabilitation.

Central questions were: 1) what is the electric field distribution, generated by tsDCS and how can it by controlled via different electrode placements 2) what are the targeted neural structures of tsDCS and could this knowledge be used to achieve a more targeted stimulation effect 3) Can the effect of tsDCS be directed via different alignments of the imposed electric field with the targeted neural structures 4) What is the best possible mode of application to achieve the maximal modulation effect. 5) Can tsDCS safely be applied to the intended target group.

To address these questions, a combination of computational and experimental approaches was chosen. Chapter 2 addresses the electric field (EF) generated during tsDCS and its interaction

with the targeted neural circuits. This includes calculation, visualization and analysis of the generated electric field as well as the identification of neural structures, likely to be most targeted by the intervention. Furthermore, a comparison with existing human tsDCS studies as well as the possible effects of electrode misplacement during application are discussed.

Thereafter, the following two chapters experimentally assess the effects of tsDCS for different protocol variations, such as electric field direction and mode of application.

Chapter 3 deals with investigating the effects of tsDCS applied with different electric field directions, and the repeatability of results previously obtained by others. The central question hereby, was to assess whether the tsDCS outcome is dependent on electric field direction. This was addressed in a randomized, double-blind placebo controlled study, whereby 10 healthy subjects received tsDCS in three different electrode configurations, plus a placebo stimulation. As a probe for the induced neural changes, the H-reflex recruitment curve was utilized.

Chapter 4 compares the effects of tsDCS during active movement and rest, to investigate during which of the two conditions the application of tsDCS leads to larger modulatory effects. The underlying hypothesis is, that the modulatory effect of tsDCS can be significantly increased when paired with ongoing neural activity. In four different experiments, subjects received real- or placebo tsDCS during either lying and walking. The resulting neural changes were measured using the H-reflex.

Lastly, chapter 5 investigates important safety aspects, when tsDCS is applied in the presence of metallic spinal implants. This is related to the fact, that the presence of metallic implants in the body is still a safety concern, in connection with electrical stimulation procedures. Since spinal implants are expected to be present in at least part of the targeted population with spinal cord injury, it is necessary to explore the safety and application specific consequences of tsDCS with the presence of a spinal metallic implant. To investigate this question, the tsDCS induced EF and current density was simulated in the presence of a metallic spinal implant.

References

[1] Lamy J-C, Ho C, Badel A, Arrigo R T and Boakye M 2012 Modulation of soleus H reflex by spinal DC stimulation in humans. *J. Neurophysiol.* **108** 906–14

[2] Hubli M, Dietz V, Schrafl-Altermatt M and Bolliger M 2013 Modulation of spinal neuronal excitability by spinal direct currents and locomotion after spinal cord injury. *Clin. Neurophysiol.* **124** 1187–95

[3] Yamaguchi T, Fujimoto S, Otaka Y and Tanaka S 2013 Effects of transcutaneous spinal DC stimulation on plasticity of the spinal circuits and corticospinal tracts in humans *2013 6th Int. IEEE/EMBS Conf. Neural Eng.* 275–8

[4] Bocci T, Marceglia S, Vergari M, Cognetto V, Cogiamanian F, Sartucci F and Priori A 2015 Transcutaneous Spinal Direct Current Stimulation (tsDCS) Modulates Human Corticospinal System Excitability *J. Neurophysiol.* jn.00490.2014

[5] Cogiamanian F, Ardolino G, Vergari M, Ferrucci R, Ciocca M, Scelzo E, Barbieri S and Priori A 2012 Transcutaneous Spinal Direct Current Stimulation *Front. Psychiatry* **3**

[6] Cogiamanian F, Vergari M, Pulecchi F, Marceglia S and Priori A 2008 Effect of spinal transcutaneous direct current stimulation on somatosensory evoked potentials in humans. *Clin. Neurophysiol.* **119** 2636–40

[7] Bocci T, Vannini B, Torzini A, Mazzatenta A, Vergari M, Cogiamanian F, Priori A and Sartucci F 2014 Cathodal transcutaneous spinal direct current stimulation (tsDCS) improves motor unit recruitment in healthy subjects *Neurosci. Lett.* **578** 75–9

[8] Bican O, Minagar A and Pruitt A A 2013 The Spinal Cord. A Review of Functional Neuroanatomy *Neurol. Clin.* **31** 1–18

[9] Chen Y, Tang Y, Vogel L and DeVivo M 2013 Causes of Spinal Cord Injury *Top. Spinal Cord Inj. Rehabil.* **19** 1–8

[10] Ho C H, Wuermser L A, Priebe M M, Chiodo A E, Scelza W M and Kirshblum S C 2007 Spinal Cord Injury Medicine. 1. Epidemiology and Classification *Arch. Phys. Med. Rehabil.* **88**

[11] Donovan W H 2007 Spinal cord injury-past, present, and future *J. Spinal Cord Med.* **30** 85–100

[12] Yu W-Y and He D-W 2015 Current trends in spinal cord injury repair *Eur. Rev. Med. Pharmacol. Sci.* **19** 3340–4

[13] McDonnell M N, Hillier S L, Miles T S, Thompson P D and Ridding M C 2007 Influence of combined afferent stimulation and task-specific training following stroke: a pilot randomized controlled trial. *Neurorehabil. Neural Repair* **21** 435–43

[14] Gerasimenko Y, Gorodnichev R, Moshonkina T, Sayenko D, Gad P and Reggie Edgerton V 2015 Transcutaneous electrical spinal-cord stimulation in humans *Ann. Phys. Rehabil. Med.* **58** 225–31

[15] Harkema S, Gerasimenko Y, Hodes J, Burdick J, Angeli C, Chen Y, Ferreira C, Willhite A, Rejc E, Grossman R G and Edgerton V R 2011 Effect of epidural stimulation of the lumbosacral spinal cord on voluntary movement, standing, and assisted stepping after motor complete paraplegia: a case study. *Lancet* **377** 1938–47

[16] Alam M, Garcia-Alias G, Jin B, Keyes J, Zhong H, Roy R R, Gerasimenko Y, Lu D C and Edgerton V R 2017 Electrical neuromodulation of the cervical spinal cord facilitates forelimb skilled function recovery in spinal cord injured rats *Exp. Neurol.* **291** 141–50

[17] Wenger N, Moraud E M, Gandar J, Musienko P, Capogrosso M, Baud L, Le Goff C G, Barraud Q, Pavlova N, Dominici N, Minev I R, Asboth L, Hirsch A, Duis S, Kreider J, Mortera A, Haverbeck O, Kraus S, Schmitz F, DiGiovanna J, van den Brand R, Bloch J, Detemple P, Lacour S P, Bézard E, Micera S and Courtine G 2016 Spatiotemporal neuromodulation therapies engaging muscle synergies improve motor control after spinal cord injury *Nat. Med.* **22** 138–45

[18] Gerasimenko Y, Lu D, Modaber M, Zdunowski S, Gad P, Sayenko D, Morikawa E, Haakana P, Ferguson A R, Roy R R and Edgerton V R 2015 Noninvasive Reactivation of Motor Descending Control after Paralysis. *J. Neurotrauma* **13** 1–13

[19] Rahman A, Reato D, Arlotti M, Gasca F, Datta A, Parra L C and Bikson M 2013 Cellular effects of acute direct current stimulation: somatic and synaptic terminal effects. *J. Physiol.* **591** 2563–78

[20] Bikson M and Rahman A 2013 Origins of specificity during tDCS: anatomical, activity-selective, and input-bias mechanisms. *Front. Hum. Neurosci.* **7** 688

[21] Bikson M, Parra L, Reato D, Rahman A, Lafon B and Radman, T 2013 Cellular Mechanism of transcranial Direct Current Stimulation (tDCS), Presentation, given at the Summit on transcranial Direct Current Stimulation, Sept 5, 2013, at the UC-Davis Center for Mind and Brain, Davis, USA

[22] Wagner S, Rampersad S M, Aydin Ü, Vorwerk J, Oostendorp T F, Neuling T, Herrmann C S, Stegeman D F and Wolters C H 2014 Investigation of tDCS volume conduction effects in a highly realistic head model. *J. Neural Eng.* **11** 16002

[23] Rampersad S M, Janssen A M, Lucka F, Aydin Ü, Lanfer B, Lew S, Wolters C H, Stegeman D F and Oostendorp T F 2014 Simulating transcranial direct current stimulation with a detailed anisotropic human head model. *IEEE Trans. Neural Syst. Rehabil. Eng.* **22** 441–52

[24] Rampersad S M, Stegeman D F and Oostendorp T F 2013 Single-layer skull approximations perform well in transcranial direct current stimulation modeling. *IEEE Trans. Neural Syst. Rehabil. Eng.* **21** 346–53

[25] Arlotti M, Rahman A, Minhas P and Bikson M 2012 Axon terminal polarization induced by weak uniform DC electric fields: a modeling study. *Conf. Proc. IEEE Eng. Med. Biol. Soc.* **2012** 4575–8

[26] Thomson W 1854 On the Theory of the Electric Telegraph *Proc. R. Soc. London* **7** 382–99

[27] Hoorweg J L 1898 Ueber die elektrischen Eigenschaften der Nerven *Arch. für die gesamte Physiol. des Menschen und der Tiere* **71** 128–57

[28] Carnevale N T and Hines M L 2006 *The NEURON Book* vol 30

[29] Bower J M and Beeman D 2003 The Book of Genesis - Exploring Realistic Neural Models with the GEneral NEural SImulation System *Genesis* 2003

Chapter II – Modeling Trans-Spinal Direct Current Stimulation for the Modulation of the Lumbar Spinal Motor Pathways

A. KUCK [1], D.F. STEGEMAN [2] and E.H.F. VAN ASSELDONK [1]

[1] University of Twente, Drienerlolaan 5, 7522 NB Enschede, The Netherlands

[2] Radboud University Medical Center, Donders Institute for Brain, Cognition and Behavior, Department of Neurology/Clinical Neurophysiology, Reinier Postlaan 4, 6500HB Nijmegen, The Netherlands.

Based on: A. Kuck et al 2017 J. Neural Eng. 14 056014
DOI: https://doi.org/10.1088/1741-2552/aa7960

Abstract

Objective. Trans-spinal direct current stimulation (tsDCS) is a potential new technique for the treatment of spinal cord injury (SCI). TsDCS aims to facilitate plastic changes in the neural pathways of the spinal cord with a positive effect on SCI recovery. To establish tsDCS as a possible treatment option for SCI, it is essential to gain a better understanding of its cause and effects. We seek to understand the acute effect of tsDCS, including the generated electric field (EF) and its polarization effect on the spinal circuits, to determine a cellular target. We further ask how these findings can be interpreted to explain published experimental results. Approach. We use a realistic full body finite element volume conductor model to calculate the EF of a 2.5 mA direct current for three different electrode configurations. We apply the calculated electric field to realistic motoneuron models to investigate static changes in membrane resting potential. The results are combined with existing knowledge about the theoretical effect on a neuronal level and implemented into an existing lumbar spinal network model to simulate the resulting changes on a network level. Main results. Across electrode configurations, the maximum EF inside the spinal cord ranged from 1.29 V/m to 2.73 V/m. Axon terminal polarization was identified to be the dominant cellular target. Also, differences in electrode placement have a large influence on axon terminal polarization. Comparison between the simulated acute effects and the electrophysiological long-term changes observed in human tsDCS-studies suggest an inverse relationship between the two. Significance. We provide methods and knowledge for better understanding the effects of tsDCS and serve as a basis for a more targeted and optimized application of tsDCS.

2.1 Introduction

Spinal cord injury poses a heavy burden on the quality of life. Depending on the severity and location of the injury, sufferers are usually left with the loss of upper and lower limb motor control, as well as other vital functions. Among other investigated treatment options, there is a recent focus on invasive and non-invasive electrical stimulation techniques with the intention of inducing an additional degree of improvement when combined with traditional rehabilitation efforts.

Stimulation protocols under investigation for spinal cord injury rehabilitation vary significantly in their degree of invasiveness and intended neural response. Whereas for non-invasive electrical

stimulation, electrodes are placed on the skin of the subject [1], invasive electrical stimulation of the spinal cord has been successfully demonstrated by using epidural electrodes [2–4].

In humans, both invasive and non-invasive electrical stimulation have been used to directly activate the targeted neural pathways in the spinal cord via supra-threshold electrical stimulation. Sub-threshold network modulation is commonly applied non-invasively and aims to modulate ongoing and future neural activity by inducing pathway specific plastic changes.

We focus here on the understanding of noninvasive sub-threshold direct current stimulation (DCS) for the modulation of the lumbar spinal motor circuits. Trans-spinal direct current stimulation (tsDCS) aims to modulate spinal motor pathways and in turn, increase and direct neural plasticity where it is most necessary (for a review see: [1]). A well understood and targeted application is essential for the success and credibility of the tsDCS technique in a rehabilitation setting. Therefore, next to existing practical efforts, a reasonable way of directing the effects of tsDCS has to be found. However, predictions of the short and long-term effects of DCS are difficult, since they require a thorough understanding of the functional and anatomical parameters of the nervous system.

Previous studies have shown, that tsDCS can have a significant effect on the pathways in the spinal cord including the descending motor pathways [5], ascending somatosensory pathways [6] and the lumbar monosynaptic reflex loop [7,8]. In the latter, modulatory effects on post activation depression [9] and presynaptic inhibition [10] have also been shown. Additionally, animal studies provide further evidence on effects of DC stimulation on the spinal circuits. Thereby, lumbar tsDCS had a wide range of influences on, for instance, the execution of descending motor signals, spontaneous firing measured in the motor nerve as well as associative plasticity when paired with trains of cortical signals [11–13]. All studies suggest a clear polarity dependency of the reported effects. The growing evidence raises hope that tsDCS may be applicable to the rehabilitation of spinal cord injury or even extend to other disorders in the future. For a successful application however, the distribution and magnitude of the applied electric field, its acute effects on the targeted neural pathways and the relationship to the long-term effects reported in literature have to be investigated.

DC stimulation generates a weak electric field (EF) of <1 V/m for tsDCS [14] as well as for the related transcranial DCS technique (tDCS) [15–17]). The interaction with a neural structure thus leads to a local shift in transmembrane potential, depending on the detailed morphology and its alignment with the electric field. Assuming a spatially static EF, membrane polarization takes place mainly at closed ends such as axon and dendrite terminals. The polarization exponentially decays with further distance to the terminal.

The molecular working mechanisms within the neuron are largely dependent on its resting membrane potential. Membrane polarization will therefore lead to an acute functional modulation of the neuron and can be measured as a change of synaptic efficacy [18]. The ultimate goal is to translate such acute effects into long term changes via mechanisms known as synaptic plasticity. This transition depends on the acute membrane polarization and the molecular mechanisms involved (cellular targets), the duration of the stimulation [18–20], the ongoing neural activity [21,22] as well as subject specific genetics factors [23].

Previous work shows that the polarization of a number of different cellular targets (e.g. soma, dendrites, axon terminals) may be eligible to produce the observed plasticity effects in synaptic efficacy. Thereby facilitation/inhibition of neuron function may be causally related to depolarization/hyperpolarization of the somatic membrane potential [18,24–26]. The polarization of incoming axons [18,25,27,28] and axon terminals [18,29,30] may further contribute to the effects of DCS. In pyramidal neurons, typically the focus of cortical tDCS studies, the polarization of apical dendrites, which polarize opposite to somas, was also found to influence synaptic processing [25,28,31].

The so far gathered knowledge underlines the importance of understanding the cellular targets of DCS as a prerequisite to a rational electrotherapy design [31]. Most previous work aimed at the understanding of DCS on cortical structures. Our focus differs in this respect, since we focus on the application of DCS on the lumbar spinal motor circuits. This requires a thorough evaluation and analysis of spinal motoneuron (MN) morphology and functioning.

Alpha MNs receive axonal connections of cortical and local (sensory) origin. Dendrites extend radially around a central soma in a seemingly random fashion. For Ia terminals, a majority of synapses are located on the proximal dendrites and follow little distinct patterns of spatial organization [32–35]. Motoneuron response and excitability may be controlled via channels exhibiting persistent inward currents (PIC) [36], located on the proximal dendrites [37,38].

Previous publications have shown that tsDCS can modulate spinal network output. The goal of our contribution is a thorough analysis of the EFs generated by tsDCS, as well as the resulting membrane polarization in neurons, sensory and descending corticospinal axon terminals (ATs). Concurrently, we seek to find the cellular target of tsDCS, including its theoretical effects on a network level. Along this line, we further aim to understand the connection between simulated, acute network effects and long-term plasticity changes reported by others as well as the impact of possible electrode misplacements.

We use a realistic full body segmented finite element model to estimate the electric field inside the spinal cord when stimulated with three different electrode configurations at an intensity of 2.5mA. We apply the electric field finite element solution to realistic neuron models to investigate changes in membrane resting potential within the neuron as well as afferent and efferent axon terminals. We further combine the observed membrane polarization effects with acute cellular changes found experimentally by others. To simulate the theoretical network effect, we make use of an existing lumbar spinal network model [39].

2.2 Methods

2.2.1 Electrode Placement

We simulated the electric field for three electrode configurations (fig. 1): A) the in previous publications used spine-shoulder configuration (active electrode on the T11 vertebrae and return electrode placed on the left posterior shoulder), B) both electrodes placed at equal distance, superior and inferior to the T11 vertebrae, C) the active electrode is placed on the T11 vertebrae and two counter electrodes are placed on the left and right anterior superior iliac crest.

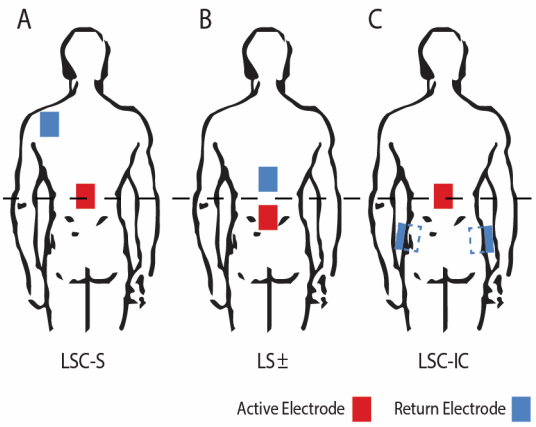

Figure 1: The simulated electrode placement configurations. A) Active electrode on the lumbar spinal cord, return electrode on the posterior left shoulder. B) Active electrode below and passive electrode above the lumbar spinal cord. C) Active electrode on lumbar spinal cord, two passive electrodes on the left and right anterior superior Iliac Crest respectively.

2.2.2 Finite Element Model

The steady state electrical potential in the inhomogeneous volume conductor model is computed using the software environment SCIrun (SCI Institute 2015) by solving the function described by Poisson's equation

$$\nabla(\sigma \nabla \Phi) = 0 \qquad (1)$$

where σ is a conductivity tensor and Φ is the electric potential. Subsequently the electric field vector E is calculated by

$$E = -\nabla \Phi \qquad (2)$$

The goal is to solve equation 1, given a mesh, a set of known conductivities, and a set of known potentials corresponding to the electrode locations. Computations were conducted using a conjugate gradient descend algorithm at varying voxel resolutions of 4mm^3 in the head and extremities, 1-2mm^3 in the torso and electrodes and 0.5mm^3 inside the spinal cord. The mesh was a pre-segmented full body model (Ella) (fig. 2), which is part of the Virtual Population Library Version 2 [41]. A segmentation of the spinal cord into white and grey matter was added using a custom-made model. Conductivities were adopted from [14] without change. White matter in the spinal cord was simulated using anisotropic conductivities with a transversal vs. longitudinal factor of 1:10 [42]. The rectangular surface electrodes (50×70×3mm) were positioned

Figure 2: The utilized finite element model (Ella), which includes 22 individual segments, stems from the Virtual Population Library (version 2) (dimensions: 500.4 × 278.9 × 1647.3 mm).

according to the corresponding electrode configuration in direct connection with the skin surface. Electrode potentials were assigned to the outer surface nodes of each electrode mesh.

2.2.3 Motoneuron Model

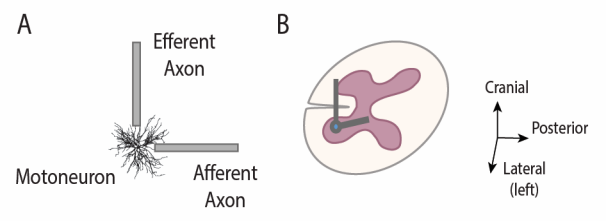

Figure 3: A) Schematic illustration of the utilized motoneuron model, essentially consisting of three separate models: a realistic neuron model and two straight, cylindrical axons. B) The location and orientation of motoneuron and axon models within the spinal cord (axon length not to scale). The motoneuron is placed within the grey matter below the T11 vertebrae.

To calculate the influence of the steady state electric field on motoneurons with a realistic morphology, six reconstructed cat motoneurons (NMO_00687, NMO_00688, NMO_00689, NMO_00690, NMO_00691, NMO_00692) initially supplied by Alvarez et al. [43] and modified by Balbi et al. [44] were used (Table 1). This was implemented via the modeling environment NEURON v.7.3 [45]. Each neuron model was placed in the ventral horn of the spinal cord between the T11 and T12 vertebrae (fig. 3). Thereafter, the previously calculated extracellular potential for each compartment is calculated via trilinear- interpolation and assigned in NEURON via the extracellular function.

Table 1: Morphometric parameters of the utilized motoneuron models.

	NeuroMorpho identification number	Number of Dendritic Sections	Number of dendritic compart-ments	Number of primary dendrites	Soma diameter (µm)	Sum of diameters of primary dendrites	Soma surface (μm^2)	Surface of dendrites tree (μm^2)	Dendrites mean terminal distance (µm)
1	NMO_00687	398	3118	10	65.02	111.42	13,280	682,012	1049.45
2	NMO_00688	92	716	8	49.97	87.38	7847	150,243	736.52
3	NMO_00689	86	540	16	65.64	158.97	13,535	166,343	456.83
4	NMO_00690	149	1425	13	52.82	89.10	8767	233,642	829.38
5	NMO_00691	249	2183	11	60.81	101.77	11,616	374,199	896.49
6	NMO_00692	270	2656	12	63.83	130.10	12,801	489,120	891.33

Two separate straight axons, representing efferent and afferent connections to the motoneuron, were assigned with the electric field strength in longitudinal and anterio-posterior direction respectively at the level of the motoneuron. Both axons were modeled as simple cylinders with a length of 40 mm and a diameter of 10 µm. Reported diameters for both axon types, including myelin, are within a range of 13 µm to 20 µm for afferent (Ia) fibers [46] and 16 µm to 20 µm for efferent axons originating from cortical Betz neurons [47,48]. The inner axonal diameter, without

myelin, was estimated via multiplication of the g-ratio (g=0.6) [49], whereby the chosen axon diameter of 10 μm is within the resulting range for both axons.

For all neural elements, the external resistivity was set to 70 Ωcm, the specific capacitance was set to 1 $\mu F/cm^2$. Na^+ and K^+ equilibrium potentials were set to +50 mV and −77 mV respectively, while the Ca^{2+} equilibrium potential dynamically changed depending on the variations of internal and external ion concentrations [44]. For a complete overview of all biophysical parameters, which were adopted unchanged, refer to [44].

2.2.4 Spinal Circuit Model

Simulations at a network level were performed using an open source lumbar spinal network model (ReMoto, Version: 2.1) developed by Cisi et al. [39]. The model employs two-compartment motoneuron models for slow (S), fast fatigue resistant (FR) and fast fatigable (FF) types and includes a population of interneurons (Ia reciprocal inhibitory interneurons, Ib interneurons, and Renshaw cells) connected to afferent connections and induced stochastic point processes associated with descending tracts. To simulate human electrophysiological experiments, the simulator incorporates external nerve stimulation with orthodromic and antidromic propagation. The generation of the H- reflex by the Ia-motoneuron pool system, its modulation by spinal cord interneurons, as well as varying possibilities for incorporating descending corticospinal motor-signals are included [39].

2.2.5 Simulation Procedure

As a first step, the local field potential distribution and electric field for a stimulation intensity of 2.5mA was computed for each electrode configuration (fig. 1). To test the sensitivity of electrode misplacements, the active lumbar electrode was shifted vertically by ±5 cm. For configuration "LSC ±" (fig. 1B) the misplacement was applied to both electrodes. Thereafter, each of the six neuron models was simulated at resting state with and without the applied electric field for each of the three electrode configurations. The application of the electric field results in a shift of the transmembrane potential.

To obtain results that can be related to experimental evidence, we used the spinal network model by Cisi et al. The model is used to approximate the resulting acute functional changes imposed by tsDCS. We therefore simulate two common functional tests used to assess (cortico-) spinal network function; these are the H- Reflex and motor evoked potentials (MEP). Both give information about spinal afferent and efferent motor pathways respectively and have been used to show effects induced by tsDCS in previous studies. We simulate the changes induced by modulation of the primary cellular target, including those during acute tsDCS, and compare the obtained network responses with experimental results obtained by others. The neural building blocks used for both scenarios are 800 slow (S), 50 fatigue resistant (FR) and 50 fast fatiguing (FF) motor units [39]. All other model parameters are left unaltered. To mimic a spinal motoneuron response similar to that of a primary MEP, we simulate soleus voluntary contraction with a pulse input. Descending efferent input to the motoneuron pool is given by a single pulse Poisson distributed firing pattern, with a mean inter-spike-interval (ISI) of 3ms for $0 \text{ ms} \leq t \leq 5 \text{ ms}$ [50] and infinite otherwise (for details, refer to [39]). Baseline synaptic maximum conductance was set to 700 nS. Parameter values were chosen in favor of resulting in

a clear model output, which is given by a simulated muscle activation in form of an EMG response. For each of the acquired EMG traces, the amplitude and delay are subsequently extracted. For H-Reflex simulation, the afferent input is a single stimulus of 1ms duration applied to the motor nerve for increasing stimulation amplitudes (H-Reflex).

2.3 Results

2.3.1 Electric Field Distribution in Spinal Cord

Figure 4 shows the calculated electric field magnitude for all configurations throughout the spinal cord. Each configuration creates a distinct pattern with a maximum electric field magnitude approximately half way between, and a smaller EF immediately adjacent to the two electrodes. The maximum field strength varies between 1.29 V/m and 2.73 V/m depending on the electrode placement.

A more thorough analysis of EF size and direction can be performed by regarding its individual vector components (fig. 5). This is helpful when considering the directional prerequisite for the modulation of neural compartments.

For each electrode configuration the figure shows the transverse mean of the electric field vector in all three dimensions. Thereby, the targeted motoneuron location is indicated by a red cross. Additionally, the figure shows the EF for both, upward and downward (± 5cm) misplacements respectively. For all configurations the transversal EF component remains small compared to anterio-posterior and longitudinal vector magnitudes. Also, though the anterio-posterior vector is largest below, the longitudinal component dominates between the electrode pair. Furthermore, a cyclic variation is visible on the anterio-posterior vector component (see also fig. 4). These appear to correlate with vertebral locations, and may therefore reflect a variation in EF magnitude caused by vertebral body anatomy.

When the active electrode is misplaced, EF amplitude and direction at the stimulation target site are altered. For cases where the active electrode is placed on top of the target region, misplacements lead to amplitude changes in anterio-posterior and field reversals in longitudinal direction (fig. 5 A and C). When two electrodes are placed in

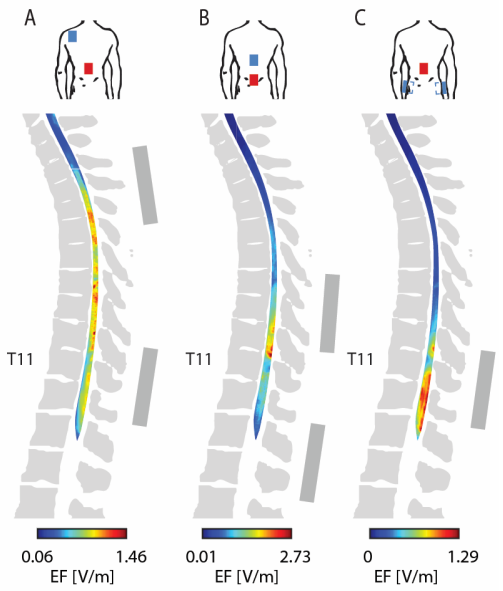

Figure 4: Electric field distribution in the spinal cord for each electrode configuration with indicated electrode locations (see also fig.1).

equal distance to the target region, a misplacement of both affects the field magnitude in longitudinal and lead to a reversal in anterio-posterior direction (fig. 5 B).

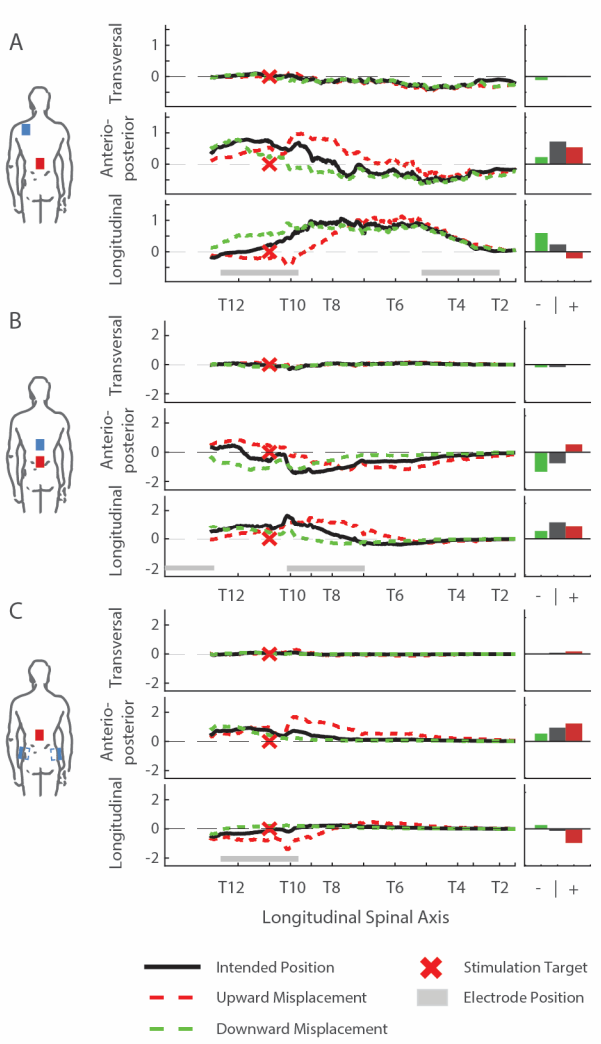

Figure 5: Individual EF vector components in the spinal cord for each electrode configuration as well as upward (+) and downward (-) electrode misplacements of ± 5cm. Additionally, the vector component magnitude at the stimulation target is shown (right column).

2.3.2 Changes in Membrane Potential

The potential distribution at motoneuron level and the resulting membrane polarization for an exemplary motoneuron is shown in figure 6. Clearly visible is the de-/hyperpolarization trend in line with the EF-vector direction. In this case, as for all tested motoneuron/configuration pairs, afferent and efferent axon terminal polarization (ranging from 0.35 mV to 2.89 mV) was dominant and multiple times stronger compared to other cellular targets (fig.7). In contrast, the soma was hardly polarized (<0.01 mV) and polarization of dendritic terminals did not exceed 0.63 mV. From further analysis, it follows that the mean polarization of dendritic membrane, specific to PIC channels and synaptic terminal locations (<0.17 mV), was approximately three times lower than the dendritic maximum (fig.7).

For electrode misplacements, efferent axon terminal polarization may increase or reverse depending on the shift direction (fig.7 A and C, col. 4) when the active electrode is placed on the target region. Afferent terminal polarization is affected little in this case, whereby amplitude is altered by preserving effect direction. For equal distance placements, misplacement may change sign and amplitude of afferent axon's terminal polarization (fig.7 B col. 5). Efferent axon terminal polarization amplitude is modulated while preserving effect direction.

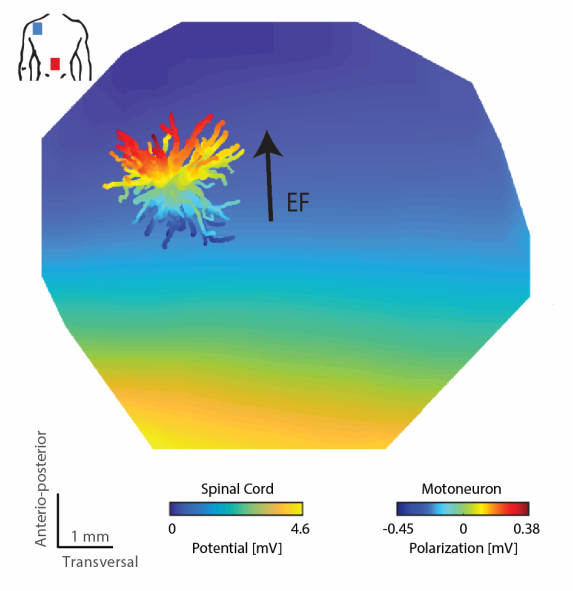

Figure 6: Stimulus induced voltages in the spinal cord and membrane polarization for an exemplary motoneuron model for electrode placement configuration LSC-S.

2.3.3 Spinal Network Simulation

In the previous subsections, we showed the acute polarization effects on lumbar spinal structures and identified the most dominant cellular target. Subsequently, we use the spinal network model developed by Cisi and Kohn, to perform a sensitivity analysis by modulating the identified cellular target to understand the resulting effects on a network level. We limit the analysis to effects caused by axon terminal polarization, representing the most prominent cellular target as shown before (fig.7). Acute, (post)synaptic effects of axon terminal polarization are known from literature [18], reporting an EF dependent change in EPSP amplitude.

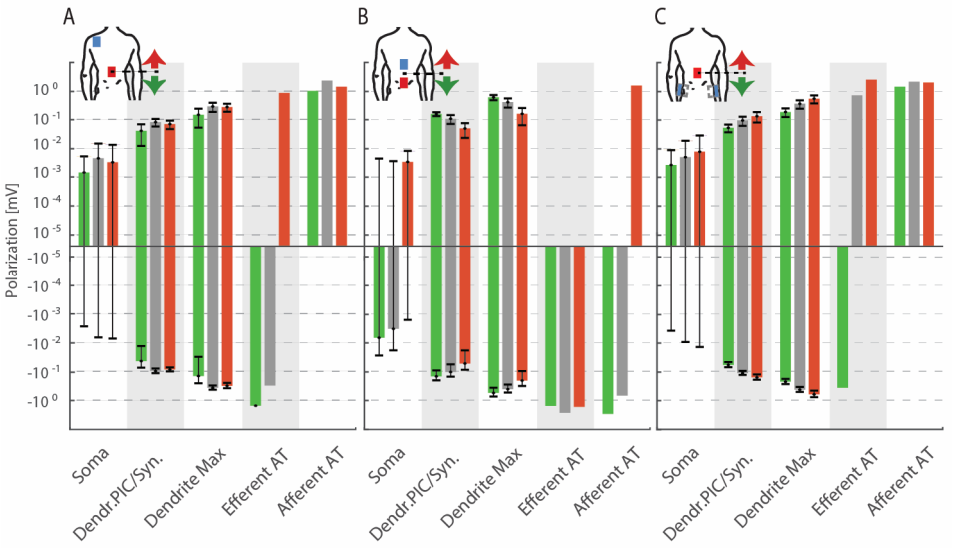

Figure 7: The average local membrane polarization and standard deviation of the six different motoneuron models. Shown are the polarization effects for: the soma, dendrites with distance to soma of less than 0.7mm (indicating the majority of PIC channels and synaptic locations) and maximum dendritic polarization. Furthermore, polarization effects are shown for the efferent and afferent axon terminals respectively. The polarization is shown for the intended electrode positions (grey) as well as downward (green) and upward (red) 5 cm electrode position misplacements. Note that polarization intensity is drawn on a hyperlog scale [51], which is linear between -10^{-5} and 10^{-5} and logarithmic otherwise.

The equation that expresses synaptic connections via the postsynaptic current I_{syn} can be written as:

$$I_{syn} = M_{synapse}\, g_{syn}(V - E_R) \tag{3}$$

where g_{syn} is the synaptic conductivity, V is the presynaptic voltage, E_R the reversal potential of the ion species involved and $M_{synapse}$ is a gain. We model synaptic modulation by changing $M_{synapse}$. According to Rahman and co-workers, axon terminal hyperpolarization/depolarization leads to an increase/decrease of postsynaptic EPSP amplitude [18]. We express the reported relationship between the EF towards the axon terminal E_{axon} and synaptic conductivity gain $M_{synapse}$ via a simple linear regression function:

$$M_{synapse} = 1 + \left(\frac{0.25}{16}\right) E_{synapse} \tag{4}$$

with "synapse" being either an efferent or afferent synapse. All previous human tsDCS studies used placement configuration 1 (figure 1, LSC-S) which we will therefore use for further analysis. The potential distribution at motoneuron level and the direction of the resulting axon terminal polarization for configuration LSC-S in both polarities is illustrated in figure 8. Efferent and afferent axon fibers point in negative longitudinal and positive sagittal directions respectively. The EF's along both terminals are $E_{efferent}$ = 0.092 V/m and $E_{afferent}$ = -0.73 V/m. This results in $M_{efferent,acute}$ = 1.00144 and $M_{afferent,acute}$ = 0.98848.

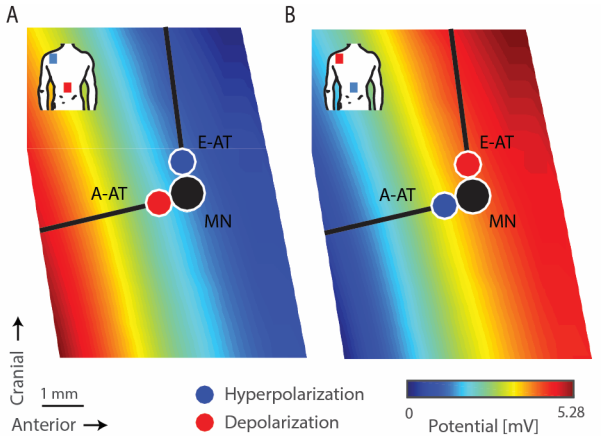

Figure 8: Simulated potential distribution in spinal cord for configuration LSC-S in both polarities as well as the estimated axon terminal polarization for efferent (E-AT) and afferent (A-AT) axon terminals in both cases.

We subsequently utilize the spinal network model, to simulate the EMG responses with either efferent or afferent neural input and respectively altering $M_{efferent}/M_{afferent}$. We simulate two conditions, pulsed descending drive soleus contraction (mimicking a primary MEP response) and the H-Reflex for varying stimulation amplitudes. We perform a sensitivity analysis of the model output by increasing/decreasing the conductivity gain $M_{efferent}$ / $M_{afferent}$ with values between 0.75 and 1.25 in increments of 0.025. To compensate for the underlying random variables in the spinal network model, the extracted variables are fit to a regression function, given their corresponding $M_{efferent}$ / $M_{afferent}$ using the least squares method. The regression function is then utilized to estimate the modulation strength for $M_{synapse,acute}$.

The simulated MEP responses for $M_{efferent}$ = [0.75, 1, 1.25] are shown in figure 9A. Thereby increasing synaptic gains result in higher peak amplitudes and decreasing latencies. Decreasing synaptic gains led to the

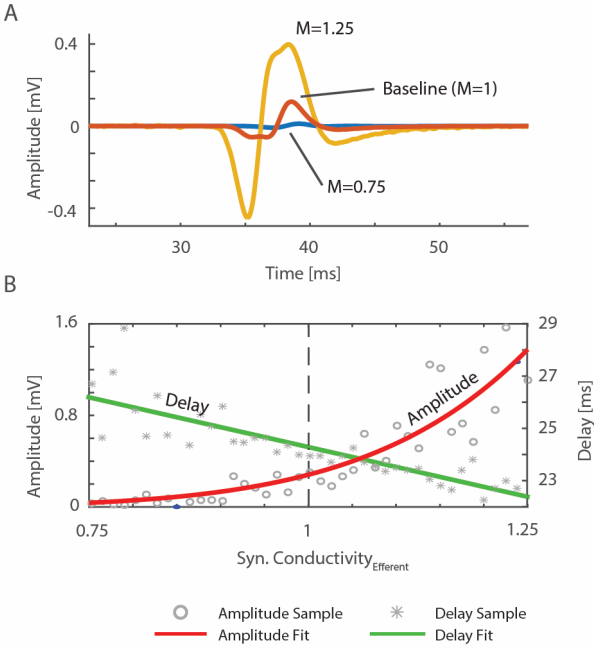

Figure 9: Simulated motor evoked potentials (MEP) for decreasing and increasing efferent synaptic conductivity ($M = M_{efferent} =$ 1, 0.75 and 1.25) (A). Individual values for MEP amplitude and delay as well as the estimated regression function for both variables, with varying $M_{efferent}$ (B).

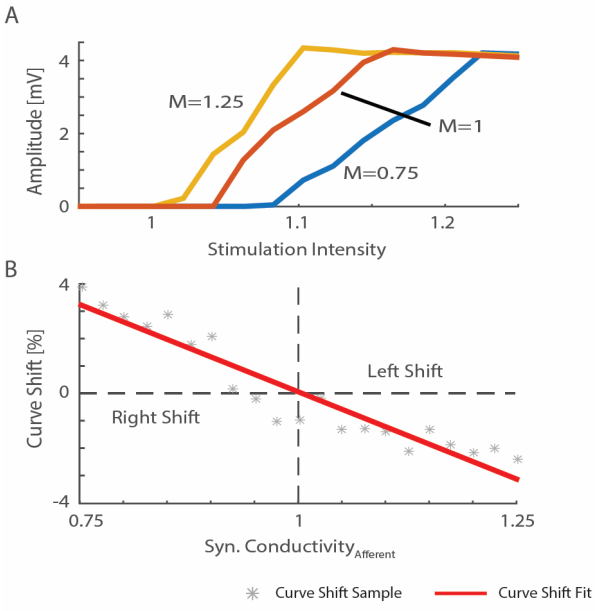

Figure 10: Simulated H-Reflex recruitment curve for varying afferent synaptic conductivity gains ($M = M_{afferent}$) (A) and the left/right shift induced by varying $M_{afferent}$ expressed as a percentage of stimulation intensity (B).

opposite effects. This is illustrated in figure 9B, which shows both EMG amplitude and delay as a function of $M_{efferent}$. Signal delay and $M_{efferent}$ followed a linear relationship, whereas the changes in amplitude were fit to an exponential of the form ax^b. For $M_{synapse} = M_{efferent,acute}$ the resulting changes in amplitude and delay were 0.0102 % and -0.0109 ms respectively.

The simulated H-reflex recruitment curves and a linear estimation of the resulting curve shift for varying $M_{afferent}$ are illustrated in figure 10. Thereby increasing/decreasing $M_{afferent}$ induces a clear left/right shift of the H-Reflex recruitment curve. This is visible in fig. 10A, which illustrates sampled recruitment curves with $M_{afferent}$ equal to 0.75, 1 and 1.25 respectively. Fig. 10B quantifies the change. For $M_{synapse} = M_{afferent,acute}$ the resulting right shift is 0.14 %.

2.4 Discussion

The goal of our work was to get a better understanding of the effects generated by lumbar trans-spinal DC stimulation. This included an understanding of the electric field strength, the resulting membrane polarization in spinal motoneurons and the axon terminals of its main incoming connections. Furthermore, we asked whether a distinct cellular target was present and the kind of acute effects this would result in. A final question was, how important a precise placement of the active electrode is at the motoneuron level and what consequences misplacement would result in.

2.4.1 Electric Field Distribution

We simulated the electric field in the spinal cord for three different electrode configurations. For all three configurations the maximum EF amplitude inside the spinal cord, typically about midway between active and return electrode, ranged from 1.29 V/m to 2.73 V/m. This is in the same

range as previously reported by Parazzini et al. (0.81 V/m to 4.97 V/m, at a 3 mA current) for tsDCS [14] as well as field strengths estimated for tDCS (0.15 mV/mm [17], 0.22 mV/mm [52]). From other studies it can be concluded, that the estimated EF magnitude is also sufficient to theoretically elicit lasting plasticity effects under the correct experimental conditions. Fritsch and co-workers thereby used a field strength of ~0.75 mV/mm to induce steadily increasing synaptic plasticity effects over a period of 60 minutes in slices from mouse primary motor cortex in vitro [22]. Furthermore, stimulation safety has to be considered. With an EF magnitude of 2.73 mV/mm, a current density of 0.07371 mA/cm² is reached in the spinal white matter. Due to the differences in conductivity, values in the gray matter are ~10 times lower than that. The values obtained here are therefore more than a hundred-fold lower than the safety limits for tissue damage reported in literature [53–55]. We further note that the EF distribution reveals a spatial pattern of cyclic in- and decrease, caused by vertebral body interference with the electric field. In locations where the EF is generally small, this may lead to an additional unexpected decrease in magnitude, which might influence the intervention outcome.

2.4.2 Cellular Target and Agreement with Functional Morphology

We further analyzed the acute polarization effects on six realistic spinal motoneuron models. On the search for a possible cellular target, we followed the assumption that the level of local membrane polarization is directly related to the resulting functional modulation. We found that the largest polarization effects were to be expected at the axon terminals, with little to negligible polarization at the proximal dendrites and soma (fig. 7). This is consistent over all six tested motoneuron models. We therefore conclude, that axon terminals are likely the most dominant cellular target in lumbar spinal DCS.

Somatic polarization is thought to be able to directly influence the generation of action potentials, which takes place close to the axon hillock. However due to the central location of the soma, with dendrites extending radially in all directions, the soma is not polarized. Therefore, a direct influence on action potential generation is unlikely.

Dendrite polarization is a second source for possible functional modulation, since they are the primary location for both, incoming synaptic terminals and channels mediating persistent inward currents. However, the dendritic membrane polarization found here is low (< 0.17 mV). We therefore conclude that dendritic polarization is unable to contribute to the functional modulation effects observed after tsDCS. This is supported by the lack of functional organization that seems to underlie dendritic and synaptic morphology. Nonetheless, in a modeling study Elbasiouny and Mushahwar have previously shown that the effect of an imposed EF on neural firing and PIC behavior is not directly proportional to the induced polarization. Whereas dendrite depolarization led to a decrease, hyperpolarization did not lead to a drastic change in persistent inward current [38]. This implies that dendrite polarization, regardless of EF orientation, is still able to lead to a depression of motoneuron function. However, due to low dendritic membrane polarization found by us, these mechanisms will likely have a relatively small impact compared to the effects induced by axon terminal polarization.

The largest polarization effect occurred at the terminals of incoming axonal connections with maxima ranging from 0.35 mV to 2.89 mV. This is several orders of magnitude larger than the

polarization values found for other neuronal structures. The correlation of direction and function for incoming axonal fibers [32], the dominance of axon terminal polarization (fig. 7) and the lack of functional organization within synaptic/PIC channels on the cellular membrane therefore implicate axon terminals to be the most likely cellular target in lumbar spinal DCS. This conclusion is backed by previous studies which provide strong evidence that the modulatory effect caused by DC stimulation is indeed dependent on axonal orientation with respect to the applied EF [28].

2.4.3 Electric Field Distribution and Polarization for Misplacements

Finding the correct vertebrae can sometimes be difficult, depending on subject anatomy. Therefore, we investigated how sensitive the EF distribution is to electrode misplacements. The results suggest that a longitudinal offset of 5 cm (ca. 1.5 vertebrae lengths) is sufficient to substantially alter EF magnitude direction and amplitude at the intended stimulation site. This is evident from figs. 5 and 7, showing that an upward/downward electrode misplacement may even reverse axon terminal polarization. When considering the curvature of the electric field, misplacements especially in cases where the stimulation site is close to the electrode may therefore have a large effect on axon terminal polarization due to the resulting change in EF direction. Therefore, electrode misplacement may be an important source of the variability experimentally observed in response to tsDCS.

2.4.4 From Cellular to Network Effects

Several studies have previously investigated the effects of tsDCS on neural function. To bridge theoretical data on a cellular level, to experimental data on a functional level is challenging. We therefore included an intermediate step, comprising of a lumbar spinal network model [39]. The characteristic effects obtained for both, simulated MEP and H-Reflex responses are in accordance with what has been shown in previous studies [5,7,8]. While changing efferent synaptic conductivity results in a modulation of the simulated MEP amplitude and latency, altering afferent synaptic conductivity leads to a well-defined left/right shift of the H-Reflex recruitment curve (fig. 10). However, the estimated acute changes in amplitude for both scenarios are much smaller than the long-term changes induced by tsDCS as reported in literature.

2.4.5 Comparison between simulated acute and reported long term effects

So far, we showed that axon terminals may be the likely main cellular target for tsDCS. The acute synaptic effects of axon terminal polarization are known from literature [18,29,30]. Additionally, we showed that synaptic conductivity changes on a network level, result in the same type of functional effects as the long-term effects reported by several previous tsDCS studies. It is therefore of special interest, how axon terminal polarization - in connection with its theoretical acute synaptic conductivity effect and the simulated spinal network responses - can be connected to the effects reported experimentally by others. In the following, we therefore individually compare the experimental results obtained by others to the simulations reported here.

Anodal tsDCS can result in a significant left shift of the H-Reflex recruitment curve [7,8]. Cathodal stimulation had no significant effect. For anodal tsDCS, afferent ATs are depolarized (fig. 8A), acutely decreasing synaptic conductivity. However, network simulations imply an increasing afferent synaptic gain to replicate the effect observed experimentally (H-Reflex left shift). Acute synaptic terminal and long-term plasticity effects are therefore in opposite directions.

Bocci et al. showed an increase/decrease in motor evoked potential area for cathodal/anodal tsDCS. Modulation of MEP area can theoretically be achieved by altering motoneuron recruitment [5]. The efferent axon terminal is depolarized/hyperpolarized for cathodal/anodal stimulation (fig. 8), leading to a theoretical increase/decrease of synaptic conductivity. Network simulation indicates a larger motoneuron response for increased synaptic conductivity and vice versa. Therefore, the simulated acute synaptic changes for both polarities are in opposite direction to the experimental results reported by Bocci et al. Winkler et al. found an increase/decrease of post activation depression (PAD) of the H-Reflex after cathodal and anodal tsDCS respectively [9]. PAD, is a reduction of synaptic efficacy due to decreased neurotransmitter release at a previous activated Ia fiber-motoneuron synapse [56] and has not been shown to be susceptible to supraspinal influences [9]. For anodal/cathodal tsDCS the afferent axon terminal is depolarized/hyperpolarized, leading to an acute suppression/strengthening of afferent synaptic conductivity. Thus, the reported experimental effects are again opposite to the acute synaptic effects estimated here. Yamaguchi et al. showed a decrease in presynaptic inhibition of Ia afferents (D1 inhibition) for anodal tsDCS. Since D1 inhibition is mediated by descending pathways via inhibitory presynaptic connections [57], effects on the efferent pathway have to be considered. For anodal tsDCS, the efferent axon terminal is hyperpolarized, leading to an acute synaptic facilitation. This stands in contrast to the depression effects reported in literature.

For all discussed human studies, we therefore note a long-term plasticity effect in opposite direction to the acute synaptic changes estimated here. A reversal of acute and after effect has previously been observed by others. For instance, a study by Ahmed [13] showed a suppression, during and potentiation, after DCS of cortically evoked potentials for anodal tsDCS in mice. Switching polarities reversed the effect. Inversion of effects during versus after DCS is therefore possible. Nonetheless, the underlying mechanisms connecting acute and longer-term plasticity effects remain elusive and need to be well understood for rational applications of DCS in clinical practice.

2.4.6 Practical Implications on Intervention Design

We estimated the EF strength at MN level for several configurations. The EFs appeared similar to those reported in previous studies in vitro [22], which showed significant modulatory effects on a cellular level. Thus, for any of the simulated electrode placements the EF is theoretically large enough for functional modulation, given the appropriate neural target structure and neural activity. However accurately estimating the applied electric field as we did, is vital since EF direction and amplitude are equally important and intervention designs solely based on EF magnitude may potentially lead to suboptimal results in application. This is especially evident when considering the effects of electrode misplacements on axon terminal polarization (fig. 7). Thereby, misplacement of 5 cm may lead to a change in electric field direction and thus result in a reversal of AT polarization. This implies that interventions should be designed such that for small misplacements, influence on EF vector angle is kept minimal, which can be achieved by either focusing on proper electrode placement or actively misplacing the electrode in a direction for which misplacement in the opposite direction would not lead to reversal of EF direction at the intended stimulation target. Additionally, vertebral bodies may lead to fluctuations of EF

magnitude. This could further be taken into account by placing the electrodes such that EF fluctuations are small with respect to the overall EF amplitude.

We identified axon terminals to be the most dominant cellular target. It may therefore be possible to modulate individual functional pathways, under the condition that both pathways are oriented in a specific, no-random direction at different angles towards each other, optimally approaching 90 degrees. This may to some degree be applicable to the descending and sensory fibers in the lumbar spinal cord such that pathway specific modulation may be feasible.

2.4.7 Limitations

We use a realistic full body, segmented, MRI model for computation of the electric field after tsDCS stimulation. However, though being a realistic anatomical representation, the model is subject specific. Thus, the results presented here are not quantitatively generalizable across subjects. Nonetheless, we expect that generalization over subjects is principally possible once knowing the individualized anatomical details.

We used realistic reconstructions of motoneurons originally obtained from cats, which may limit generalization to human subjects. However, although quantitative differences may occur we believe the models nonetheless provide a reasonable basis for the intended logical reasoning. Furthermore, we represent incoming axon terminals with a straight cylindrical compartmental model. We expect this approximation to hold for the average of all incoming axon terminals. However, in a realistic scenario, incoming axons branch out, forming a tree-like structure of axon terminals to form connections with local dendrites. Therefore, axon terminal polarization will likely be distributed within a range centered around the values similar to those estimated here.

2.5 Conclusion

We show that the tsDCS induced electric field strengths at spinal motoneuron level is similar to those that have been described for tDCS in the cortex. Furthermore, similar EF amplitudes have previously been used in vivo and vitro to evoke significant modulation in the underlying neural structures. We therefore conclude that the tsDCS generated EF in the spinal cord is of sufficient strength to evoke functional modulation. Also, axon terminal polarization is expected to be the primary cellular target, inducing the modulatory effects observed after lumbar tsDCS. However, the expected acute synaptic efficacy changes are in opposite direction to the long-term plasticity effects reported in literature. This emphasizes the need for a deeper understanding of the mechanisms involved in the transition from acute to long-term plasticity effects. Furthermore, we show that correct electrode placement is crucial for the success of the application. Possible pitfalls such as incorrect EF alignment due to electrode misplacement should be taken into consideration in the design of electrotherapeutic interventions. This may lead to better methods for predicting the outcome of tsDCS.

2.6 Acknowledgements

This research was supported by ZonMw (Grand Nr. 10-10400-98-008) as part of the NeuroControl - Assessment and Stimulation (NeurAS) consortium. We are thankful to our colleagues Herman van der Kooij and Jan Buitenweg who provided expertise that greatly assisted our research.

References

[1] Cogiamanian F, Ardolino G, Vergari M, Ferrucci R, Ciocca M, Scelzo E, Barbieri S and Priori A 2012 Transcutaneous Spinal Direct Current Stimulation *Front. Psychiatry* **3**

[2] Harkema S, Gerasimenko Y, Hodes J, Burdick J, Angeli C, Chen Y, Ferreira C, Willhite A, Rejc E, Grossman R G and Edgerton V R 2011 Effect of epidural stimulation of the lumbosacral spinal cord on voluntary movement, standing, and assisted stepping after motor complete paraplegia: a case study. *Lancet* **377** 1938–47

[3] Alam M, Garcia-Alias G, Jin B, Keyes J, Zhong H, Roy R R, Gerasimenko Y, Lu D C and Edgerton V R 2017 Electrical neuromodulation of the cervical spinal cord facilitates forelimb skilled function recovery in spinal cord injured rats *Exp. Neurol.* **291** 141–50

[4] Wenger N, Moraud E M, Gandar J, Musienko P, Capogrosso M, Baud L, Le Goff C G, Barraud Q, Pavlova N, Dominici N, Minev I R, Asboth L, Hirsch A, Duis S, Kreider J, Mortera A, Haverbeck O, Kraus S, Schmitz F, DiGiovanna J, van den Brand R, Bloch J, Detemple P, Lacour S P, Bézard E, Micera S and Courtine G 2016 Spatiotemporal neuromodulation therapies engaging muscle synergies improve motor control after spinal cord injury *Nat. Med.* **22** 138–45

[5] Bocci T, Vannini B, Torzini A, Mazzatenta A, Vergari M, Cogiamanian F, Priori A and Sartucci F 2014 Cathodal transcutaneous spinal direct current stimulation (tsDCS) improves motor unit recruitment in healthy subjects *Neurosci. Lett.* **578** 75–9

[6] Cogiamanian F, Vergari M, Pulecchi F, Marceglia S and Priori A 2008 Effect of spinal transcutaneous direct current stimulation on somatosensory evoked potentials in humans. *Clin. Neurophysiol.* **119** 2636–40

[7] Lamy J-C, Ho C, Badel A, Arrigo R T and Boakye M 2012 Modulation of soleus H reflex by spinal DC stimulation in humans. *J. Neurophysiol.* **108** 906–14

[8] Hubli M, Dietz V, Schrafl-Altermatt M and Bolliger M 2013 Modulation of spinal neuronal excitability by spinal direct currents and locomotion after spinal cord injury. *Clin. Neurophysiol.* **124** 1187–95

[9] Winkler T, Hering P and Straube a. 2010 Spinal DC stimulation in humans modulates post-activation depression of the H-reflex depending on current polarity *Clin. Neurophysiol.* **121** 957–61

[10] Yamaguchi T, Fujimoto S, Otaka Y and Tanaka S 2013 Effects of transcutaneous spinal DC stimulation on plasticity of the spinal circuits and corticospinal tracts in humans *2013 6th Int. IEEE/EMBS Conf. Neural Eng.* 275–8

[11] Ahmed Z 2013 Effects of Cathodal Trans-Spinal Direct Current Stimulation on Mouse Spinal Network and Complex Multijoint Movements *J. Neurosci.* **33** 14949–57

[12] Ahmed Z 2013 Electrophysiological characterization of spino-sciatic and cortico-sciatic associative plasticity: modulation by trans-spinal direct current and effects on recovery after spinal cord injury in mice. *J. Neurosci.* **33** 4935–46

[13] Ahmed Z 2011 Trans-spinal direct current stimulation modulates motor cortex-induced muscle contraction in mice. *J. Appl. Physiol.* **110** 1414–24

[14] Parazzini M, Fiocchi S, Liorni I, Rossi E, Cogiamanian F, Vergari M, Priori A and Ravazzani P 2014 Modeling the current density generated by transcutaneous spinal direct current stimulation (tsDCS). *Clin. Neurophysiol.*

[15] Datta A, Bansal V, Diaz J, Patel J, Reato D and Bikson M 2009 Gyri-precise head model of transcranial direct current stimulation: Improved spatial focality using a ring electrode versus conventional rectangular pad *Brain Stimul.* **2**

[16] Salvador R, Mekonnen A, Ruffini G and Miranda P C 2010 Modeling the electric field induced in a high resolution realistic head model during transcranial current stimulation. *Conf. Proc. IEEE Eng. Med. Biol. Soc.* **2010** 2073–6

[17] Rampersad S M, Janssen A M, Lucka F, Aydin Ü, Lanfer B, Lew S, Wolters C H, Stegeman D F and Oostendorp T F 2014 Simulating transcranial direct current stimulation with a detailed anisotropic human head model. *IEEE Trans. Neural Syst. Rehabil. Eng.* **22** 441–52

[18] Rahman A, Reato D, Arlotti M, Gasca F, Datta A, Parra L C and Bikson M 2013 Cellular effects of acute direct current stimulation: somatic and synaptic terminal effects. *J. Physiol.* **591** 2563–78

[19] Bindman L J, Lippold O C and Redfearn J W 1964 the Action of Brief Polarizing Currents on the Cerebral Cortex of the Rat (1) During Current Flow and (2) in the Production of Long-Lasting After-Effects. *J. Physiol.* **172** 369–82

[20] Gartside I B 1968 Mechanisms of sustained increases of firing rate of neurons in the rat cerebral cortex after polarization: reverberating circuits or modification of synaptic conductance? *Nature* **220** 382–3

[21] Ranieri F, Podda M V, Riccardi E, Frisullo G, Dileone M, Profice P, Pilato F, Di Lazzaro V and Grassi C 2012 Modulation of LTP at rat hippocampal CA3-CA1 synapses by direct current stimulation. *J. Neurophysiol.* **107** 1868–80

[22] Fritsch B, Reis J, Martinowich K, Schambra H M, Ji Y, Cohen L G and Lu B 2010 Direct current stimulation promotes BDNF-dependent synaptic plasticity: Potential implications for motor learning *Neuron* **66** 198–204

[23] Lamy J-C and Boakye M 2013 BDNF Val66Met polymorphism alters spinal DC stimulation-induced plasticity in humans. *J. Neurophysiol.* **110** 109–16

[24] Jefferys J G 1981 Influence of electric fields on the excitability of granule cells in guinea-pig hippocampal slices. *J. Physiol.* **319** 143–52

[25] Bikson M, Inoue M, Akiyama H, Deans J K, Fox J E, Miyakawa H and Jefferys J G R 2004 Effects of uniform extracellular DC electric fields on excitability in rat hippocampal slices in vitro. *J. Physiol.* **557** 175–90

[26] Radman T, Ramos R L, Brumberg J C and Bikson M 2009 Role of cortical cell type and morphology in subthreshold and suprathreshold uniform electric field stimulation in vitro *Brain Stimul.* **2**215–228.e3

[27] Arlotti M, Rahman A, Minhas P and Bikson M 2012 Axon terminal polarization induced by weak uniform DC electric fields: a modeling study. *Conf. Proc. IEEE Eng. Med. Biol. Soc.* **2012** 4575–8

[28] Kabakov a. Y, Muller P a., Pascual-Leone a., Jensen F E and Rotenberg a. 2012 Contribution of axonal orientation to pathway-dependent modulation of excitatory transmission by direct current stimulation in isolated rat hippocampus *J. Neurophysiol.* **107** 1881–9

[29] Hubbard J I and Willis W D 1962 Hyperpolarization of Mammalian Motor Nerve Terminals *J. Physiol.* **163** 115–37

[30] Hubbard J I and Willis W D 1968 The Effects of Depolarization of Motor Nerve Terminals upon the Release of Transmitter by Nerve Impulses *J. Physiol.* **194** 381–405

[31] Bikson M and Rahman A 2013 Origins of specificity during tDCS: anatomical, activity-selective, and input-bias mechanisms. *Front. Hum. Neurosci.* **7** 688

[32] Burke R E and Glenn L L 1996 Horseradish peroxidase study of the spatial and electrotonic distribution of group Ia synapses on type-identified ankle extensor motoneurons in the cat *J. Comp. Neurol.* **372** 465–85

[33] Burke B R E 1968 Group Ia synaptic input to fast and slow twitch motor units of cat triceps surae. *J. Physiol.* 605–30

[34] Segev I, Fleshman J W and Burke R E 1990 Computer simulation of group Ia EPSPs using morphologically realistic models of cat alpha-motoneurons *J. Neurophysiol.* **64** 648–60

[35] Rotterman T M, Nardelli P, Cope T C and Alvarez F J 2014 Normal distribution of VGLUT1 synapses on spinal motoneuron dendrites and their reorganization after nerve injury. *J. Neurosci.* **34** 3475–92

[36] Heckman C J, Johnson M, Mottram C and Schuster J 2008 Persistent inward currents in spinal motoneurons and their influence on human motoneuron firing patterns *Neuroscientist* **14** 264–75

[37] Powers R K, ElBasiouny S M, Rymer W Z and Heckman C J 2012 Contribution of intrinsic properties and synaptic inputs to motoneuron discharge patterns: a simulation study *J. Neurophysiol.* **107** 808–23

[38] Elbasiouny S M and Mushahwar V K 2007 Suppressing the excitability of spinal motoneurons by extracellularly applied electrical fields: insights from computer simulations. *J. Appl. Physiol.* **103** 1824–36

[39] Cisi R R L and Kohn A F 2008 Simulation system of spinal cord motor nuclei and associated nerves and muscles, in a Web-based architecture. *J. Comput. Neurosci.* **25** 520–42

[40] SCI Institute 2015 SCIRun: A Scientific Computing Problem Solving Environment, Scientific Computing and Imaging Institute (SCI), Download from: http://www.scirun.org

[41] Christ A, Kainz W, Hahn E G, Honegger K, Zefferer M, Neufeld E, Rascher W, Janka R, Bautz W, Chen J, Kiefer B, Schmitt P, Hollenbach H-P, Shen J, Oberle M, Szczerba D, Kam A, Guag J W and Kuster N 2010 The Virtual Family--development of surface-based anatomical models of two adults and two children for dosimetric simulations. *Phys. Med. Biol.* **55** N23–38

[42] Miranda P C 2013 Chapter 29 - Physics of effects of transcranial brain stimulation *Brain Stimulation* Handbook of Clinical Neurology vol 116, ed A M Lozano and M Hallett (Elsevier) pp 353–66

[43] Alvarez F J, Pearson J C, Harrington D, Dewey D, Torbeck L and Fyffe R E 1998 Distribution of 5-hydroxytryptamine-immunoreactive boutons on alpha-motoneurons in the lumbar spinal cord of adult cats. *J. Comp. Neurol.* **393** 69–83

[44] Balbi P, Martinoia S and Massobrio P 2015 Axon-somatic back-propagation in detailed models of spinal alpha motoneurons. *Front. Comput. Neurosci.* **9** 15

[45] Carnevale N T and Hines M L 2006 *The NEURON Book* vol 30

[46] Boron W F and Boulpaep E L 2016 *Medical Physiology* (Elsevier)

[47] Hall J E and Guyton A C 2006 *Textbook of Medical Physiology*

[48] Patestas M and Gartner L P 2006 A Textbook of Neuroanatomy *A Textb. Neuroanat.* 454

[49] Midroni G and Bilbao J M 1995 CHAPTER 3 - Quantitative Techniques BT - Biopsy Diagnosis of Peripheral Neuropathy (Butterworth-Heinemann) pp 35–43

[50] Di Lazzaro V [1], Oliviero A [2], Pilato F [2], Mazzone P [3], Insola A [4], Ranieri F [2] and Tonali P A [5. 2003 Corticospinal volleys evoked by transcranial stimulation of the brain in conscious humans *Neurol. Res.* **25** 143–50

[51] Bagwell C B 2005 HyperLog - A flexible log-like transform for negative, zero, and positive valued data *Cytom. Part A* **64** 34–42

[52] Miranda P C, Lomarev M and Hallett M 2006 Modeling the current distribution during transcranial direct current stimulation *Clin. Neurophysiol.* **117** 1623–9

[53] Bikson M, Datta A and Elwassif M 2009 Establishing safety limits for transcranial direct current stimulation *Clin. Neurophysiol.* **120** 1033–4

[54] Nitsche M A, Liebetanz D, Lang N, Antal A, Tergau F and Paulus W 2013 Safety criteria for transcranial direct current stimulation (tDCS) in humans. *Clin. Neurophysiol.* **133** 285

[55] Liebetanz D, Koch R, Mayenfels S, König F, Paulus W and Nitsche M A 2009 Safety limits of cathodal transcranial direct current stimulation in rats *Clin. Neurophysiol.* **120** 1161–7

[56] Grey M J, Klinge K, Crone C, Lorentzen J, Biering-Sørensen F, Ravnborg M and Nielsen J B 2008 Post-activation depression of Soleus stretch reflexes in healthy and spastic humans *Exp. Brain Res.* **185** 189–97

[57] Rudomin P 2009 In search of lost presynaptic inhibition *Exp. Brain Res.* **196** 139–51

Chapter III – Changes in H- Reflex Recruitment after trans-Spinal Direct Current Stimulation with Multiple Electrode Configurations

A. KUCK [1], D.F. STEGEMAN[2], H. VAN DER KOOIJ[1,3] and E.H.F. VAN ASSELDONK[1]

[1] Laboratory of Biomechanical Engineering, Department of Engineering Technology, University of Twente, Drienerlolaan 5, 7522 NB Enschede, The Netherlands

[2] Radboud University Medical Center, Donders Institute for Brain, Cognition and Behavior, Department of Neurology/Clinical Neurophysiology, Reinier Postlaan 4, 6500HB Nijmegen, The Netherlands

[3] Department of Biomechanical Engineering, Faculty of Mechanical, Maritime and Materials Engineering, Delft University of Technology, Mekelweg 2, Delft, 2628CD, Netherlands

Abstract

Trans-spinal direct current stimulation (tsDCS) is an electro-modulatory tool with possible application in the rehabilitation of spinal cord injury. TsDCS generates a small electric field, aiming to induce lasting, functional neuromodulation in the targeted neuronal networks. Earlier studies have shown significant modulatory effects after application of lumbar tsDCS. However, for clinical application, a better understanding of application specific factors is required. Our goal was to investigate the effect of different electrode configurations using lumbar spinal tsDCS on spinal excitability. We applied tsDCS (2.5 mA, 15 minutes) in 10 healthy subjects with three different electrode configurations: 1) Anode and cathode placed over vertebra T11, and the posterior left shoulder respectively (LSC-S) (one polarity), and 2) Both electrodes placed in equal distance (ED) (7cm) above and below vertebra T11, investigated for two polarities (ED-Anodal)/Cathodal). The soleus H-Reflex is measured before, during and after tsDCS in either electrode configuration or a sham condition. To account for genetic predispositions in response to direct current stimulation, subject BDNF genotype was assessed. Stimulation in configuration ED-Cathodal induced an amplitude reduction of the H-reflex, 30 minutes after tsDCS with respect to baseline, whereas none of the other configurations led to significant post intervention effects. BDNF genotype did not correlate with post intervention effects. Furthermore, we failed to replicate effects shown by a previous study, which highlights the need for a better understanding of methodological and subject specific influences on tsDCS outcome. The H-reflex depression after tsDCS (Config. ED-Cathodal) provides new insights and may foster our understanding of the working mechanism of tsDCS.

3.1 Introduction

The targeted application of electrotherapy to the rehabilitation of nervous system disorders has been a lasting vision in rehabilitation research. In recent years, trans-spinal direct current stimulation (tsDCS), a variant of transcranial Direct Current Stimulation (tDCS), has received an increasing scientific interest as a proposed novel electrotherapeutic protocol. Aiming to modulate pathways in the Spinal Cord, tsDCS imposes a small electric field (EF) to the spinal neural circuitry. The ultimate goal is the ability to facilitate spinal plasticity and promote rehabilitation after neural

injury of the spinal cord, via a meaningful and targeted application of tsDCS, in combination with established rehabilitation techniques.

Earlier research on the neural effects of DC stimulation, which originates mainly from studies on direct current stimulation of the cortex, has revealed a collection of multiple neural working mechanisms [1–3] depending on electric field magnitude and direction [4–6], the underlying neuroanatomy and its alignment with the imposed EF [7–10] as well as the ongoing neural activity [3,11–13] and genetic predispositions [3,14,15].

Consequently, previous studies which have applied tsDC-stimulation on the lumbar spinal cord, also revealed a complex picture of its effects on the spinal motor circuitry (for a thorough overview, see: [16]). It has been shown, that anodal tsDCS can lead to a significant increase [17], or more specifically, a left shift of the H-reflex recruitment curve [18], whereas cathodal stimulation had no significant effect. Also, cathodal and anodal tsDCS, were able to up- and downregulate cortically evoked motor evoked potentials (MEPs) at lumbar spinal level respectively [19]. Furthermore, it was shown that lumbar tsDCS has a significant modulatory effect on spinal reflex presynaptic inhibition [20] and post-activation depression [21]. As for tDCS, also in tsDCS genetic factors have been implicated to have an effect on the outcome of DC stimulation protocols [14]. In particular, a polymorphism (*Val66Met*) of Brain-derived Neurotropic Factor (*BDNF*), has been of particular interest. Thereby, Lamy and Boakye showed that the H-reflex recruitment curve modulation after tsDCS significantly differs in carriers and non-carriers of the BDNF Met allele [15].

For a successful application of tsDCS in a clinical setting, a better understanding of its application specific effects is needed. This includes knowledge about proper electrode placement, the resulting electric field at the target region and its effects on the targeted neural circuitry. Based on studies simulating the electric field generated by transcutaneous DC stimulation, the EF-vector for a pair of surface electrodes is expected to be largest and tangential to the skin – surface about half-way between electrodes. Below the electrodes the EF vector will be comparably lower and perpendicular to the skin-surface [22]. Given that the neural effect of DC stimulation is dependent on EF strength and direction, the modulatory outcomes are expected to vary across tsDCS protocols employing different electrode configurations. However, since all previous studies utilized a similar electrode configuration (passive electrode on the shoulder, active electrode above the lumbar spinal cord), current knowledge does not allow conclusions about electrode placement specific effects of tsDCS.

In this study, our goal was therefore to investigate the effect of tsDCS on the soleus H-reflex with three electrode configurations (fig. 1). We compared the commonly used electrode configuration to a new bipolar electrode placement, with both electrodes placed in equal distance, above and below the lumbar spinal cord. We measured the soleus H-Reflex before, during and after tsDCS with both configurations and a sham condition. The commonly used placement was tested in anodal configuration only, which had previously shown to be effective in modulating the soleus H-Reflex [17,18]. To probe for polarity specific effects, for the new electrode placement both anodal and cathodal configuration were investigated. We were primarily interested in the changes in H-Reflex amplitude post-tsDCS with respect to baseline. Additionally, we tested for a

relationship between the amplitude changes during- compared to those after tsDCS. To take into account the possible differences in tsDCS modulatory response for BDNF met allele carriers [15], we assessed BDNF genotype in all subjects.

3.2 Methods

3.2.1 Subjects

We included 10 healthy volunteers with a mean age of 23 (range: 20 to 29) years. All participants gave their written informed consent before data collection and the study protocol was approved by the local ethics committee of Twente (Enschede, The Netherlands).

3.2.2 tsDCS

As announced, tsDCS was applied in two different electrode placement configurations (fig. 1). The amplitude was 2.5 mA and the duration 15 minutes using a NeuroConn DC-Stimulator PLUS (neuroCare Group GmbH, Munich, Germany). The electrode configurations chosen were: LSC-S: Lumbar Spinal Cord (T11)- left posterior Shoulder (fig. 1A) and ED: Equal Distance 7 cm above and below T11 (Lumbar Spinal Cord) (fig. 1B). LSC-S was applied in anodal configuration only, whereas for configuration ED the effect of both polarities was investigated. We refer to the polarity of the lower electrode for configuration naming for all configurations (e.g. ED-A and ED-C). Vertebra T11 was determined via manual palpation of the spinal processes, staring at vertebra C7 and counting until vertebra T11 was reached. This process was repeated three times, with the final position estimate determined by taking the mean of the three initial estimates. Sham stimulation, included in the utilized stimulation device, was achieved by applying a 110 μA pulse with a pulse-width of 3 ms and an interval of 550 ms for a duration of 15 minutes.

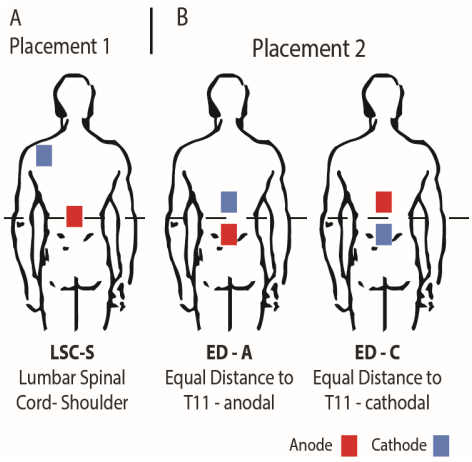

Figure 1: Illustration of the electrode placement configurations investigated. From left to right: A) The traditionally used placement with one anodal electrode centered on the lumbar spinal cord and a return electrode placed on the left posterior shoulder (LSC-S). B) Both electrodes placed in equal distance to the lumbar spinal cord, for opposite polarities.

3.2.3 H-reflex measurement

To determine the changes induced to the H-reflex by tsDCS in one of the three configurations, we chose to characterize the H-reflex recruitment curve at four characteristic points (fig. 2): H-Reflex threshold (H_{Thresh}), 50% of H-reflex maximum ($H_{max50\%}$), the point at which the ascending part of the recruitment curve begins to settle (H_{Settle}) as well as the maximum H-wave (H_{max}). These points were chosen for their ability: 1) to reflect the anticipated changes of the H-

reflex recruitment curve (left/right shift, based on [18]), or overall amplitude modulation, as well as 2) to sufficiently approximate the ascending part of the recruitment curve. The points were determined from a detailed H-reflex recruitment curve, recorded at the start of each experiment. The recruitment curve was sampled at stimulation intervals I (see: Experimental Protocol). Thereby, M_{max}, H_{max} and H_{Thresh} were determined manually, with H_{max} defined as the peak value of the average H-wave recruitment curve and M_{max} the amplitude immediately after peak settling amplitude of the M-wave recruitment curve. H_{Thresh} was defined as the first visible H-Wave, in response to a stimulus. H_{Settle} and $H_{max50\%}$ were determined via fitting of a sigmoid function $f(s)$ to the recorded recruitment curve: $f(s) = H_{max}/(1 + e^{-m(s-S_{max50\%})})$. Thereby, m is the function slope at $f(S_{max50\%})$, $S_{max50\%}$ the stimulus needed to evoke 50% of H_{max}, H_{max} the maximum value of the recruitment curve and s_{max} the corresponding stimulation amplitude. $H_{max50\%}$ and H_{Settle} are then defined as $f(s_{max50\%})$ and $f(s_{Settle})$ respectively, given $f''(s_{Settle}) = \min(f''(s))$. For each point, the closest multiple of I was chosen as a stimulation amplitude.

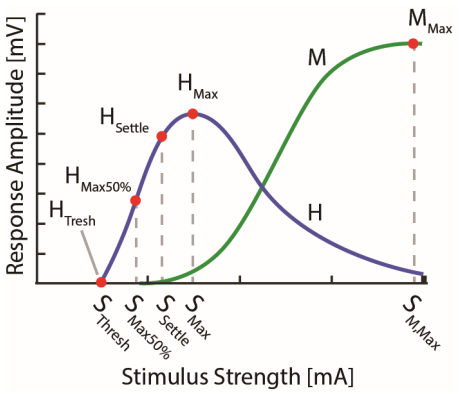

Figure 2: Overview of the distinct points measured within the H- and M- Wave recruitment curves: H-Reflex threshold (H_{Thresh}), 50% of H-reflex maximum ($H_{max50\%}$), the point at which the ascending part of the recruitment curve begins to settle (H_{Settle}), the maximum H wave (H_{max}) as well as the maximum M-wave (M_{max}).

3.2.4 EMG measurement

Bipolar, EMG was recorded using a TMSi Porti amplifier (TMSi, Oldenzaal, NL) from the belly of the right lateral soleus muscle with electrode centers placed approximately 3 cm apart, 4 cm below the initiation of the gastrocnemius tendon. The sampling frequency was set to 2048 samples/s.

3.2.5 Tibial nerve stimulation

H-Reflex responses were evoked using electrical stimulation of the tibial nerve (Micromed Matrix Light, Micromed S.p.A., Mogliano Veneto, Italy). Adhesive active-cathodal (1.5 × 1.5cm) and return -anodal (5 × 5 cm) electrodes were placed over the tibial nerve in the popliteal fossa and above the patella respectively. The stimulation consisted of a biphasic pulse with a pulse width of 0.5 ms and stimulation amplitudes ranging from 0 mA to 80 mA.

3.2.6 BDNF genotyping

Saliva samples were collected (Oragene Dx, DNA Genotek Inc., Ottawa, Canada) from each subject. Subsequently all samples were analyzed to detect the BDNF Val66Met polymorphism using Taqman (rs6265). Additionally, BDNF concentration and sample purity (260/280) were detected.

3.2.7 Experimental protocol

The experiment was set up in a randomized double-blind placebo controlled design, whereby both experimenter and subject were blinded with respect to the intervention type (real or sham). Interventions consisted of the three stimulation configurations and one sham stimulation. For each intervention, an individual experiment was performed in a randomized order with experiments planned with an interval of at least seven days. The configuration by which sham was performed was randomized across subjects.

Subjects were instructed to avoid drinking coffee or consume other stimulants on the day of the experiment. Preparatory steps before attachment of EMG and tibial nerve stimulation electrodes included skin disinfection with alcohol, shaving and exfoliating of the desired skin section. With the subject lying on a medical bench in a prone position, EMG electrodes and nerve stimulation counter electrode in place, a handheld stimulation probe was used to determine the optimal position to stimulate the tibial nerve. Indicators for an appropriate stimulation position were a clear EMG response and visible contraction of the soleus, while excluding the contraction of other muscles such as the tibialis anterior, to avoid stimulation of the peroneal nerve. Additionally, an approximate H-reflex threshold was determined during this procedure, used for the determination of the needed stimulation increment for recruitment curve sampling.

After placement of the active stimulation amplitude, the subject was comfortably seated in an inclined medical chair, head and arms supported (Ankle angle: ~110°, Knee angle: ~150°, Hip angle: ~120°, similar to [18]). Thereafter, the protocol was executed as shown in fig. 3, for which the subject was instructed to remain entirely still and to avoid movement or muscle tension throughout the course of the experiment.

As a first step, an entire recruitment curve was measured at small intervals, later used to determine the stimulation amplitude of four relevant H-wave points (fig. 2). Starting at a stimulation amplitude at which no response was visible, the amplitude was increased gradually in predetermined intervals I, while measuring six times at each increment. I was set according to the previously approximated threshold amplitude. For thresholds below 10 mA, increments were set to threshold/10, otherwise an interval of 1 mA was used. The recruitment curve was sampled until reaching its declining portion after H_{max}, after which the amplitude was increased at larger increments, until after the maximum M-wave was reached.

After completion of the initial curve mapping process, the stimulation amplitudes for H_{Thresh}, $H_{Max50\%}$, H_{Settle}, H_{Max} and M_{max} were identified within the recorded recruitment curve (see: H-reflex measurement). These stimulation amplitudes were then held constant throughout the experiment.

After an additional baseline measurement, the tsDCS intervention was started. Post measurements were performed immediately after (t0) and 30 minutes following the intervention (t30). To assess the acute stimulation effects, additional measurements, two (S1) and nine minutes (S2) in the course of the intervention, were conducted. To reduce interference with effects of tsDCS, only $H_{max50\%}$, H_{Settle} and M_{max} were measured at S1 and S2. The protocol was repeated for each electrode configuration and a sham condition.

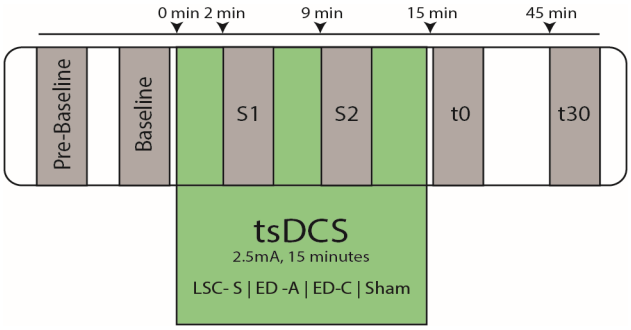

Figure 3: Overview of experimental protocol. At Pre-Baseline an initial recruitment curve mapping took place to determine characteristic points within the H- and M- Wave recruitment curves (see fig. 2). After an additional baseline measurement, the tsDCS intervention was started with an amplitude of 2.5mA and a duration of 15 minutes. During tsDCS, the H-reflex is probed after two minutes (S1) and nine minutes (S2), measuring only H_{Settle}, H_{max} and M_{max}. Post tsDCS measurements follow immediately (t0) and 30 minutes (t30) after the intervention.

3.2.8 Data analysis

Data processing was performed with a custom Matlab script (Matlab v.2015a, MathWorks Inc., Natick, USA). EMG signals were high pass filtered at 5 Hz after which H- and M- wave peak-to-peak amplitudes were determined automatically. Thereafter, all amplitudes were normalized with their corresponding M_{max}. Extreme outliers, such as null responses, were removed manually.

We expressed each obtained data point by its difference to baseline. This difference is normalized by the value of H_{max} at baseline and therefore expressed as a fraction of initial, overall H-reflex amplitude allowing comparison between sessions.

As an additional outcome-measure, we calculated the area below the sampled characteristic points, which gives an indication about the curve as a whole. Again, the area was expressed as its difference to the area calculated for its respective baseline. The resulting area difference was normalized by the overall area at baseline.

Because H-reflex during stimulation was only measured at two sample points ($H_{max50\%}$ and H_{Settle}), we also calculated the area difference to baseline restricted to the interval between $H_{max50\%}$ and H_{Settle}. This was done in order to compare measurements during, to those before and after tsDCS.

3.2.9 Statistics

Statistical analysis was performed using IBM SPSS Statistics v.23 (IBM Corporation, New York, USA). For each stimulation condition a Friedman's one-way ANOVA was used to test for significant effects in time and for each time interval for significant effects of stimulation configuration. This was performed on changes in curve area and data point amplitudes at H_{max} and $H_{max50\%}$. The significance level was set to p=0.05. Post-hoc pairwise comparison is performed using Dunn's–test [23] with an adjusted p-value of 0.0083. Effect size r is calculated via $r = Z/\sqrt{2N}$ with N being the number (10) of subjects [24]. Furthermore, we calculate the mean (m_{abs}) and interquartile range (IQR_{abs}) of the absolute difference from baseline for conditions found to be significant by post hoc comparison.

To differentiate between a recruitment curve threshold shift and overall amplitude shift, we use Friedman repeated measures ANOVA to compare within measurement values for $H_{max50\%}$ and H_{max} for post-hoc measurements significant with respect to baseline. We thereby assume that a change in recruitment curve threshold, which is visible in a left or right shift of the recruitment curve, will result in a significantly larger amplitude change measured at $S_{max50\%}$ compared to those at S_{max}. Consequently, an overall amplitude decrease will result in no significant difference between the changes at $H_{max50\%}$ and H_{max}.

Furthermore, correlation analysis is used to rule out that changes in H wave could be attributed to a change in M_{max}. In order to investigate differences between genotype groups, a Kruskal-Wallis test is performed for each measurement in which a significant difference was found, with the genotype as between group factor. For conditions across which a significant difference was found, we assess two-tailed Pearson and Spearman correlations by using the area between the corresponding measurement and baseline in a range from $H_{max50\%}$ to H_{Settle}.

3.3 Results

3.3.1 Subject safety

Throughout the course of the study, all subjects underwent the experiments without adverse effects, neither during or after the applied tsDCS, nor during the tibial nerve stimulation.

3.3.2 Changes in H-reflex

A typical measurement for an exemplary subject, including sampled H- and M-wave datapoints and average EMG traces at $s_{max50\%}$, for condition ED-C is illustrated in Figure 4. An overview of all H-Reflex datapoints, expressed as a percentage difference of H_{max} at baseline, for all subjects and conditions is shown in figure 5. The total area, as a percentage difference of the area at baseline (see also fig. 4.), quantifies the overall change (see fig. 6), whereas differences in mean datapoint amplitudes for H_{max} and $H_{max50\%}$ (fig. 5) can be interpreted as changes in overall amplitude and threshold respectively.

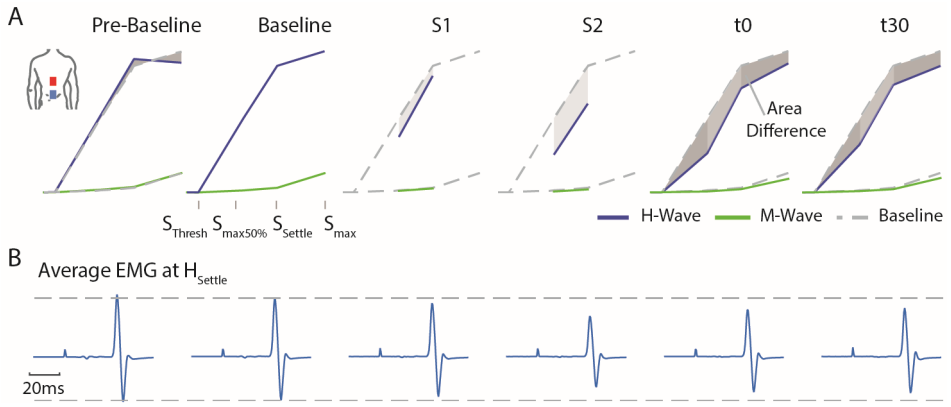

Figure 4: For an exemplary subject (A) all average H- and M- Wave datapoints are shown. For clarity, the figure exemplifies the area between a corresponding measurement and baseline. (B) Average EMG traces at H_{Settle} for configuration ED-C.

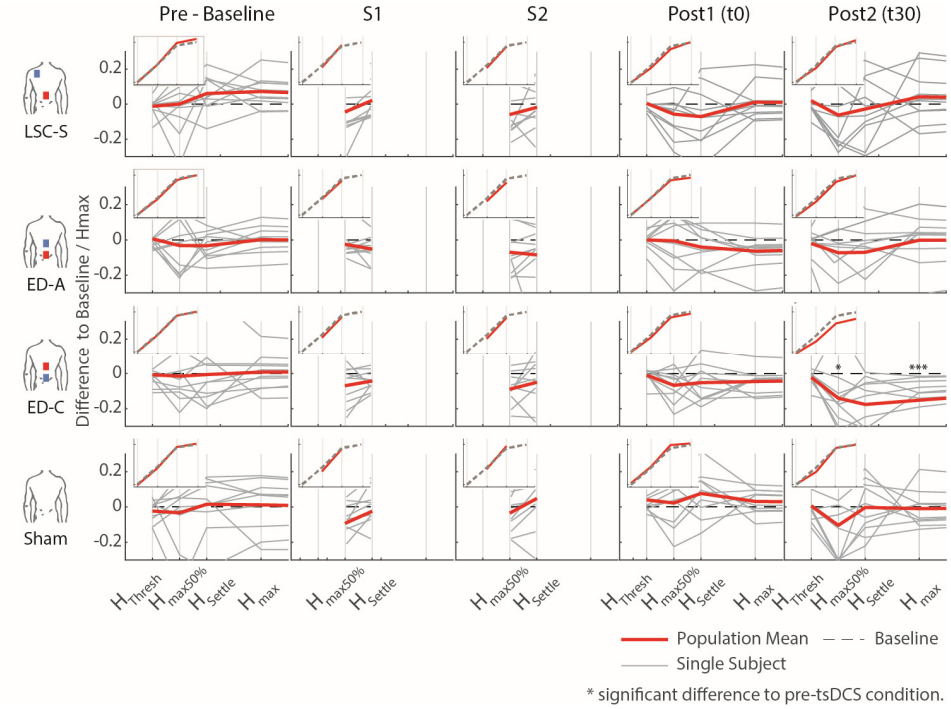

Figure 5: Overview of all differences to baseline, as a percentage of the corresponding H_{max} at baseline, for all configurations and measurements. The inlays show the average trend over all subjects with respect to a generic s-function representing baseline. Significant differences with respect to pre-intervention measurements arose for configuration ED-C, 30 minutes after intervention (last column).

Responses to the different stimulation paradigms show high inter and intra subject variability. The changes observed for all sham measurements and those obtained during curve mapping before baseline give an indication of the natural changes that can be expected without intervention. Thereby the fluctuation in changes in area for all combined pre-baseline and sham measurements normalized by their baseline had an interquartile range of 21 %. Similarly, for H_{max}: IQR=13 %, and $H_{max50\%}$: IQR=45 %. Across subjects, most post-intervention changes are within the amplitude range of effects observed without intervention, as visible in figs. 5 and 6.

For configurations LSC-S and ED-A, observed changes lie within the same standard deviation range as the sham condition. Furthermore, for both stimulation conditions, responses in either direction are visible, resulting in no statistically significant net-change with respect to baseline (tab. 1). Similarly, for the sham condition, responses in both directions resulted in no statistically significant changes with respect to baseline.

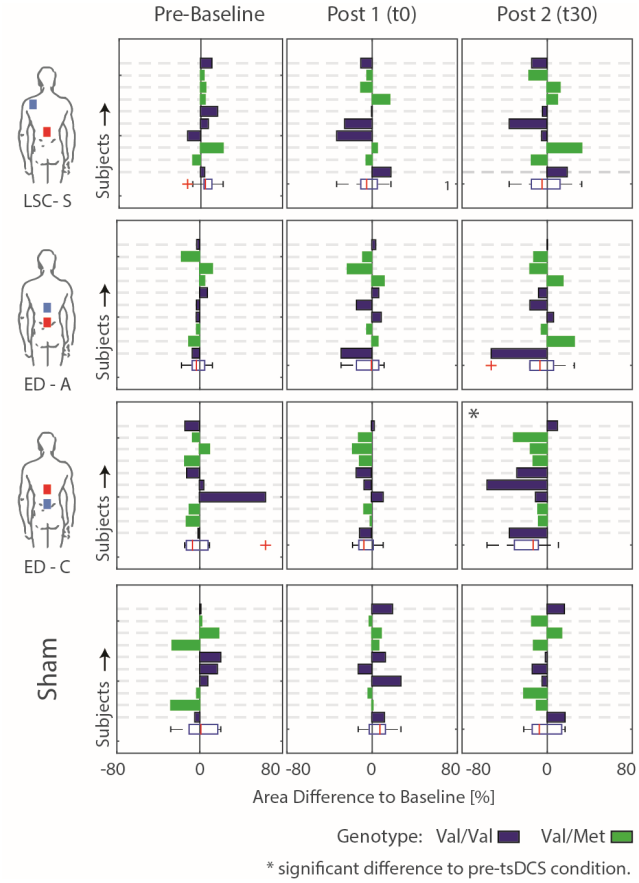

Figure 6: Difference areas between baseline and pre-baseline as well as post tsDCS (t0 and t30) for all subjects. Rows/Bars within each graph correspond to the measured subjects. Additionally, the subject genotype is color coded: Val/Val=Blue, Val/Met=Green. Significant differences to pre-tsDCS measurements are detected for configuration ED-C at time t30.

Table 1: Statistical analysis of general differences within conditions and measurement times, across conditions, after Friedman repeated measures analysis.

Configuration	Significance		
	Area Difference	H_{max}	$H_{max50\%}$
LSC-S	0.51	0.16	0.51
ED-A	0.66	0.24	0.073
ED-C	0.033*	0.001***	0.033*
Sham	0.26	0.54	0.15
Measurement Time			
Pre-Baseline	0.16	0.39	0.78
t0	0.06	0.05*	0.52
t30	0.095	0.06	0.78

($p \leq 0.05$) *, ($p \leq 0.01$) **, ($p \leq 0.001$) ***

For configuration ED-C, differences in curve area (fig. 6) as well as data points $H_{max50\%}$ and H_{max} (fig. 5) reveal clear tsDCS effects post-intervention compared to baseline. This is indicated by overall significant changes in area ($\chi2(3) = 8.76$, p=0.033), H_{max} ($\chi2(3) = 16.56$, p=0.001) and $H_{max50\%}$ ($\chi2(3) = 8.76$, p=0.033). Post hoc analysis reveals a significant difference of t30 to pre-baseline (H_{max}: Z=1.8, p=0.011, r = 0.4, m_{abs}= 0.15, IQR_{abs} = 0.19) and baseline (area: Z=1.7, p=0.019, r= 0.38, m_{abs} = 0.22, IQR_{abs} = 0.24; H_{max}: Z=2.2, p<0.001, r= 0.49, m_{abs} =0.15, IQR_{abs} = 0.19; $H_{max50\%}$: Z=1.7, p=0.019, r=0.38, m_{abs} = 0.4, IQR_{abs} = 0.24) measurements. To constrain the character of the observed recruitment curve changes, we compared the data points at $H_{max50\%}$ with those at H_{max}, within configuration ED-C at time t30. Thereby no significant differences were found (p=0.114). Thus, the population trend with respect to baseline for condition ED-C appears to be an overall H-reflex decrease instead of a curve shift to the right, revealed by a significant decrease in area, $H_{max50\%}$ and H_{max}.

The observed effects in $H_{max50\%}$, H_{max} and curve area could not be explained by changes in nervous excitation during tibial nerve stimulation as changes in these measures were unrelated to changes in M_{max}. We also explored whether changes during tsDCS (measurements S1 and S2) were predictive for changes post intervention. However, from correlation analysis it appeared that this was not the case.

Testing for time effects across configurations, Friedman's test reveals differences in H_{max} for measurements at t0 ($\chi2(3) = 7.8$, p=0.05). However, whereas the highest difference was found between configuration ED-A and sham (Z=-1.4, p=0.09), post hoc pairwise comparisons did not lead to significant results. Furthermore, analysis reveals a notable statistical trend ($\chi2(3) = 7.56$, p=0.06) across conditions at time t30.

To explain the high variability across subjects, BDNF genotype was tested. Thereby, 5 out of 10 subjects were tested positive for the Vall66Met polymorphism. The corresponding subjects' genotype is included by coloring the bars in figure 6. Generally, there is no consistent difference

in stimulation response between genotype groups. For conditions exhibiting significant differences compared to baseline, Kruskal-Wallis' test reveals no significant differences between the responses exhibited by the two genotype groups. Thus, the high intersubject variability, which remains within genotype groups, cannot be explained by or, otherwise stated, prohibits explanation of an effect of subject genotype.

3.4 Discussion

The goal of this study was to investigate electrode placement specific changes of lumbar trans-spinal direct current stimulation on the soleus H-reflex before, during and after intervention. We introduced a new electrode placement configuration (ED), which generates an electric field vector dominant in longitudinal direction at lumbar spinal motoneuron level, by placing both electrodes equidistant above and below the lumbar spinal cord [22]. We show that the newly introduced electrode configuration (ED-C) was able to induce significant changes to the approximated H-reflex recruitment curve 30 minutes after intervention. This was indicated by a significant and consistent depression of H_{max}, $H_{max50\%}$ and area. The equal distance placement in anodal setting (ED-A) had no significant effect, which confirms the polarity dependency often observed in DC stimulation protocols. Additionally, the effects observed post tsDCS were unrelated to the deviations from baseline measured during DC stimulation. Strikingly, we were not able to observe the effects previously reported for configuration LSC-S (Lumbar Spinal Cord – Shoulder), which had been shown to induce a significant left shift of the H-reflex recruitment curve [18].

The specific post intervention response to stimulation with configuration ED-C appears to be an overall amplitude reduction of the H –reflex, indicated by a relative decrease in H_{max}, $H_{max50\%}$ and area. This is qualitatively different from the left shift reported after anodal tsDCS (LSC-S) in previous studies and may consequently indicate the involvement of different working mechanisms. Cellular targets of lumbar spinal DCS that have been suggested by previous studies, are the Ia-motoneuron synapse [17,18,22], Ia-presynaptic inhibition [20] or channels mediating persistent inward current excitability [25].

We argue, that conductivity changes at the Ia-motoneuron synapse seem less likely, as this would lead to a left shift or right shift of the H-Reflex recruitment curve, not an amplitude modulation [22]. Thus, also changes in Ia-presynaptic inhibition appear unlikely. It can however not be excluded, that the observed effect in H-Reflex reduction could in part be caused by a downregulation of Ca2+ persistent inward current. Elbasiouny and Mushahwar investigated the effect of motoneuron polarization on spinal motoneuron firing and PIC modulation [25]. Thereby a constant EF was able to directly surpress motoneuron firing by reducing Ca^{2+} current. In analogy to that, the tsDCS generated electric field in this study, could have led to a similar polarization profile of the lumbar spinal motoneurons [22], which may in turn have resulted in a downregulation of motoneuron activity.

In an effort to understand inter-individual response differences, we investigated the relationship between tsDCS acute and after effects as well as differences in BDNF genotype. To test the relationship between acute and after effects, we correlated the conditions found to be significant,

to the changes from baseline measured during tsDCS within the same experiment. However, no relationship was detected.

A possible reason that a relation between acute and long-term effects was not found in this study, could be that the stimulation intensities usually used for human subjects were too low to elicit measurable acute effects. This is different in animal and in in-vitro DC experiments, which show measurable acute effects during DC stimulation, which scale with stimulation intensity [26,27]. The relationship between DCS acute and after effects is complex, as shown by Ahmed [27], whereby MEP evoked muscle twitches in the hindlimb where inversed during, compared to after tsDCS. Furthermore, this directional relationship was altered by associative stimuli during tsDCS.

Genetic dependencies for the response to tsDCS have been shown for Met allele carriers of brain derived neurotropic factor (BDNF) (Val66Met polymorphism) [15,28]. However, BDNF genotyping in our subject population reveals that the level of variability remains within the two genotype groups and thus no statistical difference between the responses exhibited by the two subject groups was found. This does however not rule out the influence of other genetic dependencies [28].

We did not observe a consistent recruitment curve left shift after tsDCS with configuration LSC-S, as reported previously [18]. Based on Lamy et al., we had expected a substantial increase of $H_{max50\%}$ with respect to baseline (for configuration LSC-S at time T30). However, with a mean difference from baseline for $H_{max50\%}$ of -6.3 % (95 % CI [-20.81 %, 8.26 %]), the population response observed here is substantially different from that. However, this is in line with observations by Hubli et al., who showed no significant modulatory effects after anodal tsDCS tested in healthy individuals [17]. We therefore assume that the absence of a modulatory effect after tsDCS in configuration LSC-S, must be attributed to experimental and/or subject-specific factors.

The two main methodological differences between the protocol used here and the one of Lamy et al., are the amount of measurements taken during tsDCS as well as sample size. For the former, Lamy et al. sampled two complete H-reflex recruitment curves during tsDCS at a stimulus frequency of 0.33 Hz, and a measurement time of 3-4 minutes for each curve. In contrast to that, we intentionally reduced the number of measurements during tsDCS, to prevent interactions with the artificially induced neural activity and therefore influence intervention outcome. With each measurement lasting approximately 1-2 minutes (thus overall 2-4 minutes during tsDCS), the amount of induced neural activity was substantially lower as compared to the protocol performed by Lamy et. al (6-8 minutes during tsDCS). Along this line, Hubli and colleagues did not measure during tsDCS and stimulation was applied during rest, thus reducing neural activity during DC stimulation to a resting level [17]. Since the outcome of DC stimulation is thought to be neural activity dependent [3], the agreement of our results with those reported by Hubli et al. [17] and the discrepancies with those observed by Lamy et al. may be explained via the differences in induced neural activity during tsDCS.

With regards to sample size, we included a smaller number of subjects (10) compared to Lamy et al. (17), which may suggest limited statistical power to show an otherwise significant effect.

However, based on the mentioned population mean for $H_{max50\%}$, 30 minutes after tsDCS with configuration LSC-S, the responses obtained here are substantially different from those reported by Lamy et al. Furthermore, our results agree with those of Hubli et al., who had included the same number of subjects (17) as Lamy et al. Out of these reasons, it is unlikely that sample size is able to account for the mentioned differences in intervention outcome.

3.5 Conclusion

The presented results are a further step towards forming a basic understanding of tsDCS and may potentially contribute to a more targeted application in the future. In the light of the knowledge obtained by others, the overall reduction of the H-reflex after stimulation with configuration ED-C indicates that by changing EF direction with respect to the target structure the network response can be changed. This implies that different cellular targets may be dominant depending on EF orientation, which is in line with current state of the art knowledge. Against our expectations, we were not able to observe the same recruitment-curve left shift for configuration LSC-S as previously reported by others, which could be accounted for by methodological or subject specific differences as discussed. In addition to the depression effects discussed earlier, this highlights the complexity of the underlying mechanisms, which have to be understood before tsDCS can find its way into clinical application.

References

[1] Ruf G, Wendling F, Merlet I, Molaee-ardekani B, Mekonnen A, Salvador R, Soria-frisch A, Grau C, Dunne S and Miranda P C 2013 Transcranial Current Brain Stimulation (tCS): Models and Technologies **21** 333–45

[2] Miranda P C 2013 Chapter 29 - Physics of effects of transcranial brain stimulation *Brain Stimulation* Handbook of Clinical Neurology vol 116, ed A M Lozano and M Hallett (Elsevier) pp 353–66

[3] Bikson M and Rahman A 2013 Origins of specificity during tDCS: anatomical, activity-selective, and input-bias mechanisms. *Front. Hum. Neurosci.* **7** 688

[4] Rampersad S M, Janssen A M, Lucka F, Aydin Ü, Lanfer B, Lew S, Wolters C H, Stegeman D F and Oostendorp T F 2014 Simulating transcranial direct current stimulation with a detailed anisotropic human head model. *IEEE Trans. Neural Syst. Rehabil. Eng.* **22** 441–52

[5] Salvador R, Mekonnen A, Ruffini G and Miranda P C 2010 Modeling the electric field induced in a high resolution realistic head model during transcranial current stimulation. *Conf. Proc. IEEE Eng. Med. Biol. Soc.* **2010** 2073–6

[6] Dmochowski J P, Datta A, Bikson M, Su Y and Parra L C 2011 Optimized multi-electrode stimulation increases focality and intensity at target. *J. Neural Eng.* **8** 46011

[7] Arlotti M, Rahman A, Minhas P and Bikson M 2012 Axon terminal polarization induced by weak uniform DC electric fields: a modeling study. *Conf. Proc. IEEE Eng. Med. Biol. Soc.* **2012** 4575–8

[8] Tranchina D and Nicholson C 1986 A model for the polarization of neurons by extrinsically applied electric fields. *Biophys. J.* **50** 1139–56

[9] Radman T, Ramos R L, Brumberg J C and Bikson M 2009 Role of cortical cell type and morphology in subthreshold and suprathreshold uniform electric field stimulation in vitro *Brain Stimul.* **2**215–228.e3

[10] Kabakov a. Y, Muller P a., Pascual-Leone a., Jensen F E and Rotenberg a. 2012 Contribution of axonal orientation to pathway-dependent modulation of excitatory transmission by direct current stimulation in isolated rat hippocampus *J. Neurophysiol.* **107** 1881–9

[11] Reato D, Rahman A, Bikson M and Parra L C 2010 Low-Intensity Electrical Stimulation Affects Network Dynamics by Modulating Population Rate and Spike Timing *J. Neurosci.* **30** 15067–79

[12] Ranieri F, Podda M V, Riccardi E, Frisullo G, Dileone M, Profice P, Pilato F, Di Lazzaro V and Grassi C 2012 Modulation of LTP at rat hippocampal CA3-CA1 synapses by direct current stimulation. *J. Neurophysiol.* **107** 1868–80

[13] Lapenta O M, Minati L, Fregni F and Boggio P S 2013 Je pense donc je fais: transcranial direct current stimulation modulates brain oscillations associated with motor imagery and movement observation. *Front. Hum. Neurosci.* **7** 256

[14] Chhabra H, Shivakumar V, Agarwal S M, Bose A, Venugopal D, Rajasekaran A, Subbanna M, Kalmady S V, Narayanaswamy J C, Debnath M and Venkatasubramanian G 2015 Transcranial direct current stimulation and neuroplasticity genes: implications for psychiatric disorders *Acta Neuropsychiatr* 1–10

[15] Lamy J-C and Boakye M 2013 BDNF Val66Met polymorphism alters spinal DC stimulation-induced plasticity in humans. *J. Neurophysiol.* **110** 109–16

[16] Cogiamanian F, Ardolino G, Vergari M, Ferrucci R, Ciocca M, Scelzo E, Barbieri S and Priori A 2012 Transcutaneous Spinal Direct Current Stimulation *Front. Psychiatry* **3**

[17] Hubli M, Dietz V, Schrafl-Altermatt M and Bolliger M 2013 Modulation of spinal neuronal excitability by spinal direct currents and locomotion after spinal cord injury. *Clin. Neurophysiol.* **124** 1187–95

[18] Lamy J-C, Ho C, Badel A, Arrigo R T and Boakye M 2012 Modulation of soleus H reflex by spinal DC stimulation in humans. *J. Neurophysiol.* **108** 906–14

[19] Bocci T, Marceglia S, Vergari M, Cognetto V, Cogiamanian F, Sartucci F and Priori A 2015 Transcutaneous Spinal Direct Current Stimulation (tsDCS) Modulates Human Corticospinal System Excitability *J. Neurophysiol.* jn.00490.2014

[20] Yamaguchi T, Fujimoto S, Otaka Y and Tanaka S 2013 Effects of transcutaneous spinal DC stimulation on plasticity of the spinal circuits and corticospinal tracts in humans *2013 6th Int. IEEE/EMBS Conf. Neural Eng.* 275–8

[21] Winkler T, Hering P and Straube a. 2010 Spinal DC stimulation in humans modulates post-activation depression of the H-reflex depending on current polarity *Clin. Neurophysiol.* **121** 957–61

[22] Kuck A, Stegeman D and van Asseldonk E 2017 Modeling trans-spinal direct current stimulation for the modulation of the lumbar spinal motor pathways *J. Neural Eng.* **14** 56014

[23] Dunn O J 1964 Multiple Comparisons Using Rank Sums *Technometrics* **6** 241–52

[24] Pallant J 2013 *SPSS survival manual: a step by step guide to data analysis using SPSS*

[25] Elbasiouny S M and Mushahwar V K 2007 Suppressing the excitability of spinal motoneurons by extracellularly applied electrical fields: insights from computer simulations. *J. Appl. Physiol.* **103** 1824–36

[26] Rahman A, Reato D, Arlotti M, Gasca F, Datta A, Parra L C and Bikson M 2013 Cellular effects of acute direct current stimulation: somatic and synaptic terminal effects. *J. Physiol.* **591** 2563–78

[27] Ahmed Z 2011 Trans-spinal direct current stimulation modulates motor cortex-induced muscle contraction in mice. *J. Appl. Physiol.* **110** 1414–24

[28] Wiegand A, Nieratschker V and Plewnia C 2016 Genetic Modulation of Transcranial Direct Current Stimulation Effects on Cognition *Front. Hum. Neurosci.* **10**

Chapter IV – Task Dependency of trans-Spinal Direct Current Stimulation

A. KUCK [1], S.S. FRICKE [1], H. VAN DER KOOIJ[1,3], D.F. STEGEMAN[2] and E.H.F. VAN ASSELDONK[1]

[1] Laboratory of Biomechanical Engineering, Department of Engineering Technology, University of Twente, Drienerlolaan 5, 7522 NB Enschede, The Netherlands

[2] Radboud University Medical Center, Donders Institute for Brain, Cognition and Behavior, Department of Neurology/Clinical Neurophysiology, Reinier Postlaan 4, 6500HB Nijmegen, The Netherlands

[3] Department of Biomechanical Engineering, Faculty of Mechanical, Maritime and Materials Engineering, Delft University of Technology, Mekelweg 2, Delft, 2628CD, Netherlands

Abstract

Trans- spinal direct current stimulation (tsDCS) is a neuromodulatory tool with potential application to injuries or dysfunctions of the spinal cord, whereby recent studies have shown that tsDCS may be able to modulate the networks of the corticospinal pathways. When aiming to apply tsDCS in a rehabilitation setting, the utilized protocol needs to be tailored to achieve optimal stimulation effects. Motivated by similar studies in the brain, we therefore investigated whether the effect of tsDCS depends on the task that is performed during the stimulation. Real and sham tsDCS were applied during rest and while active in ten healthy subjects. TsDCS was applied in cathodal configuration (cathode above T11, anode on left shoulder) at 2.5mA and 15 minutes duration. Changes of the spinal reflex pathways were assessed by measuring the H-reflex during standing and walking before, five minutes after (T5) and 30 minutes after tsDCS (T30). Our results show, that the H-reflex amplitude was significantly more modulated, when compared to sham, at time T30 when tsDCS was applied while active. This was the case for both, the H-reflex measured during standing and walking. However, the direction of modulation was inconsistent across subjects, with post-tsDCS responses being either suppressed or increased depending on a subject specific basis. Our results suggest that a larger effect size is to be expected when tsDCS is paired with ongoing neural activity in the stimulated target region. The directional inconsistency across subjects highlights the importance of a more thorough screening of the influence of protocol and subject specific variables on the intervention outcome.

4.1 Introduction

Transcutaneous Spinal Direct Current Stimulation (tsDCS) is a non-invasive neurostimulation technique to modulate spinal cord neuronal networks [1]. During tsDCS, a small, constant electric field is applied to the desired spinal pathways, aiming to induce a lasting, functional change to the targeted neural circuitry. Due to its neuromodulatory characteristics, tsDCS may therefore be beneficial for the rehabilitation of disorders or damage of the spinal cord.

Spinal cord injury typically leads to the dysfunction of corticospinal- and spinal network function. Depending on the severity and location of the injury, resulting symptoms may include a decrease in voluntary motor control, spasticity, or the loss of certain organ functions [2]. Previous research has shown, that transcutaneous- spinal DCS can have significant effect on the spinal neural networks, including lumbar spinal reflexes [3,4] as well as ascending [5] and descending

corticospinal connections [6] (for a thorough overview, see: [7]). Since both, ascending and descending pathways may be damaged in patients with spinal cord injuries (SCIs) and spinal reflexes are often increased [8,9], tsDCS may therefore be a promising tool to promote rehabilitation after SCIs.

However, before tsDCS can be used appropriately in clinical practice, more should be known about its influencing factors and the optimal way of application [1]. Previous studies have shown, that the effects of DC stimulation on the nervous system may depend on electric field strength and direction [10–12], neural activity during stimulation [13–18], morphology of the targeted neural circuitry [19] and genetic predisposition [10,20,21]. For the latter, specific genetic dependencies where detected for genotypes of brain-derived-neurotrophic-factor (BDNF), which result in different post tsDCS modulation effects of the H-reflex recruitment curve [20]. In other words, the resulting modulatory effects may be significantly different (e.g. in direction or amplitude), or non-existent, across tsDCS protocols for different electric field strengths, neural activities or other aforementioned factors.

To improve the control of tsDCS protocols, this study focusses on the dependency of tsDCS outcome on the neural activity during stimulation. This dependency is referred to as activity-selectivity, which is the preferential modulation of a neuronal network that is already active, while not modulating separate neuronal networks that are inactive [10]. Indications that such dependencies exist, have been shown for transcutaneous DC stimulation applied to the brain (in the form of transcranial Direct Current Stimulation, or tDCS) and spinal cord [13–16,22], as well as in-vitro and animal experiments [17,23]. For example, Kim et al. showed a two-fold increase in MEP amplitude after combining anodal tDCS with voluntary grip exercise, compared to anodal tDCS or grip exercise alone [22]. Furthermore, various animal and in-vitro studies show a similar trend [10,17,23].

Based on these results, we hypothesized that a similar task-dependency might be observed for tsDCS. Specifically, we were interested in whether a larger modulatory effect could be expected, when lumbar- tsDCS is applied during walking compared to tsDCS during rest. The two conditions were chosen due to their contrast in ongoing neural activity, which is expected to be substantially lower during rest compared to walking.

The modulation effect on spinal excitability was measured by using the H-reflex during standing and walking. TsDCS was applied in a real or sham condition, during either lying or walking. We also tested BDNF genotype, a known genetic dependency [20], to counteract possible between subject differences.

4.2 Methods

4.2.1 Subjects

Ten healthy subjects (22.8±2.2 years, 7 women and 3 men) participated in this study. The study was approved by the Medical Ethical Committee Twente (Enschede, The Netherlands) and subjects signed an informed consent after receiving verbal and written information.

4.2.2 Study design and protocol

The experimental protocol was randomized double-blind and placebo controlled, whereby both experimenter and subject were blinded with respect to the applied stimulation (real or sham). Each subject participated in four experiments, with a minimum inter-session-interval of 72 hours. In each experiment, real or sham tsDCS was applied during one of the two tasks: 1) at rest, lying in a supine position, or 2) actively walking at a speed of 2.5 km/h. Five subjects received tsDCS during walking in experiment one and two, whereas the other five subjects received tsDCS during rest in sessions one and two.

At the beginning of each experiment, the EMG level at maximum voluntary contraction (MVC) and the resting EMG amplitude during standing (target EMG) were measured (fig. 1). These were used to determine an appropriate EMG background activity level for the H-reflex measurements during standing. Thereafter, the H-reflex recruitment curve was measured during both standing and walking, succeeded by a five minutes period of rest. Subsequent measurements were conducted before (baseline), five minutes after (T5) and 30 minutes after (T30) tsDCS.

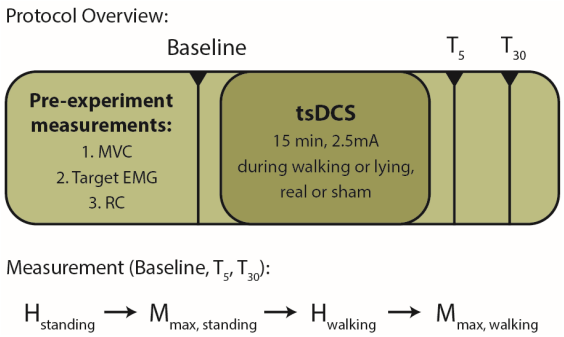

Figure 1: Overview of the experimental protocol. At the beginning of each experiment, maximal voluntary contraction (MVC), the average background EMG activity during standing (target EMG) as well as the H-reflex recruitment curve (RC) were measured during standing and walking respectively. Thereafter, a baseline measurement was conducted, after which the tsDCS intervention was applied for a duration of 15 minutes. Post measurements were conducted five (T_5) and 30 minutes (T_{30}) after tsDCS. The measurements at baseline, T_5 and T_{30} consist of sampling the H-wave and maximum M-wave during standing and walking.

4.2.3 Transcutaneous spinal direct current stimulation

TsDCS was delivered using a DC stimulator (Magstim DC-stimulator PLUS, Carmarthenshire, Wales UK) at a current of 2.5 mA and a duration of 15 minutes. This resulted in a current density of 0.07 mA/cm² and a total charge of 0.064 C/cm², which is far below the limits for tissue damage (14.29 mA/cm² and 5.24 C/cm²) [24]. For the sham condition small current pulses of 110 μA were applied at a 550 ms interval (110 μA for 15 ms) resulting in an average current of 2 μA, shown to result in no therapeutic effect [25].

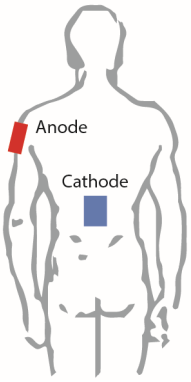

Figure 2: Location of the tsDCS electrodes on the upper left arm (anode) and half way between vertebrae Th11 and Th12 (cathode).

Before the tsDCS electrodes were placed, the skin was cleaned with alcohol. The electrodes (5 cm x 7 cm) were covered with saline-soaked sponges and the cathode was positioned longitudinally on the midpoint between the spinous processes of the 11th and 12th thoracic vertebrae [4] (fig.2). The anode was placed on the upper left arm (lateral deltoid muscle). This configuration was chosen based on a previous study that reported a significant change of motor evoked potentials (MEPs) after applying cathodal tsDCS [6]. The electrodes were taped down and a rubber strap was used to ensure that the cathode was firmly attached to the skin.

4.2.4 EMG recording

A differential surface EMG electrode was used to record reflexes from the soleus muscle of the dominant leg. Before electrode attachment, the skin was shaved, scrubbed and cleaned with alcohol. The electrode was placed on the dominant leg, distal to the belly of the medial gastrocnemius and medial to the Achilles tendon [26]. The reference electrode was placed on the lateral malleolus. Using an analog signal amplified (Bagnoli-16, Delsys, Boston, USA), the EMG signal was bandwidth filtered with cutoff frequencies at 20Hz and 450 Hz, amplified (1000x) and sampled at a rate of 2000 samples/s.

4.2.5 Maximal voluntary contraction and target EMG level

During maximal voluntary contraction (MVC) the subject was seated on an adjustable chair and the dominant leg was fixed in a frame, which enabled isometric plantarflexion against a static resistance. The hip, knee and ankle angle were approximately 90 degrees. Three isometric MVC contractions were performed with a break of one minute between the subsequent trials. The subject was instructed to increase the force until a maximum was reached, hold it for three seconds and then relax. The mean value of the highest rectified EMG signal within a 100 ms window was calculated for each trial. The maximum of the three trials was taken as the MVC.

The H-reflex during standing was measured by controlling the neural background activity in form of muscle activation (see below). The EMG level at which this was done is referred to here as the "target EMG level". To determine the target EMG level, the EMG signal was measured during one minute of quiet standing. For this, the subject was instructed to stand at ease, hold the arms by the side. The feet were separated by a distance approximately corresponding to pelvic width [8,27]. The average of the filtered and rectified EMG signal over one minute was used as the target EMG level for the H-reflex measurements during standing.

4.2.6 Tibial nerve stimulation

For eliciting the H-reflex, a circular cathode electrode (diameter 20 mm, Plaquette, Technomed Europe, The Netherlands) was placed above the tibial nerve in the popliteal fossa. The optimal electrode position was determined by palpating the skin with a hand-held electrode probe, stimulating at low intensities while the subject was standing. Proper electrode positioning was indicated by an H-reflex that could be evoked at low intensities, without the occurrence of an M-wave [28]. The anode (41 × 41 mm^2, TENS electrode, Maxpatch, UK) was placed proximal to the patella. A constant current stimulator (Digitimer DS7A, Hertfordshire, UK) was used to generate monophasic pulses with a stimulus width of 500 μs and an inter-stimulus interval varying randomly between four and seven seconds.

4.2.7 H-reflex recording

At the beginning of each experiment, detailed recruitment curves of the H-reflex and M-wave were measured, to determine the stimulation intensities needed for the succeeding H-reflex measurements. Starting below the H-reflex threshold, the stimulus intensity was increased in steps of 1 mA until reaching the maximum H-wave (H_{max}). If the threshold to elicit an H-reflex was lower than 10 mA, steps of 10% of the threshold were applied. After reaching H_{max}, the stimulus intensity was increased in steps of 5 mA until the maximum M-wave (M_{max}) was reached. Four stimuli were applied for each stimulation intensity and separate recruitment curves were measured during standing and walking.

For the subsequent pre- and post-intervention outcome, the H-reflex was measured during standing and walking, respectively ($H_{standing}$ and $H_{walking}$). For both conditions, standing and walking, the corresponding stimulation amplitudes were chosen at an intensity that would result in an H-wave with an amplitude of 50% H_{max}. This was determined based on the initially recorded recruitment curves and allowed to monitor facilitation and depression of the H-reflex. The M-wave was monitored during the experiment, to ensure consistent nerve stimulation [29]. Therefore, if no M-wave was visible at the stimulus intensity that elicited an H-reflex of 50% H_{max}, a higher stimulus intensity was chosen with the strength between for 50% H_{max} and for H_{max}.

In addition to the H-wave, M_{max} was measured for normalization in each measurement block during standing and walking, respectively. The stimulation intensity to elicit M_{max} was chosen based on the recruitment curve for the M-wave at the point where the M-wave curve reached a plateau. Five stimuli were given at this intensity.

All measurements during standing were conducted with a background EMG level of the predetermined target EMG level ± 8% EMG level at MVC, which was achieved on visual screen judgement.

During walking, the H-reflex was elicited during mid-stance, at 35% of the gait cycle [30–32] which was determined based on detected heel contacts. This was done by measuring vertical ground reaction forces during walking on a split-belt, instrumented treadmill (Y-Mill, Force Link, Culemborg, The Netherlands). Heel strikes were detected by using a threshold of 10 N [33].

To counteract possible variations in stimulation intensity at the tibial nerve, the M-wave was monitored in the course of the experiment and the stimulation intensity was adjusted if the M-wave did not stay within the range of the target M-wave ± 5 % M_{max} for four out of five stimuli [34]. The target M-wave was defined as the average M-wave that was measured during the recruitment curve measurements at the chosen intensity.

4.2.8 BDNF genotyping

Saliva samples were collected from each subject (Oragene Dx, DNA Genotek Inc., Ottawa, Canada) and all samples were analyzed using Taqman (rs6265) to determine BDNF genotype. Additionally, BDNF concentration and sample purity (260/280) were measured.

4.2.9 Data analysis

The peak-to-peak value was calculated for the H-reflex and M-Wave in Matlab2014b (Mathworks, Natick, USA) and averaged for each subject. The average peak-to-peak value was normalized with the M_{max} within the same measurement block. Subsequently, the change of each measurement was expressed as a percentage of baseline (H_{norm}), by subtracting the amplitude at baseline from the amplitude at T5 or T30 and dividing by the baseline amplitude (for instance: $H_{norm,standing\ at\ T5} = (Hreflex_{standing\ at\ T5} - Hreflex_{standing\ at\ baseline})/Hreflex_{standing\ at\ baseline}$). As an additional outcome measure variant, expressing only modulatory effect amplitude, we calculated the absolute difference from baseline ($|H_{norm}|$).

Due to the presence of outliers and unequal variances in the obtained data, a robust paired t-test (Yuen-Welch-test) [35–37] was utilized for statistical analysis, which was implemented and performed in R (version 3.4.1). The Yuen-Welch-test was chosen for its robustness in the presence of outliers or other nonnormalities [35,37]. This is achieved by using the trimmed mean, with a trimming factor of 0.2. We therefore, pairwise compared each of the included stimulation conditions and timepoints, to its corresponding sham counterpart using Yuen-Welch-test. The significance level was set to 0.05. This was conducted for 1) the normalized difference from baseline (H_{norm}), to test for directionally coherent modulation, as well as 2) for the absolute normalized difference from baseline ($|H_{norm}|$), to test for differences in only effect size.

For conditions shown to be significantly modulated with respect to sham, additional statistics were performed. Since we assumed that significant changes induced by tsDCS would be visible in the H-reflex during walking and standing, we assessed the correlation for changes in H_{norm} between standing and walking. To further exclude a significant influence of other factors on the soleus H-reflex amplitude, e.g. changes in neural activation or electrode position, we correlated H_{norm} with the corresponding normalized difference from baseline for M_{max} and the background EMG level. Data points initially flagged as outliers, or those that had a Mahalanobis distance >1.5*IQR were excluded from correlation analysis. The Mahalanobis distance [38] is a standardized distance measure widely applied for outlier detection [39]. It measures the distance between a single data vector and the vector of means of all the variables (centroid) [38].

To investigate possible genetic dependencies of the Val66Met BDNF genotype, we directly compared the responses of the two genotype groups using the normalized difference from baseline, via an independent samples t-test. This was performed for all conditions, earlier shown to be significant.

4.3 Results

Subjects underwent all tsDCS stimulation procedures without adverse side effects. Representative examples of EMG traces for $H_{norm,standing}$ and $H_{norm,walking}$ can be seen in figure 3.
With regards to data quality, the amplitudes of M_{max} and the M-wave during standing and walking remained approximately constant with interquartile ranges (IQR) of $IQR_{M_{max,standing}} = 8\%$ and $IQR_{M_{max,walking}} = 7{,}5\%$ as well as $IQR_{M-wave_{standing}} = 1\%$ and $IQR_{M-wave_{walking}} = 1{,}3\%$ (all expressed with respect to the amplitude of M_{max} at baseline). Similarly, the average background

EMG levels during standing and walking varied with $IQR_{EMG_{standing}} = 3.7\%$ and $IQR_{EMG_{Walking}} = 6\%$ (expressed as a percentage of the average EMG during MVC).

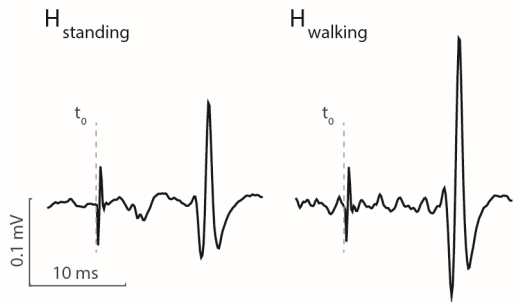

Figure 3: Example of EMG traces for all measurements in one subject. t_0 indicates the time of the stimulus.

4.3.1 Changes of the H-reflex

The relative changes of $H_{norm,walking}$ in an exemplary subject are illustrated in figure 4. The particular example suggests an increased $H_{norm,walking}$ after applying real tsDCS during walking and lying, while the H-reflex for both sham conditions appears to have been comparably more stable. The increasing trends observed after tsDCS during walking are similar to what can be seen on a group level.

Considering the data of all subjects, general trends are visible. Primarily, the data suggests an increase in variability in H_{norm}, after tsDCS was applied during walking. This can be interpreted as an increase in absolute H-reflex amplitude compared to baseline and sham (fig. 5A). The H-reflex further appears to be increased for both real as well as sham stimulation, when applied during lying. In addition to that, the data is characterized by the presence of a number of extreme outliers, which are mainly observed in recordings performed during standing (fig. 5).

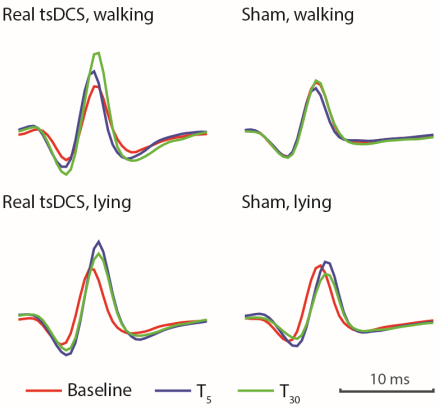

Figure 4: Results for the H-reflex during walking in one subject. The data is normalized by baseline and traces show the average of 10 samples.

The results of Yuen-Welch's-test for both, H_{norm} and $|H_{norm}|$, are summarized in table 1. Analyzing $H_{norm,standing}$ and $H_{norm,walking}$, no significant differences from sham can be detected. Consequently, tsDCS resulted in no directionally coherent shift in mean H-reflex amplitude across subjects.

However, analysis of $|H_{norm}|$ suggest that the H-reflex was modulated significantly more compared to sham 30 minutes after tsDCS was applied during walking. This is indicated by a significant increase in $|H_{norm,standing}|$ and $|H_{norm,walking}|$ at T30 after tsDCS while being

active compared to their corresponding sham condition for both $H_{norm,walking}$ (t(5)= 3.85, p=0.01) and $H_{norm,standing}$ (t(5)= 2.73, p=0.04) (see fig. 5B).

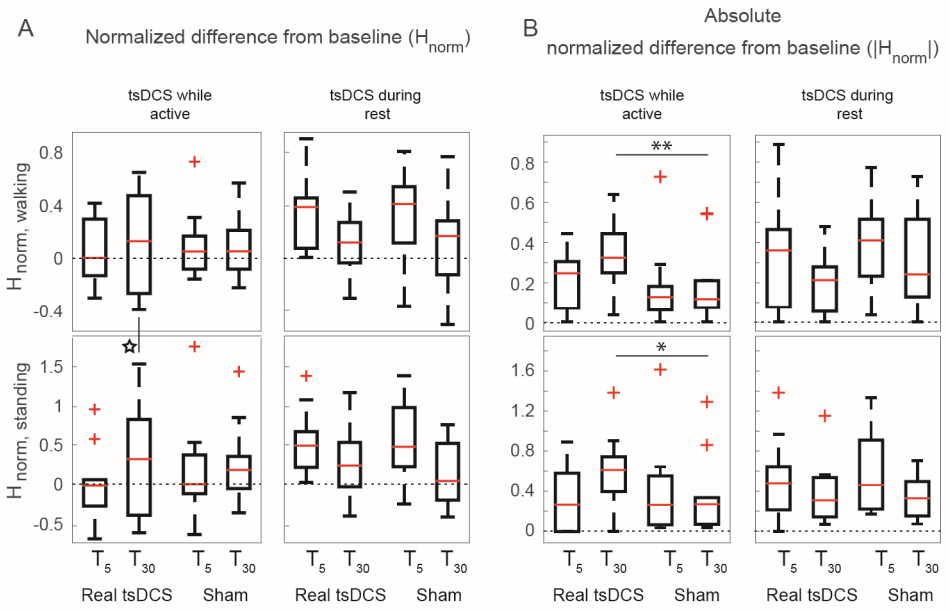

Figure 5: Boxplots of all H-reflex measurements and conditions. A) shows the "normalized difference from baseline", which is the percentual change with respect to baseline. B) is the "absolute normalized difference from baseline", which is the absolute value of (A) and therefore shows only modulation amplitude without considering directionality.

☆ Significant correlation (r_P=0.74, p=0.021), * significant at p < 0.05, ** significant at p < 0.01

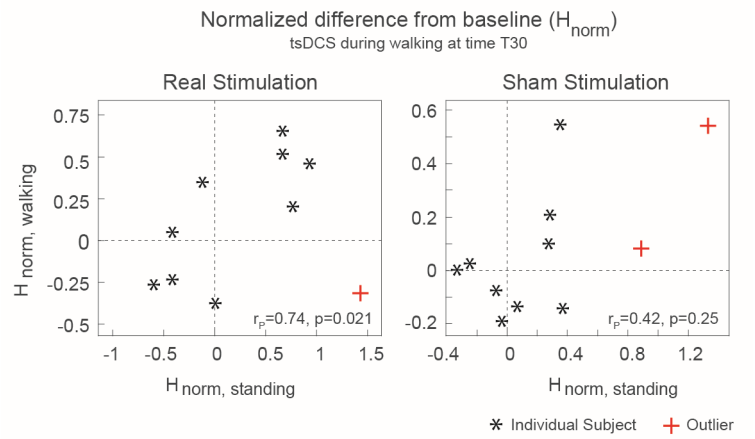

Figure 6: Individual subject values for the normalized difference to baseline (H_{norm}) for the H-reflex measurements during standing ($H_{norm,standing}$) and walking ($H_{norm,walking}$), 30 minutes after (T30) real or sham tsDCS was applied during walking. The values of both measurements were significantly correlated (r_P=0.74, p=0.021) after real tsDCS (Outliers excluded from correlation analysis based on Mahalanobis distance).

Subsequent Pearson correlation analysis revealed that $H_{norm,standing}$ and $H_{norm,walking}$ at time T30, when tsDCS was administered during walking, are significantly correlated (r_P=0.74, p=0.021) (fig. 5 and fig. 6). As a counter-test, we correlated $H_{norm,walking}$ and $H_{norm,standing}$ for the same condition and time after sham tsDCS, which led to no significant outcome (r_P=0.42, p=0.25) (fig. 6). Furthermore, within the same condition no significant dependencies were observed for each, $H_{norm,standing}$ and $H_{norm,walking}$ correlated with their corresponding changes of M_{max} and background EMG level.
With regards to the performed genetic analysis, BDNF Vall66Met genotype distribution was as follows: Val/Val: 6 subjects, Val/Met: 3 subjects, Met/Met: 1 subject. Subsequent analysis, conducted for $H_{norm,walking}$ and $H_{norm,standing}$ (real tsDCS, T30), did however not reveal a significant modulation difference between genotype groups.

Table 1: Results of Yuen-Welch's-test on the H-reflex normalized difference- (H_{norm}) and absolute normalized difference from baseline ($|H_{norm}|$) (see fig. 5). Each condition and timepoint was compared to its corresponding sham condition.

Normalized difference from baseline (H_{norm}):		**H-reflex during standing**		**H-reflex during walking**	
		t(5)	**p-value**	**t(5)**	**p-value**
Task	**tsDCS while active**				
Time	T5	-1.16	0.29	0.03	0.97
	T30	0.4	0.7	0.15	0.88
Task	**tsDCS during rest**				
Time	T5	-0.57	0.59	-0.44	0.67
	T30	0.61	0.56	-0.05	0.95
Absolute normalized difference from baseline ($\|H_{norm}\|$):					
Task	**tsDCS while active**				
Time	T5	-0.13	0.89	1.76	0.13
	T30	2.73	0.04*	3.85	0.01**
Task	**tsDCS during rest**				
Time	T5	-0.57	0.59	-0.86	0.42
	T30	-0.14	0.89	-0.71	0.50

* significant at p < 0.05, ** significant at p < 0.01

4.4 Discussion

The goal of this study, was to determine whether applying tsDCS during walking could induce a larger modulation effect on the soleus H-reflex, as compared to tsDCS applied during rest. The outcome is twofold. On the one hand, cathodal lumbar tsDCS during walking was able to significantly alter the soleus H-reflex amplitude 30 minutes after intervention, compared to the sham condition. On the other hand, this modulation was not directionally coherent across subjects. Whereas in some subjects a decrease was observed, the H-reflex was increased in others.

This led to insignificant differences in population means when modulation-direction was taken into account.

The strength of this result is supported by the fact that the amplitudes of both H-reflex measures during walking and standing were significantly different from sham. Furthermore, the directional changes within subjects were significantly correlated with each other across the two different measures (fig. 6). This can be regarded as evidence that our results are not coincidental, since the detected changes are visible and directionally coherent within subjects in both H-reflex measures. Furthermore, these modulatory effects were not correlated with variations in background EMG or the maximum M-wave of the corresponding condition. Therefore, there is no evidence that these changes occurred due to other influences, such as alterations in electrode-nerve connection or voluntary activity level.
The results are in line with the concept of activity-selectivity, which hypothesizes that ongoing activity in a network makes it sensitive to modulation by DC stimulation [10]. Furthermore, they agree with work done by others, which suggests that the modulatory effects of DC stimulation are highly influenced by the neural activity during the intervention. This has been shown in animal studies for tsDCS [23], DC stimulation in vivo [17] as well as tDCS in human subjects [13–16]. Whereas, to our knowledge this is the first study that investigated the activity dependency for tsDCS in the lumbar spinal cord, a particularly similar study by Kim et al. demonstrated that a combination of tDCS and voluntary grip exercises was more effective in increasing MEP amplitude, as compared to anodal tDCS or voluntary grip exercise alone [22].

As mentioned, these changes were not consistent in directionality across subjects. This implies that, although modulation magnitude was enhanced for tsDCS during walking, other components of the protocol were inadequate to foster response consistency across subjects. Based on what is known to influence stimulation outcome, many such factors exist [10]. Inconsistent responses across subjects are a common observation in human direct current stimulation studies [40]. In accordance to the data presented here, other studies, mainly using transcranial- DCS, report a poor response consistency across subjects [40–43] or within subjects across sessions [42,44]. Often, different subject groups are identified, such as responders and non-responders [40,44], or responders in both positive- and negative- directions [42]. In both scenarios, the resulting overall effect decreases or may vanish when response differences across subjects are not considered specifically. This can be achieved by identifying population sub-groups, or including the analysis of absolute changes such as we did here.

One possible source of variation shown by others [20,21,45], are the different polymorphisms of BDNF due to its involvement in neuroplasticity and synapse function [46–48]. However, our analysis does not show such a clear dependency for the data presented here. Nonetheless, since genetic influences have shown to be important in regulating electromodulatory responses [21] it cannot be excluded that there are other genetic factors, that have an influence on tsDCS effects.

4.4.1 Clinical and scientific implications

In recent years, electrotherapeutic therapies for injuries of the spinal cord have received growing attention. Particularly invasive, pulsed stimulation techniques, applied in combination with

intensive manual therapy, have led to the successful restoration of some voluntary movement control in a limited number of human subjects.

Since tsDCS has shown to be able to modulate corticospinal circuitry, the technique could possibly be considered as a non-invasive counterpart to the mentioned invasive approaches. Part of the appeal of DC stimulation are its ease of application, as well as the high tolerability due to the relatively low stimulation intensity.

However, a challenging question is how tsDCS must be applied in a rehabilitation setting. We attempted to contribute to this question with this study. In conformity with previous research [10], our results suggest that increased neural activity in the targeted pathways during direct current stimulation can create favorable conditions for fostering long term plasticity changes and thus lead to larger post intervention effects. For the application in a neurorehabilitation setting, this suggests that tsDCS should be paired with meaningful functional movements such as walking therapy.

That subjects responded differently leads to the conclusion that future efforts should focus on understanding and controlling intersubject response variability. This applies specifically to effect directionality, which refers to either-up or downregulation of neural signaling. In a clinical application, the ability to control modulation direction would be especially relevant. For instance, whereas reducing spasticity may require the downregulation of the reflexive pathways, an increase in corticospinal connection strength is required when aiming to aid voluntary motor control. Further investigation in this direction could be performed by varying electric field amplitude and direction [10,11,49] in combination with pathway specific neural activity [10]. In parallel to that, screening for other, known genetic dependencies may additionally help to explain response differences across subjects [21].

4.5 Conclusion

We showed that the H-reflex amplitude was significantly more modulated when tsDCS was applied during walking as opposed to tsDCS during lying, which conforms with the results shown in previous studies. This suggests, that future studies aiming to modulate motor function in the spinal cord using sub-threshold electrical stimulation, should consider combining tsDCS with voluntary activation. The direction of modulation was, however, inconsistent across subjects. Although this is not uncommon in DC stimulation studies, it highlights the importance of a more thorough screening of the influence of protocol specific variables on subject specific intervention outcome, which is needed if tsDCS is to find its way into clinical practice.

References

[1] Priori A, Ciocca M, Parazzini M, Vergari M and Ferrucci R 2014 Transcranial cerebellar direct current stimulation and transcutaneous spinal cord direct current stimulation as innovative tools for neuroscientists. *J. Physiol.* **592** 3345–69

[2] Ho C H, Wuermser L A, Priebe M M, Chiodo A E, Scelza W M and Kirshblum S C 2007 Spinal Cord Injury Medicine. 1. Epidemiology and Classification *Arch. Phys. Med. Rehabil.* **88**

[3] Lamy J-C, Ho C, Badel A, Arrigo R T and Boakye M 2012 Modulation of soleus H reflex by spinal DC stimulation in humans. *J. Neurophysiol.* **108** 906–14

[4] Hubli M, Dietz V, Schrafl-Altermatt M and Bolliger M 2013 Modulation of spinal neuronal excitability by spinal direct currents and locomotion after spinal cord injury. *Clin. Neurophysiol.* **124** 1187–95

[5] Cogiamanian F, Vergari M, Pulecchi F, Marceglia S and Priori A 2008 Effect of spinal transcutaneous direct current stimulation on somatosensory evoked potentials in humans. *Clin. Neurophysiol.* **119** 2636–40

[6] Bocci T, Marceglia S, Vergari M, Cognetto V, Cogiamanian F, Sartucci F and Priori A 2015 Transcutaneous Spinal Direct Current Stimulation (tsDCS) Modulates Human Corticospinal System Excitability *J. Neurophysiol.* jn.00490.2014

[7] Cogiamanian F, Ardolino G, Vergari M, Ferrucci R, Ciocca M, Scelzo E, Barbieri S and Priori A 2012 Transcutaneous Spinal Direct Current Stimulation *Front. Psychiatry* **3**

[8] Nakazawa K, Kawashima N and Akai M 2006 Enhanced stretch reflex excitability of the soleus muscle in persons with incomplete rather than complete chronic spinal cord injury *Arch. Phys. Med. Rehabil.* **87** 71–5

[9] Thompson A K, Pomerantz F R and Wolpaw J R 2013 Operant conditioning of a spinal reflex can improve locomotion after spinal cord injury in humans. *J. Neurosci.* **33** 2365–75

[10] Bikson M and Rahman A 2013 Origins of specificity during tDCS: anatomical, activity-selective, and input-bias mechanisms. *Front. Hum. Neurosci.* **7** 688

[11] Rahman A, Reato D, Arlotti M, Gasca F, Datta A, Parra L C and Bikson M 2013 Cellular effects of acute direct current stimulation: somatic and synaptic terminal effects. *J. Physiol.* **591** 2563–78

[12] Kuck A, Stegeman D and van Asseldonk E 2017 Modeling trans-spinal direct current stimulation for the modulation of the lumbar spinal motor pathways *J. Neural Eng.* **14**aa7960

[13] Bortoletto M, Pellicciari M C, Rodella C and Miniussi C 2015 The interaction with task-induced activity is more important than polarization: A tDCS study *Brain Stimul.* **8** 269–76

[14] Kaski D, Dominguez R O, Allum J H, Islam a F and Bronstein a M 2014 Combining physical training with transcranial direct current stimulation to improve gait in Parkinson's disease: a pilot randomized controlled study. *Clin. Rehabil.* **28** 1115–24

[15] Gill J, Shah-Basak P P and Hamilton R 2015 It's the thought that counts: Examining the task-dependent effects of transcranial direct current stimulation on executive function *Brain Stimul.* **8** 253–9

[16] Sriraman A, Oishi T and Madhavan S 2014 Timing-dependent priming effects of tDCS on ankle motor skill learning *Brain Res.* **1581** 23–9

[17] Kronberg G, Bridi M, Abel T, Bikson M and Parra L C 2016 Direct Current Stimulation Modulates LTP and LTD: Activity Dependence and Dendritic Effects *Brain Stimul.* **10** 51–8

[18] Radman T, Su Y, An J H, Parra L C and Bikson M 2007 Spike Timing Amplifies the Effect of Electric Fields on Neurons: Implications for Endogenous Field Effects *J. Neurosci.* **27** 3030–6

[19] Radman T, Ramos R L, Brumberg J C and Bikson M 2009 Role of cortical cell type and morphology in subthreshold and suprathreshold uniform electric field stimulation in vitro *Brain Stimul.* **2**215–228.e3

[20] Lamy J-C and Boakye M 2013 BDNF Val66Met polymorphism alters spinal DC stimulation-induced plasticity in humans. *J. Neurophysiol.* **110** 109–16

[21] Wiegand A, Nieratschker V and Plewnia C 2016 Genetic Modulation of Transcranial Direct Current Stimulation Effects on Cognition *Front. Hum. Neurosci.* **10**

[22] Kim G W and Ko M H 2013 Facilitation of corticospinal tract excitability by transcranial direct current stimulation combined with voluntary grip exercise *Neurosci. Lett.* **548** 181–4

[23] Ahmed Z 2011 Trans-spinal direct current stimulation modulates motor cortex-induced muscle contraction in mice. *J. Appl. Physiol.* **110** 1414–24

[24] Liebetanz D, Koch R, Mayenfels S, König F, Paulus W and Nitsche M A 2009 Safety limits of cathodal transcranial direct current stimulation in rats *Clin. Neurophysiol.* **120** 1161–7

[25] Winkler T, Hering P and Straube a. 2010 Spinal DC stimulation in humans modulates post-activation depression of the H-reflex depending on current polarity *Clin. Neurophysiol.* **121** 957–61

[26] Zehr E P 2002 Considerations for use of the Hoffmann reflex in exercise studies *Eur. J. Appl. Physiol.* **86** 455–68

[27] Tokuno C D, Garland S J, Carpenter M G, Thorstensson A and Cresswell A G 2008 Sway-dependent modulation of the triceps surae H-reflex during standing. *J. Appl. Physiol.* **104** 1359–65

[28] Knikou M 2008 The H-reflex as a probe: pathways and pitfalls. *J. Neurosci. Methods* **171** 1–12

[29] Pierrot-Deseilligny E and Burke D 2012 The Circuitry of the Human Spinal Cord of Movement: Spinal and Corticospinal Mechanisms of Movement - Back Matter *The Circuitry of the Human Spinal Cord of Movement: Spinal and Corticospinal Mechanisms of Movement* pp 33–5

[30] Stein R B, Estabrooks K L, McGie S, Roth M J and Jones K E 2007 Quantifying the effects of voluntary contraction and inter-stimulus interval on the human soleus H-reflex *Exp. Brain Res.* **182** 309–19

[31] Simonsen E B, Alkjær T and Raffalt P C 2012 Reflex response and control of the human soleus and gastrocnemius muscles during walking and running at increasing velocity *Exp. Brain Res.* **219** 163–74

[32] Knikou M, Angeli C A, Ferreira C K and Harkema S J 2009 Soleus H-reflex modulation during body weight support treadmill walking in spinal cord intact and injured subjects *Exp. Brain Res.* **193** 397–407

[33] O'Connor C M, Thorpe S K, O'Malley M J and Vaughan C L 2007 Automatic detection of gait events using kinematic data *Gait Posture* **25** 469–74

[34] Simonsen E B and Dyhre-Poulsen P 1999 Amplitude of the human soleus H reflex during walking and running. *J. Physiol.* **515 (Pt 3** 929–39

[35] Yuen K K 1974 The two-sample trimmed t for unequal population variances *Biometrika* **61** 165–70

[36] Erceg-Hurn D M and Mirosevich V M 2008 Modern robust statistical methods: An easy way to maximize the accuracy and power of your research. *Am. Psychol.* **63** 591–601

[37] Wilcox R 2005 *Introduction to Robust Estimation and Hypothesis Testing* vol 47

[38] De Maesschalck R, Jouan-Rimbaud D and Massart D L L 2000 The Mahalanobis distance *Chemom. Intell. Lab. Syst.* **50** 1–18

[39] Finch W H 2012 Distribution of variables by method of outlier detection *Front. Psychol.* **3**

[40] Wiethoff S, Hamada M and Rothwell J C 2014 Variability in response to transcranial direct current stimulation of the motor cortex *Brain Stimul.* **7** 468–75

[41] Horvath J C, Vogrin S J, Carter O, Cook M J and Forte J D 2016 Effects of a common transcranial direct current stimulation (tDCS) protocol on motor evoked potentials found to be highly variable within individuals over 9 testing sessions *Exp. Brain Res.* **234** 2629–42

[42] Strube W, Bunse T, Nitsche M A, Nikolaeva A, Palm U, Padberg F, Falkai P and Hasan A 2016 Bidirectional variability in motor cortex excitability modulation following 1 mA transcranial direct current stimulation in healthy participants. *Physiol. Rep.* **4** 307–21

[43] López-Alonso V, Cheeran B, Río-Rodríguez D and Fernández-Del-Olmo M 2014 Inter-individual variability in response to non-invasive brain stimulation paradigms *Brain Stimul.* **7** 372–80

[44] López-Alonso V, Fernández-del-Olmo M, Costantini A, Gonzalez-Henriquez J J and Cheeran B 2015 Intra-individual variability in the response to anodal transcranial direct current stimulation *Clin. Neurophysiol.* **126** 2342–7

[45] Fritsch B, Reis J, Martinowich K, Schambra H M, Ji Y, Cohen L G and Lu B 2010 Direct current stimulation promotes BDNF-dependent synaptic plasticity: Potential implications for motor learning *Neuron* **66** 198–204

[46] Lu B 2003 BDNF and Activity-Dependent Synaptic Modulation *Learn. Mem.* **10** 86–98

[47] Crozier R a, Bi C, Han Y R and Plummer M R 2008 BDNF modulation of NMDA receptors is activity dependent. *J. Neurophysiol.* **100** 3264–74

[48] Bramham C R and Messaoudi E 2005 BDNF function in adult synaptic plasticity: The synaptic consolidation hypothesis *Prog. Neurobiol.* **76** 99–125

[49] Kuck A, Stegeman D and van Asseldonk E 2017 Modeling trans-spinal direct current stimulation for the modulation of the lumbar spinal motor pathways *J. Neural Eng.* **14** 56014

Chapter V – Modeling Trans-Spinal Direct Current Stimulation in the Presence of Spinal Implants

A. KUCK [1], D.F. STEGEMAN[2] and E.H.F. VAN ASSELDONK[1]

[1] University of Twente, Drienerlolaan 5, 7522 NB Enschede, The Netherlands

[2] Radboud University Medical Center, Donders Institute for Brain, Cognition and Behavior, Department of Neurology/Clinical Neurophysiology, Reinier Postlaan 4, 6500HB Nijmegen, The Netherlands.

Abstract

Objective. Trans-spinal Direct Current Stimulation (tsDCS) is a technique considered for the treatment of corticospinal damage or dysfunction. TsDCS aims to induce functional modulation in the corticospinal circuitry via a direct current (DC) generated electric field. To ensure subject safety, subjects with metallic implants are generally excluded from receiving neural DC stimulation. However, spinal injuries often require spinal implants for stabilization. Our goal was to investigate implant imposed changes to electric field (EF) and current density (CD) magnitude during tsDCS. Approach. We simulated the EF and CD, generated by tsDCS in the presence of spinal rods for two electrode configurations and four implant locations along the spinal cord. For each scenario a no-implant condition was computed for comparison. We assessed changes in EF and CD at the implant location and the EF inside the spinal cord. Main results. Our results show that implant presence was able to influence peak CD, compared to the no-implant condition. Nonetheless, the highest calculated CD levels were a factor six lower than those thought to lead to hazardous tissue damaging effects. Additionally, implant presence did not considerably affect the average EF inside the spinal cord. Our findings do therefore not indicate potentially unsafe CD levels, or significant alterations to stimulation intensity inside the spinal cord, caused by a spinal implant during tsDCS. Significance. Our results are relevant to the safety of transcutaneous spinal stimulation applied in the presence of metallic spinal implants.

5.1 Introduction

Trans-spinal direct current stimulation (tsDCS) is an emerging neuromodulatory tool under development, aiming to alter neural function in the spinal cord. If successful the intervention may be suitable for the rehabilitation of spinal cord injury (SCI), or the treatment of other neural dysfunctions of the cortico-spinal tract. TsDCS is part of a collection of tools, which have the goal to modulate nervous system function via an imposed electric field [1]. Whereas the application of most neural DC stimulation methods has mainly been limited to the cortex, tsDCS has the goal to modulate neural function in a spinal target region, via a subthreshold Direct Current (DC) generated electric field (EF), applied with electrodes placed on the skin. Modulation effects of tsDCS on the corticospinal circuitry have thereby been shown for H-Reflex recruitment [2,3], presynaptic inhibition [4], lower limb somatosensory evoked potentials [5] and lower limb motor evoked potentials (for a more comprehensive review, see [6]).

While intervention efficacy is necessary, safety is paramount for a successful clinical application. Safety concerns are thereby related to stimulation induced tissue damage, which can be caused by an improperly designed stimulation protocol [7]. In past studies, tissue damage has been associated with a prolonged accumulation of charge in the stimulated tissue, above a certain tolerable threshold. The most relevant proposed predictor, for DC stimulation evoked tissue damage, is thus local current density magnitude (A/m^2) [8] in combination with the time of exposure. Recent estimates, based on animal studies in combination with computer simulations, suggest current density thresholds for neural tissue damage of 6.3 A/m^2 to 17 A/m^2, [9]. In comparison to that, conventionally used tDCS and tsDCS protocols in humans, produce current densities that are approximately one order of magnitude lower than these estimates (at currents $\leq$ 4 mA) without leading to serious adverse effects. For a comprehensive review we refer to [9].

Due to possible interaction effects, the administration of DC stimulation is commonly restricted by a number of exclusion criteria which, among others, includes the presence of metallic or highly conductive objects in the body. In theory, the implant may lead to an altered current flow in the surrounding tissue and increase the chance of locally high current concentrations with potentially damaging effects. However, although initial studies have not been able to support these initial safety concerns [9,10], there is still insufficient evidence to support the development of clear safety guidelines for the administration of tsDCS or tDCS in the presence of metal implants.

A central goal is to utilize tsDCS for the treatment of an injury or dysfunction of the spinal cord. Since spinal implants are prevalent in patients with spinal cord injury, some patients may be restricted from receiving tsDCS. Albeit not always the case, spinal cord injury is often caused by a fracture of the spinal vertebrae. When vertebrae are severely damaged metal implants are used to stabilize the affected spinal region. It is therefore important, to understand the implications of the presence of a spinal implant during tsDCS. Thereby the first question is whether the presence of an implant can alter the tsDCS generated electric field and current density to result in potentially hazardous scenarios, such as a large increase in current density. The second question is, to which extent the electric field inside the spinal cord, intended to stimulate neural circuitry, is affected by the presence of a spinal implant.

To address these questions, we simulated the electric field generated by tsDCS in the presence of a spinal implant. We took into account two different electrode configurations, as well as four varying spinal implant locations in the cervical, thoracic and thoracolumbar spinal cord. The effect of an implant at each of the four locations, in combination with one of the two electrode configurations, was calculated separately. Additionally, a no-implant scenario was computed for each of the possible combinations. We assessed local changes in electric field and current density at the implant location, as well as the electric field inside the entire spinal cord.

5.2 Methods

5.2.1 Model

All computations were based on an MRI derived, segmented finite element body model (Ella), which is part of the publicly available virtual population library (version 2.0) [11] and consists of 22 individual tissue compartments. Four spinal implants, as well as spinal grey matter which were

not included in the original model, were added manually. Spinal implants and grey matter were modeled in 3ds Max (2015) (Autodesk, Inc., San Rafael, CA, USA). Model implementation and finite element calculations were conducted using the open-source program SCIrun (version 4.7) [12].

We considered two different electrode configurations: 1) the active and passive electrodes positioned on the 11th thoracic vertebra and the left, posterior shoulder respectively (lumbar spinal cord – shoulder: LSC-S) and 2) both electrodes positioned in equal distance, 7 cm above and below vertebra T11 (LSC ±) (fig. 1). Both configurations have been used in previous studies to target the neural structures in the lumber spinal cord, located at the level of vertebra T11. The rectangular surface electrodes (50 × 70 × 4 mm, 35 cm^2 skin contact) were positioned according to the corresponding electrode configuration in direct contact with the skin surface. Electrode potentials, inducing a 2.5mA current, were assigned to the outer surface nodes of each electrode mesh.

Tissue conductivity values were adopted from Parazzini et al. without change [13]. The electrode was assigned the conductivity of saline (1.4 S/m). Metallic implants in the body are enclosed by a double layer impedance, generated by electrochemical processes at the tissue-metal interface [7]. Whereas metal is as an electron current carrier, current carried through the body is ionic. Therefore, a large impedance is expected between the metal implant and the surrounding tissue [7,9]. According to Theeuwen et al., this double layer impedance Z can be described by

$$Z(\omega) = \frac{K}{\left(i\frac{\omega}{2\pi}\right)^{v}} \qquad (1)$$

as a function of the angular velocity $\omega = 2\pi f$ with f the frequency [14]. Also, K is a proportionality constant, $i = \sqrt{-1}$ and v an empirical factor. For a constant EF, it follows that $\lim_{f \to 0} \frac{K}{(if)^{v}} = \infty$, and thus the double layer acts as an insulator, or very large resistor. We therefore assign the implant with a conductivity of 10^{-8} S/m to act as large resistor with respect to all other tissue model compartments.

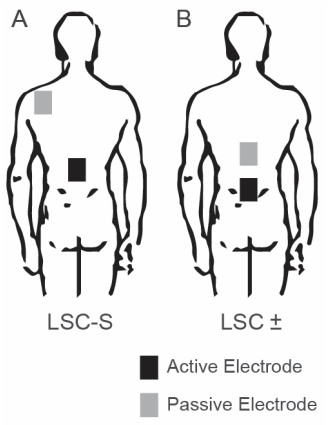

Figure 1: The simulated electrode placement configurations. A) Active electrode on the lumbar spinal cord (LSC), return electrode on the posterior left shoulder (LSC - S). B) Active electrode below and passive electrode above the lumbar spinal cord (LSC ±).

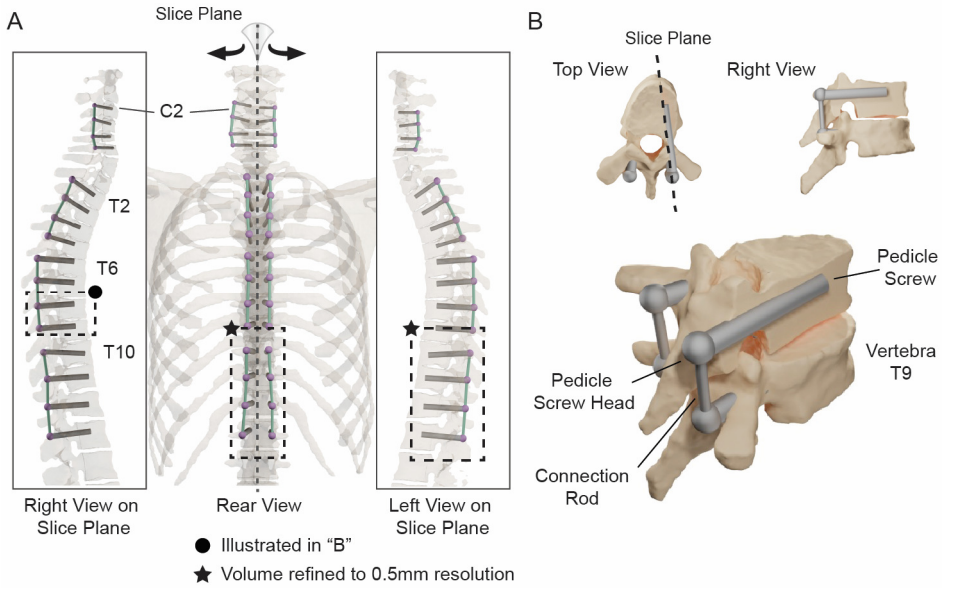

Figure 2: A) Illustration of all four implants and their locations in the spinal cord of the utilized FE model. A vertical slice plane is used to show the left and right sections of each implant separately. B) Detail view of the lower two pedicle screw segments of the third spinal implant (as indicated in A). Vertebra T8 is vertically sliced in line with the screw (see top view), entering through the right pedicle to illustrate screw placement within the vertebral body. Additionally, the volume used for resolution refinement (2mm to 0.5mm) is illustrated for an exemplary implant (A).

5.2.2 Spinal Implant Geometry

Four spinal implants were modeled resembling the geometry of the Harrington rod, each bridging four vertebrae in the cervical (C2-C5) as well as upper (T2-T5), middle (T6-T9) and lower(T10-L1) thoracic spinal cord (fig. 2 and table 1). We refer to each implant by using the highest of the four vertebrae it spans (e.g. implant C2).

Each implant was assembled out of simplified representations of its three main components: pedicle screw (cylinder), pedicle screw head (sphere) and connection rod (cylinder) (table 2), by adhering to dimensions and placements similar to those used in medical practice [15–17].

Table 1: Reference and location for all modeled implants.

Implant Number:	1	2	3	4
Implant Reference:	C2	T2	T6	T10
Vertebrae:	C2 - C5	T2 – T5	T6 - T9	T10 – L1

Table 2: Specification of the individual parts, each implant was assembled with. Dimensions of pedicle screw diameter and length were adapted based on implant location.

Part:	**Simplified as:**	**Dimensions [mm]:**				
Pedicle Screw	Cylinder	Implant:	C2	T2	T6	T10
		Diameter:	3	4.35	6	6
		Length:	25	30	40	45
Pedicle Screw Head	Sphere	Diameter: 8				
Connection Rod	Cylinder	Diameter: 3				

5.2.3 Finite Element Computation:

The steady state electrical potential in the inhomogeneous volume conductor model is computed by solving the function described by Poisson's equation

$$\nabla (\sigma \nabla \Phi) = 0 \quad (2)$$

where σ is a conductivity tensor and Φ is the electric potential. Subsequently the electric field vector E is calculated by

$$E = -\nabla \Phi. \quad (3)$$

The corresponding current density J is approximated via

$$J = \sigma E. \quad (4)$$

Equation 1 is solved, given a hexagonal element mesh, a set of known conductivities as well as potentials corresponding to the electrode locations. Finite element calculations were done in two stages using a conjugate gradient descend algorithm with a target error of 10^{-18}. During the first stage, a solution for the entire body was computed at varying voxel resolutions of $8mm^3$ in the head and extremities, 4-2 mm^3 in the torso as well as $2mm^3$ at the implant, electrodes and inside the spinal cord. In a second stage, the resolution around the spinal implant was increased to 0.5 mm^3 by separately computing the implant in isolation within a cubic space, factor 1.4 times the size of the implant (see fig. 2). Thereby the outer boundary nodes of the isolated model were assigned with the solution of the first stage via a first-order linear interpolation.

5.2.4 Simulation Conditions and Data Reporting

We computed the electric field and current density for both electrode configurations (see fig. 1) at the location of each implant as well as in the entire spinal cord, with and without the implant present. The effect of each implant was thus considered separately to take into account the impact of varying implant location. Computationally, the same mesh was used for both, implant and no-implant, scenarios. In the implant scenario, a mask of the implant was applied and the affected tissue conductivity values were replaced with those of the implant.

Since our main motivations are safety considerations related to the presence of spinal implants during tsDCS, we focus on reporting peak field amplitudes, determined within a volume of 10mm distance around the corresponding implant surface. For each implant location and electrode configuration, we thus report the peak electric field and current density magnitudes within this volume for each: the Spinal Cord (includes white and grey matter), bone as well as the surrounding soft tissue (all remaining soft tissue, excluding corticospinal fluid).
In addition to that, we report the EF in the spinal grey matter, to obtain an estimate of the possible consequences on the intended tsDCS application.

5.3 Results

Representative examples of the obtained results can be seen in figure 3. Shown are two cross sections through the implant when placed at location T10 for electrode configurations LSC-S and LSC ±. For each cross section, model compartments (e.g. tissue type or implant), the EF with and without the implant as well as the difference between the two scenarios are illustrated. When an implant was present, this led to a change in EF magnitude at- and in close proximity to the implant surface.

5.3.1 TsDCS without the presence of implants

For configuration LSC-S, without the presence of implants, peak electric field density values measured around each of the corresponding implant sites reached maximum magnitudes of 7.028 V/m in the bone, at implant location T6 (fig. 4A). Electric field strengths in the tissue and Spinal Cord reached maximum values of 4.94 V/m (T2) and 2.6 V/m (T6) respectively. The lowest EF magnitudes were measured in the cervical spinal cord (C2), which were decreased to approximately one-fifth compared to the peak amplitudes at thoracic spinal cord locations. The overall largest peak current density values were observed the surrounding tissue with maximum values of 0.55 A/m^2 (T6). Peak magnitudes in bone and Spinal Cord reached 0.11 A/m^2 (T6) and 0.4 A/m^2 (T6) respectively.

Due to the lower placement position of both stimulation electrodes, tsDCS with configuration LSC ± resulted in a weaker electric field magnitude in higher locations (C2 and T2) compared to configuration LSC-S, while overall reaching similar peak EF magnitudes of 7.7 V/m (T6) in the bone, 5.38 V/m (T10) in the tissue and 3.6 V/m (T10) in the spinal cord (fig. 4B). Current density was highest inside the tissue at implant location T10 with 0.66 A/m^2. Values in the bone and spinal cord peaked at 0.15 A/m^2 (T6) and 0.59 A/m^2 (T10) respectively.

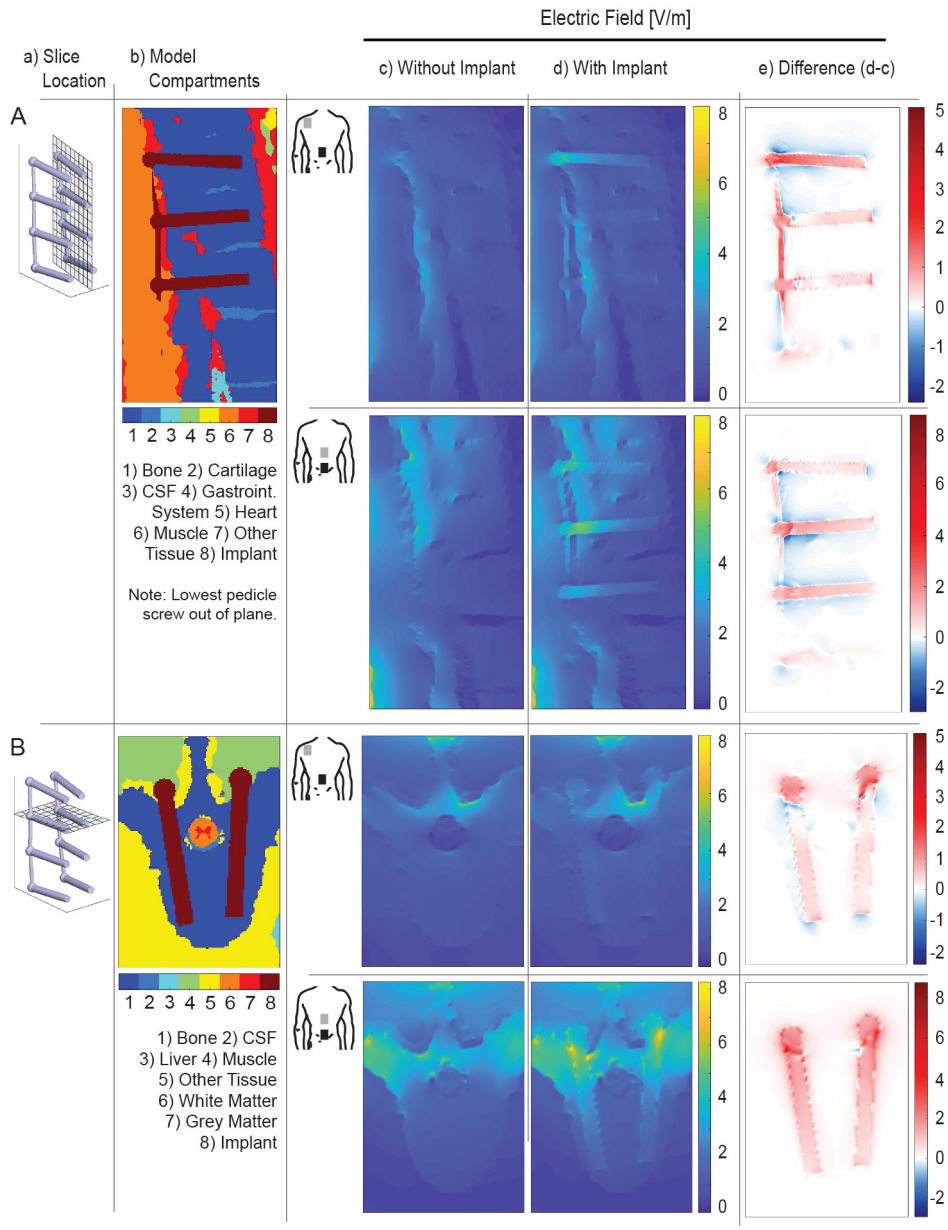

Figure 3: Representative examples of the simulated electric field for both electrode configurations with the implant located at T10. Longitudinal (row 1) and transverse (row 2) cross section through the implant, showing: the slice location (column a), model compartments (col. b) as well as the electric field magnitude without (col. c) and with (col. d) the implant present. Additionally, the difference between the two scenarios (d-c) is shown (col. e). Note: in row 1, the lowest pedicle screw is out of plane and thus not visible in the slice.

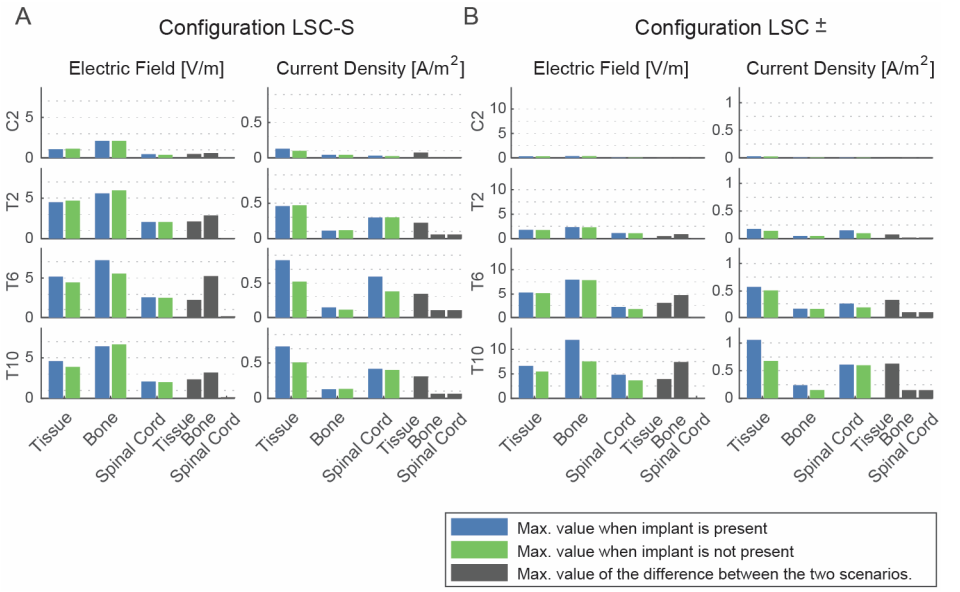

Figure 4: Maximum electric field and current density magnitude for all implant sites and both configurations (A/B). Results are shown with and without the corresponding implant, as well as for the difference between the two conditions. Note: The reported maxima may not occur at the same physical location in the model.

5.3.2 The impact of implant presence on EF and CD amplitude

Simulation in the presence of implants predominantly resulted in values of similar magnitude, compared to the scenarios with no implant present. However, in some instances the presence of implants led to considerable increases of the maximum electric field and, consequently, current density amplitude.

For configuration LSC-S, a maximum local increase of 5.57 V/m in the bone, 2.32 V/m in the surrounding tissue and 0.15 V/m in the Spinal Cord (implant at T6, for all), were observed. Accordingly, with little influence on maximum current density values, current density increased locally by a maximum of 0.37 A/m² (T16) in the adjacent tissue and 0.11 A/m² (T6) in the bone and Spinal Cord. For implant locations T6 and T10, this consequently led to a mentionable increase in overall peak current density inside the tissue, of 60 % and 45 % respectively (fig. 4A, rows 3 and 4).

For configuration LSC ±, the electric field and current density magnitudes were increased compared to the no-implant scenario, when the implant was placed at position T10. This led to peak EF magnitudes of 11.78 V/m in the bone and 6.52 V/m in the surrounding tissue (fig. 4B, row 4). Accordingly, maximum current density amplitudes were 1.04 A/m² and 0.23 A/m² for tissue and bone respectively. This corresponds to a respective peak current density increase of 58% (in tissue) and 64% (in bone) compared to the no implant scenario.

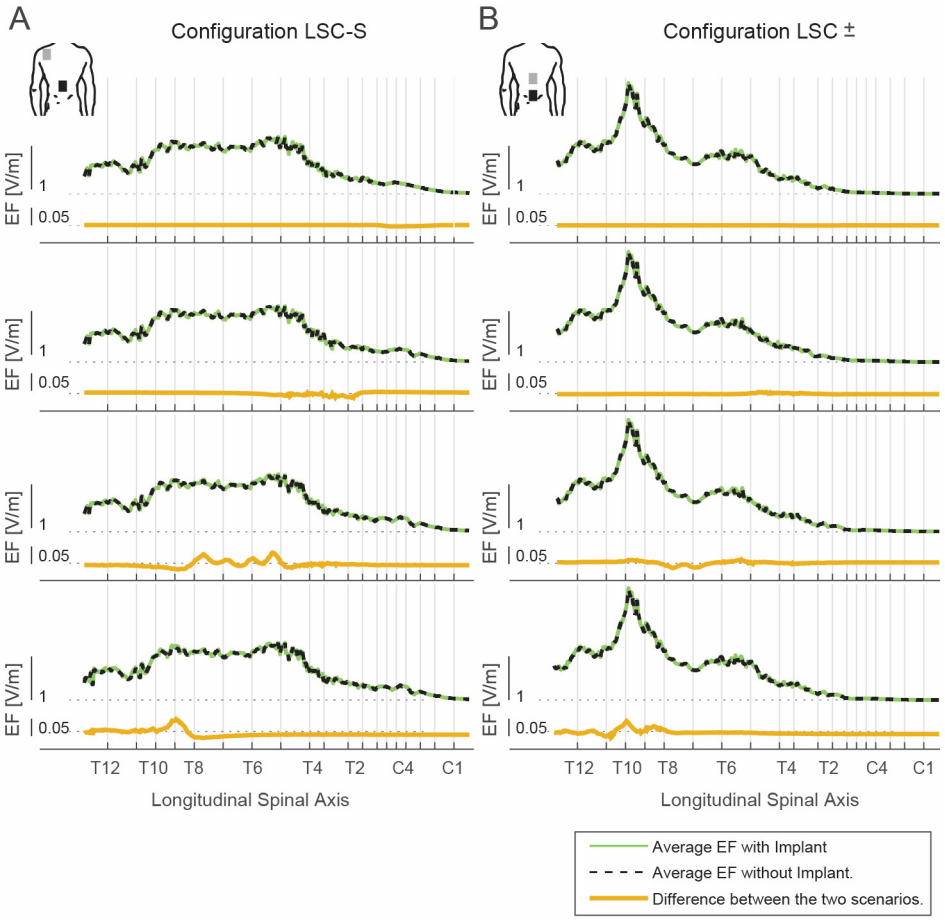

Figure 5: Transverse average of the electric field magnitude inside the spinal cord, calculated over 2mm transverse slices of the spinal grey matter along the longitudinal spinal axis, for both electrode configurations with and without the corresponding implant present, as well as the difference between the two.

5.3.3 Electric Field inside the Spinal Cord

Since tsDCS is a potential intervention option for the treatment of disorders, or injuries, of the spinal cord, it is important to probe to which extend the presence of a spinal implant may affect the electric field magnitude inside the spinal cord. Figure 5 shows the transverse mean EF magnitude in longitudinal direction, inside the spinal grey matter for each of the four spinal implants and both electrode configurations. For all implant placements and both electrode configurations, the absolute deviations introduced by the presence of each implant are marginal. Thereby, all induced EF magnitude differences were below 0.1 V/m and restricted to the area surrounding the implant location.

5.4 Discussion

Our goal was to investigate the changes in tsDCS induced electric field and current density magnitude, caused by the presence of a spinal implant. The central question was, whether the associated changes in current density magnitude could reach potentially harmful levels, which have been associated with tissue damage. Furthermore, we asked whether the presence of a spinal implant could have a disruptive influence on the magnitude of a tsDCS induced electric field meant to target the neural structures in the spinal cord.

We addressed these questions by calculating the electric field and current density, in an MRI-derived representation of a female volunteer, for two different tsDCS electrode configurations at a current of 2.5 mA, with four varying implant locations along the spinal cord. For comparison, a healthy control scenario with no implant present was computed for each of the above-mentioned combinations of implant location and electrode configuration.

Our results show that, expectedly, the electric field and thus current density were changed at each of the four investigated implant locations when an implant was present compared to the no implant scenario. While not generalizable to all implant locations, in some instances this resulted in a substantial increase in current density magnitude in the surrounding tissue. This was the case for implant locations T6 and T10 for configuration LSC-S, as well as location T10 for configuration LSC ±. However, the resulting current density levels in implant presence were well below the magnitudes previously reported to lead to tissue damage [9]. Furthermore, the average EF magnitude inside the spinal cord was not significantly affected by the presence of the implant, compared to the no-implant condition.

5.4.1 Implant induced electric field and current density changes

When tsDCS was applied without an implant present, peak electric field magnitudes were observed inside, as well as at the surface of the vertebral bone. This may be attributed to the higher resistance of the bone (0.02 S/m), compared to the surrounding tissue (muscle: 0.16 S/m, other (lumped) tissue: 0.08 S/m).

When an implant was present, this led to a change in EF magnitude at- and in close proximity to the implant surface (fig. 3). This "edge effect" can be observed around the boundary of a model compartment (such as a tissue or the implant), with a high conductivity difference compared to the surrounding tissue, e.g. stimulation electrodes [18], accumulations of corticospinal fluid [19] or metallic skull plates [10]. In our case, the implant imposed changes to the surrounding EF magnitude were in proportion to the surrounding electric field (fig. 4). Our results are similar to those reported by Datta et al., [10] who showed no significant increase in EF magnitude due to the presence of skull plates during tsDCS, despite local changes in proximity to the implant.

5.4.2 Clinical Considerations

TsDCS is being developed as a possible neuromodulatory intervention for the rehabilitation of spinal cord injury. As some percentage of spinal cord injuries will result in the placement of spinal implants, this may pose an obstacle to the successful clinical application of tsDCS, since the presence of metallic parts in the human body is still considered to be a reason for the exclusion from electrotherapeutic intervention. Especially, if we assume that the likelihood for a patient to

receive a spinal implant increases with the associated damage to the spinal cord, this may lead to the exclusion of some patients within the targeted patient population.

In the no-implant scenario, current density magnitude reached a maximum of 0.55 A/m^2 (in tissue, T6, config. 1). The current density in the spinal cord reached values of up to 0.4 A/m^2. The peak value inside the grey matter is calculated to be approximately ten times lower compared to that observed in the white matter. Since, 1) this is at least one order of magnitudes lower than the estimated DC current density threshold for tissue damage (6.3 A/m^2 to 17 A/m^2) [9] and 2) the same intensity has previously been applied in human tsDCS experiments without adverse effects [2–4,6,20], there are no indications to regard these levels as unsafe for human use.

When an implant is present, current density increases at- and close to the border of the implant (fig. 3). Importantly, the largest determined peak current density magnitude across all implant positions and electrode configurations (1.04 A/m^2) was a factor of six lower, than the most pessimistic estimated DC current density threshold for tissue damage (6.3 A/m^2) [9] (fig. 4). Our results do therefore not indicate the occurrence of potentially unsafe current density levels due to the presence of a spinal implant during tsDCS.

Furthermore, there is no indication that the presence of a spinal implant would result in significant changes in stimulation effect when compared to the control condition. The central working mechanism, by which direct current stimulation enables the modulation of neural function, is thought to be the polarization of neural structures via an imposed electric field [21]. As we show (fig. 5), the average electric field magnitude inside the spinal cord is little affected by the presence of an implant, even when located in close proximity. The EF in the spinal cord located further from the implant was not affected.

5.4.3 Limitations

The modeling approach we utilized encompassed several simplifications, which is important for the interpretation of the presented results. Primarily, our results should be regarded from a qualitative perspective. Quantitative accuracy is thus limited by the properties of the model, such as model geometry and parametrization. The chosen model geometry is the segmented MRI model of a female volunteer, which has been simplified to 22 tissue compartments. The segmentation fails to describe smaller anatomical details, e.g. nerves or blood vessels, as well as within organ inhomogeneities, such as the difference between compact and spongy bone. Furthermore, the custom-made implant models are simplified representations of spinal rod geometry, which were intended to resemble spinal implant location and dimensions. They therefore do not include geometric details, e.g. screw threads. In addition to that, we used isotropic conductivity values for all, but one (white matter), model compartments. Real conductivity values are generally anisotropic, whereby directional conductivity is governed by the microscopic anatomic structure of the corresponding tissue, such as muscular- or neural fiber orientation. Based on the mentioned limitations, it is evident that our results cannot be quantitatively generalized to human experiments in vivo. Rather, they should be viewed as first step and serve as a basis for further investigation.

5.5 Conclusion

We conclude, that our results do not suggest a risk of tissue damage due to increases in current density, when tsDCS is applied in the presence of a metallic spinal implant. Although we observed a current density increase, which resulted in a substantial difference in EF and CD amplitude in proximity to the implant, this did not lead to a hazardous increase in peak current density magnitude. Also, there is no indication that the presence of an implant may drastically alter the desired tsDCS stimulation effects, given that the average EF magnitude inside the spinal cord was little affected, compared to the no-implant scenario. Our results indicate the safety of tsDCS in combination with implanted spinal rods. Since quantitative generalization of our results is limited, further experimental evidence should be gathered to support the establishment of clear safety guidelines for spinal DC stimulation in the presence of metallic implants.

5.6 Acknowledgements

This research was supported by ZonMw (Grant Nr. 10-10400-98-008) as part of the NeuroControl - Assessment and Stimulation (NeurAS) consortium.

References

[1] Guleyupoglu B, Schestatsky P, Edwards D, Fregni F and Bikson M 2013 Classification of methods in transcranial Electrical Stimulation (tES) and evolving strategy from historical approaches to contemporary innovations *J. Neurosci. Methods* **219** 297–311

[2] Lamy J-C, Ho C, Badel A, Arrigo R T and Boakye M 2012 Modulation of soleus H reflex by spinal DC stimulation in humans. *J. Neurophysiol.* **108** 906–14

[3] Hubli M, Dietz V, Schrafl-Altermatt M and Bolliger M 2013 Modulation of spinal neuronal excitability by spinal direct currents and locomotion after spinal cord injury. *Clin. Neurophysiol.* **124** 1187–95

[4] Yamaguchi T, Fujimoto S, Otaka Y and Tanaka S 2013 Effects of transcutaneous spinal DC stimulation on plasticity of the spinal circuits and corticospinal tracts in humans *2013 6th Int. IEEE/EMBS Conf. Neural Eng.* 275–8

[5] Cogiamanian F, Vergari M, Pulecchi F, Marceglia S and Priori A 2008 Effect of spinal transcutaneous direct current stimulation on somatosensory evoked potentials in humans. *Clin. Neurophysiol.* **119** 2636–40

[6] Cogiamanian F, Ardolino G, Vergari M, Ferrucci R, Ciocca M, Scelzo E, Barbieri S and Priori A 2012 Transcutaneous Spinal Direct Current Stimulation *Front. Psychiatry* **3**

[7] Merrill D R, Bikson M and Jefferys J G R 2005 Electrical stimulation of excitable tissue: Design of efficacious and safe protocols *J. Neurosci. Methods* **141** 171–98

[8] Nitsche M A, Liebetanz D, Lang N, Antal A, Tergau F and Paulus W 2013 Safety criteria for transcranial direct current stimulation (tDCS) in humans. *Clin. Neurophysiol.* **133** 285

[9] Bikson M, Grossman P, Thomas C, Zannou A L, Jiang J, Adnan T, Mourdoukoutas A P, Kronberg G, Truong D, Boggio P, Brunoni A R, Charvet L, Fregni F, Fritsch B, Gillick B, Hamilton R H, Hampstead B M, Jankord R, Kirton A, Knotkova H, Liebetanz D, Liu A, Loo C, Nitsche M A, Reis J, Richardson J D, Rotenberg A, Turkeltaub P E and Woods A J 2016 Safety of Transcranial Direct Current Stimulation: Evidence Based Update 2016 *Brain Stimul.* **9** 641–61

[10] Datta A, Bikson M and Fregni F 2010 Transcranial direct current stimulation in patients with skull defects and skull plates: high-resolution computational FEM study of factors altering cortical current flow. *Neuroimage* **52** 1268–78

[11] Christ A, Kainz W, Hahn E G, Honegger K, Zefferer M, Neufeld E, Rascher W, Janka R, Bautz W, Chen J, Kiefer B, Schmitt P, Hollenbach H-P, Shen J, Oberle M, Szczerba D, Kam A, Guag J W and Kuster N 2010 The Virtual Family--development of surface-based anatomical models of two adults and two children for dosimetric simulations. *Phys. Med. Biol.* **55** N23–38

[12] SCI Institute 2015 SCIRun: A Scientific Computing Problem Solving Environment, Scientific Computing and Imaging Institute (SCI), Download from: http://www.scirun.org

[13] Parazzini M, Fiocchi S, Liorni I, Rossi E, Cogiamanian F, Vergari M, Priori A and Ravazzani P 2014 Modeling the current density generated by transcutaneous spinal direct current stimulation (tsDCS) *Clin. Neurophysiol.* **125** 2260–70

[14] Theeuwen M M H J, Gootzen T H J M and Stegeman D F 1993 Muscle electric activity I: A model study on the effect of needle electrodes on single fiber action potentials *Ann. Biomed. Eng.* **21** 377–89

[15] Haaker R G, Eickhoff U, Schopphoff E, Steffen R, Jergas M and Krämer J 1997 Verification of the position of pedicle screws in lumbar spinal fusion *Eur. Spine J.* **6** 125–8

[16] Puvanesarajah V 2014 Techniques and accuracy of thoracolumbar pedicle screw placement *World J. Orthop.* **5** 112

[17] Zheng X, Chaudhari R, Wu C, Mehbod A A and Transfeldt E E 2010 Subaxial cervical pedicle screw insertion with newly defined entry point and trajectory: Accuracy evaluation in cadavers *Eur. Spine J.* **19** 105–12

[18] Rampersad S M, Stegeman D F and Oostendorp T F 2013 Single-layer skull approximations perform well in transcranial direct current stimulation modeling. *IEEE Trans. Neural Syst. Rehabil. Eng.* **21** 346–53

[19] Wagner T, Fregni F, Fecteau S, Grodzinsky A, Zahn M and Pascual-Leone A 2007 Transcranial direct current stimulation: A computer-based human model study *Neuroimage* **35** 1113–24

[20] Bocci T, Marceglia S, Vergari M, Cognetto V, Cogiamanian F, Sartucci F and Priori A 2015 Transcutaneous Spinal Direct Current Stimulation (tsDCS) Modulates Human Corticospinal System Excitability *J. Neurophysiol.* jn.00490.2014

[21] Bikson M and Rahman A 2013 Origins of specificity during tDCS: anatomical, activity-selective, and input-bias mechanisms. *Front. Hum. Neurosci.* **7** 688

Chapter VI – Discussion

The goal of this dissertation was to add to the fundamental knowledge needed to use and evaluate tsDCS in modulating the lumbar spinal motor circuitry. The central question was, how tsDCS needs to be applied to induce meaningful neural changes in a well-controlled manner. An optimal scenario would allow for the selective up- or downregulation of neural pathways and circuitry, consistent across subjects.

To address these goals, it is meaningful to analyze the underlying chain of mechanisms and make inferences on feasibility, limits of application and correct utilization of tsDCS. TsDCS generates an electric field, which locally interacts with neural structures via membrane polarization, thought to be able to lead to long term changes in neural function. Functional change is thus dependent on membrane polarization, which is coupled to neural morphology and its alignment with the surrounding electric field vector. Therefore, the distribution, magnitude and direction of the generated electric field in the body needs to be understood first. Subsequently, the interaction with the targeted neural tissue must be determined, by considering neural- morphology and location. This was addressed in chapter 2, whereby the electric field, as well as its interaction with an alpha motoneuron and two incoming axons was simulated. This resulted in an improved understanding of how electric field direction and magnitude in the spinal cord can be controlled via different electrode configurations. Furthermore, it led to knowledge about how polarization of lumbar spinal motoneurons and axon terminals could be controlled by altering electric field magnitude and direction. Additional analyses focused on estimating the resulting acute, spinal network effects and discussing their correlation to long term changes observed in-vivo. In this respect, long-term refers to the neuroplastic changes within the neuron that can be observed in the order of several minutes to hours after application of the stimulation. This is opposed to acute effect, which refers to the neurocomputational changes observed as a direct consequence of the stimulus.

Having established an estimation of electric field direction and magnitude in the spinal cord, the question arose, whether it is possible to optimize the desired tsDCS modulatory response based on this knowledge. In this respect, it was useful to evaluate the network response after application of an electric field with different magnitudes and directions. This was addressed in chapter 3, whereby tsDCS was applied with two different electrode placements, of which one was tested in two polarities. The H-reflex response was used as the outcome measure of modulation. The results suggest a clear dependency on electric field magnitude and directionality of the modulatory effects after tsDCS. Additionally, the study in chapter 3 raised questions about the reliability of tsDCS effects across subjects, as it was not possible to replicate the results obtained by others.

For optimization of tsDCS outcome, an additional variable, which had been shown to influence the tsDCS neuromodulatory effect, is the ongoing neural activity during intervention. It was therefore hypothesized that higher ongoing neural activity during stimulation, may facilitate the modulation by tsDCS. This was investigated by a study described in chapter 4. The results confirm the initial hypothesis, showing a larger modulatory effect when tsDCS was applied during walking.

When tsDCS was applied during rest, no such effect was observed. However, the study also underlined the high complexity of tsDCS and the difficulty to control inter-subject variability. This applies mainly to response direction, referring to the fact that the H-reflex was either up- or downregulated without an apparent overall trend in modulation direction.

An important consideration regarding usability, is to take into account possible complications specific to the intervention group in combination with the desired intervention. Since the target group in the case of tsDCS are people with injuries of the spinal cord, a frequent complication is the presence of metallic spinal implants. The presence of metallic implants in the body is traditionally a major safety concern regarding electrotherapeutic interventions. It was therefore investigated, to which extent a metallic spinal implant in combination with tsDCS may lead to possible hazardous scenarios related to tissue damage. The results, which are discussed in chapter 5, show how the electric field is changed by the presence of a metallic spinal implant, which however does not lead to potentially hazardous scenarios.

The above notions will be discussed in more detail in the forthcoming paragraphs.

6.1 Selectivity of tsDCS

For application in the nervous system, an important factor is to which extend the intervention can be guided toward the modulation of specific functions, pathways or neural sub-populations.

As shown in chapter 2 and as expected, the electric field generated by tsDCS is widely distributed throughout the body, with little spatial selectivity [1–3]. Although the field distribution can be altered by utilizing different sizes, shapes and arrangements of electrodes [3,4], the spatial resolution of transcutaneous electrical stimulation is still several orders of magnitudes lower compared to invasive electrostimulation procedures. However, the question remains if tsDCS could still be used in a targeted manner, despite this reduced spatial precision of the applied electric field.

Recent research has shown that the outcome of neuromodulatory interventions such as DC stimulation, are highly dependent on factors such as the electrode configuration [5–7] (chapters 2&3), stimulation intensity [8,9], genetics [10–13], ongoing neural activation and brain state [14–17] (chapter 4), protocol timing known as homeostasis [18], as well as other protocol specific factors (for a thorough overview, see [14]). Although currently posing a challenge, in a future scenario this may also offer the possibility to achieve a highly specific modulatory response by precisely controlling the necessary intervention variables in a subject specific manner. A more selective control over the intervention outcome could be especially useful for the rehabilitation of spinal cord injury (SCI). These patients often suffer from deteriorated voluntary movement control and an increase in reflexive behavior, resulting in spasticity [19]. Being able to up- and downregulate voluntary and reflexive spinal pathways, respectively, could therefore have a substantial impact on the quality of life of those affected with SCI.

To improve our basic knowledge and provide clues on how to control intervention outcome, the tsDCS induced electric field and resulting membrane polarization for a set of motoneurons with different morphologies, as well as two ideal, typical incoming axons was calculated in chapter 2.

It was shown that axon terminal polarization was dominant over dendritic or somatic polarization. Assuming that the locally induced modulation effect increases with membrane polarization, it is expected that axon terminal polarization will contribute proportionally more to the overall modulation effect, compared to dendritic or somatic polarization. One can speculate that to achieve functional modulation of a single pathway from axon terminal polarization alone, a large portion of the axons that belong to the same functional subgroup need to be polarized simultaneously. The prerequisite is, that the corresponding axons need to be aligned in parallel to one another and the electric field. Two main intended targets of lumbar spinal neuromodulation are the afferent and efferent pathways, which are involved in postural feedback and voluntary activation respectively [20]. Prior to entering the lumbar spinal cord, afferent fibers are bundled in a nerve passing through the ventral root and efferent fibers descend through the corticospinal tract. Therefore, it can be assumed that the axons within both pathways are to a large degree directionally dependent. Given this reasoning, the implication is that, despite the initially low spatial selectivity of the generated electric field, pathway selectivity may be achieved via alignment of the electric field with the axon terminals of the targeted pathway.

To allow for further specificity, such as pathway up-or downregulation, as well as to improve intervention selectivity, modulation outcome could be influenced by controlling the neural activity on the corresponding pathway [14,15,21–23] (chapter 4), or neural polarization direction [7,14]. In conformity to what was shown in chapter 4, other studies have also suggested substantially different modulation effects, depending on the neural activation of the involved neural structures [15,23–26]. This is referred to as activity-selectivity, denoting the preferential modulation of a functional neural pathway that is already active during stimulation [14]. For instance, in rodents, pairing repetitive cortical-activation and lumbar-tsDCS led to a substantial increase in tsDCS modulation response on the corticospinal pathway [23]. In a similar example in humans, transcranial electrical stimulation was shown to preferentially modulate networks with heightened activity [16].

Given the appropriate neural activation, the modulation outcome could further be influenced via controlled de- or hyperpolarization of the targeted neural structures. For example, in a study by Rahman et al, the acute effect of axon terminal polarization on the extracellular postsynaptic potential was directionality dependent on the terminal polarization of the incoming axon [7]. For in vivo applications, axon terminal polarization may be controlled via electric field direction (chapter 2, and [7,27]) and alignment with the targeted pathway terminals.

Thus, although it is not clarified how these in-vitro findings will transfer to applications in vivo, these examples show that a tighter control on experimental factors could lead to better and more selective outcomes given an appropriately, well designed stimulation protocol.

6.2 Reliability and limits of application

Despite many developments in the field of electromodulation, the application of tsDCS as a clinical intervention is still challenging. This is owed to several factors that hamper the development of empirically individualized stimulation protocols in a resource efficient manner.

A first hurdle, is that DC stimulation protocols are applied at a low dose due to safety concerns. Therefore, the acute- as well as the after- effects in an individual subject after a single session are often too small to be distinguished from other, naturally occurring neural fluctuations. Since this makes it necessary to test the effects of direct current stimulation (DCS) in a placebo controlled trial with multiple subjects and across multiple sessions, optimization of stimulation protocols asks for tedious and long-lasting procedures. Given the high complexity of the underlying mechanisms of action, it is therefore difficult, time and resource intensive to perform a complete, empirical sensitivity analysis for transcutaneous DCS protocols.

In addition to that, DCS responses are often inconsistent across- and even within subjects [28–30], as well as difficult to replicate by others [31,32] (see also chapter 4). Although this does not imply that protocols that produce reliable results do not exist, it underlines the current inability to control the desired stimulation outcome sufficiently. Since repeatability is a prerequisite for the successful control and modeling of physical systems, this not only adds an additional factor of uncertainty, but also raises questions about the general feasibility and controllability of DC stimulation outcomes.

Potential sources of variability are 1) subject specificity in tsDCS modulatory response, and 2) inaccuracies in the utilized measurement methods.

With regards to subject specificity, anatomy, neuroanatomy, neural injury and genetic predisposition can potentially have a large impact on protocol outcome. Furthermore, research has shown that neuroplasticity seems to be influenced by a process referred to as homeostasis. This denotes the dependency of neuroplastic changes based on neural activation history [18]. As the history of neural activation prior to the experiment may not regularly be considered in DC stimulation research, this may add to the response variability observed in DCS experiments.

In addition, the utilized measurement methods may not be able to accurately detect the neural changes imposed by tsDCS alone, due to inherent noise sources like neural fluctuations. Resulting in an unfavorable signal- to- noise- ratio, the small changes induced by tsDCS may thereby be overshadowed by natural neural fluctuations. This could be the case for H-reflex and MEP measurements, which are susceptible to subtle environmental changes [33,34]. For example, research has shown that slight changes in body state, such as raising ones' arm, or eye closing can have a significant impact on the H-reflex recruitment curve [33].

A vital and necessary step towards the clinical application of DC stimulation protocols is therefore the improvement of overall intervention reliability [28–31,35]. This may be achieved via multidisciplinary methods comprising extensive experimental validation and computational modeling. Although resource intensive, groups working on invasive, pulsed- neurostimulation protocols have successfully demonstrated the added benefit of this polyangular approach [36–38], by leading to a meaningful protocol design based on qualitative theoretical models and hypotheses. Steps that can be beneficial for a similarly successful approach in non-invasive tsDCS could be: 1) the development of a multiscale model, predicting neural plasticity based on electric field distribution and neural activity; 2) empirical model validation and development, as well as 3) the improvement of measurement accuracy for the assessments of neural states in humans.

6.3 Safety

Besides functionality, an essential prerequisite for the clinical application of tsDCS is safety. Since tsDCS involves the electrical stimulation of tissue, stimulation protocols need to be designed with rigorous care and foresight. The resulting side effects of incorrectly applied or ill-designed DCS protocols may thereby lead to nerve damage, tissue damage or other unwanted complications. While tissue damage is a prevalent risk factor, the underlying mechanisms of tissue damage are poorly understood [39] . Still, it has been shown that the risk of tissue damage increases with current density magnitude and time of exposure. Since current density depends on subject anatomy, as well as biophysical tissue and material properties, verification is necessary about whether the utilized tsDCS protocol could possibly result in unsafe scenarios. This includes healthy individuals as well as people with a spinal cord injury, who often have metallic spinal implants that may lead to possible complications during stimulation.

Concerning the general safety of tsDCS, the results obtained here (chapter 5), are in line with those reported by others [40], who showed that the current densities induced by tsDCS are well below the determined thresholds for tissue damage [41]. This suggests that the occurrence of potentially hazardous current density levels is unlikely when adhering to the currently accepted safety recommendations [41–43].

Furthermore, these results indicate that the utilized stimulation current can in theory be increased above the currently used value of 2.5 mA without the risk of neural tissue damage. This may be beneficial for the development and empirical sensitivity analysis of tsDCS, whereby an increase in stimulation amplitude may potentially lead to an increase in tsDCS modulatory effects. According to recent estimates, current density thresholds for neural tissue damage are in the range of 6.3 A/m^2 to 17 A/m^2 [41]. In comparison to that, the calculated maximum current density in the spinal cord was, with 0.4 A/m^2, at least one order of magnitude lower. Theoretically, the stimulation amplitude could therefore be increased, while still retaining a safety margin of multiple factors. For example, doubling tsDCS amplitude to 5 mA would lead to a maximum current density of 0.8 A/m^2 in the spinal cord and still a resulting safety factor of over 6.

Most importantly, it was shown that tsDCS can potentially be safely applied in scenarios in which a metallic spinal implant is present in the body (chapter 5). Similar to what was shown previously for metallic skull plates during tDCS [44], the presence of a metallic spinal rod during tsDCS did not lead to hazardous current density levels within the tissue surrounding the implant. Therefore, although general hypotheses dictate otherwise, safety concerns connected to the presence of metallic implants cannot be confirmed by the presented evidence. This implies, that carriers of a metallic implant may potentially be able to benefit from receiving tsDCS or other electrotherapeutic interventions in the future. This is related to the fact that a high impedance double layer builds up between the tissue and the metal, making the latter an effective isolator instead of a low impedance short-cut, as often is expected [45].

Although the above predicts that tsDCS can in theory be considered as safe, it must be emphasized that these theoretical assumptions are based on partly idealized computational models, which do not allow the generalization across all possible stimulation scenarios and subjects.

Therefore, further empirical research is needed to determine the safety of both, higher stimulation amplitudes as well as the stimulation in the presence of metallic implants.

6.4 Comparison with other spinal stimulation protocols

The focus of this dissertation was to investigate tsDCS as a possible intervention option for spinal cord injury or other spinal cord dysfunctions. However, tsDCS is only one of the currently investigated techniques under development for the rehabilitation of SCI. To discuss its applicability to spinal neuromodulation, in terms of reliability, selectivity and safety, it is therefore appropriate to compare tsDCS to other possible intervention options.

Besides tsDCS, other forms of stimulation protocols for SCI rehabilitation mainly consist of applying pulsed spinal electrical stimulation via epidural, intra-spinal or transcutaneous electrodes. Pulsed stimulation protocols predominantly utilize bipolar waveforms, which consist of a positive-, followed by a negative, rectangular waveform. A consequence of using biphasic-pulsed- compared to DC stimuli, is the possibility to safely employ larger stimulation amplitudes, with studies having employed pulses of up to 200mA (in relation to the 1mA to 4mA generally used in DCS [41]) [38,39]. Thus, whereas tsDCS generate small sub-threshold membrane potential changes in the order of a few millivolts [3] (see chapter 2), pulsed protocol types are able to induce much larger membrane potential changes, up to directly evoking neural activation. The main advantage of pulsed-, compared to constant waveforms, is therefore a larger operating range with which neural activity can be modulated safely.

In recent years, several groups utilizing spinal stimulation with pulsed waveforms have been able to make substantial advances in the rehabilitation of SCI. Using both invasive [36,37,46,47] and noninvasive [38,48] approaches, as well as either sub- [38,46,48] and supra-threshold [38,47] pulsed stimulation, a variety of studies have reported significant long or short-term improvements on voluntary motor control, weight bearing or other clinical outcome parameters [36–38,46–49]. For instance, in a study by Gerasimenko and colleagues, several subjects diagnosed with motor complete paralysis were able to partly regain voluntary movement control after an 18-week training program, including weekly transcutaneous pulsed, supra-threshold spinal stimulation in combination with pharmaceutical intervention. Thus, while the more substantial improvements in voluntary control have only been achieved after long periods of combined manual training and electrical stimulation [36–38,46–49], immediate acute effects can already be observed during the first application [47,50].

In contrast to that, less effort has been invested into the development of tsDCS. While previous research has confirmed the neuromodulatory effect of DCS protocols on the spinal pathways and clinical tsDCS devices have become available, no long-term training studies on SCI subjects have been performed so far. Nonetheless, based on the advances reported here and those published by others, it seems that tsDCS can indeed lead to modulatory responses in a polarity dependent and direction specific manner [3,5,6,51]. However, whereas consistent in some studies, post-tsDCS responses in other studies showed high directional intersubject variability (chapter 4) and poor replicability (chapter 3). The variability across subjects can therefore not accurately be controlled. Since DCS is usually applied at lower electric field amplitudes, the resulting post

stimulation effect is subtle, and a study including multiple subjects is necessary to empirically optimize DC stimulation interventions. Whereas this is similar for the post stimulation effects of pulsed waveform protocols, due to the higher amplitude waveform an acute stimulation effect is visible [47,50]. This offers immediate neurophysiological feedback, which may readily be used for protocol optimization within a single experiment. Therefore, although DC stimulation may be applicable for the use in SCI rehabilitation, pulsed waveform protocols are currently more widely used, perhaps due to their immediately visible acute stimulation effects.

6.5 Contribution and implications

While focusing on the optimization of tsDCS for the modulation of the lumbar spinal circuitry, a central aim was to add to the fundamental understanding and methodology that could be used as a basis for further investigation of tsDCS and also other forms of electrotherapeutic interventions.

Most prior work on spinal DC stimulation did not focus on intervention development based on a mechanistic understanding, serving primarily as initial empirical exploratory studies. Referring to a more explanatory method, a modeling approach was chosen to serve as a theoretical framework (chapter 2), able to be extended by others in the future and with a possible application to not only tsDCS, but to most other electrostimulation procedures. Within this framework, the electric field generated in the body and spinal cord, as well as its impact on the membrane potential of spinal neural structures was computed. This established a direct link between the macroscopic level, visible to the experimenter (such as the electrical stimulator and transcutaneous electrodes), and the microscopic level in form of the targeted neuron. Since the target of non-invasive electrical stimulation is the modulation of neural networks in the body, the understanding of this macro-micro relationship is important for a hypothesis driven experimental design. The gathered knowledge can subsequently be used as a starting point for further hypothesis driven investigation on the working mechanisms of electrotherapeutic protocols, with tsDCS as an important example. The only limitation to qualitative generalization of stimulation waveforms is formed by the use of high(er) frequencies due to the frequency dependency of tissue impedance [52].

A central question addressed in chapter 2, is the relationship between stimulation acute- and after effect. Whereby acute, refers to the neural effects that result immediately due to the induced stimulus, after effects can be detected long after stimulation offset and are a result of anatomical changes in the neuron, known as neuroplasticity. While the presented work did not model the transition between acute and long term after effects directly, it was possible to establish a comparative relationship between the simulated acute-, and the long-term effects observed experimentally in humans. Although this relationship was consistently in opposite direction as initially expected, it can nonetheless be used as an initial working hypothesis for future tsDCS or other neuromodulation experiments. It can subsequently serve as a basis for establishing a working model for the effects of electrical stimulation on neuroplasticity by utilizing data obtained from human experiments.

In the chapters 3&4, the effect of different stimulation protocol variations on the lumbar spinal circuitry is assessed. The resulting findings may therefore help with the further development of electrotherapeutic protocols. In chapter 3, only one in three tested electrode configuration

variations was able to induce a significant modulation effect across subjects, 30 minutes after tsDCS. While the specific depression of the H-Reflex response had not been shown before, more importantly, this implies a high response-dependency on electric field direction. Based on this dependency, it is evident that besides the traditional electrode placements (active electrode over target region, passive electrode further away), a number of other electrode configurations can be thought of that differ significantly in the produced modulation response. With one of the tested electrode configurations, the study furthermore attempted to replicate the results obtained by Lamy et al. [5], who showed a significant left shift of the H-reflex recruitment curve. Since the results were not replicated, this supports the argument, that tsDCS alone may not be effective in a straight manner. Other protocol parameters, such as the suggested neural activity during stimulation, should be controlled in addition to that.

In chapter 4, the effect of cathodal-tsDCS during either walking or rest was evaluated. The two application conditions correspond to increased neural activity for walking, in comparison to background level neural activity at rest. In line with what is known from previous research [14], the result of this study suggests that to heighten the chance of inducing a larger post-stimulation effect, tsDCS may need to be applied with increased neural activity in the pathway of interest. Nonetheless, due to the directional-variability across subjects, the stimulation protocol has to be improved further to allow generalized, directional control over the induced modulatory effects.

Finally, since tsDCS is being developed for the rehabilitation of spinal cord disorders or injuries, intervention safety with a special focus on the intended target group needs to be verified. This especially relates to the presence of metallic spinal implants, as often the case in people with a spinal cord injury, in combination with tsDCS. The simulations outlined in chapter 5 were thereby able to show, that the presence of a metallic spinal implant during tsDCS will not result in potentially harmful scenarios. This was the case even for implant locations directly adjacent to the transcutaneous electrode. This result implies that patients with a metallic implant may not be restricted from receiving electrotherapeutic spinal stimulation in the future.

6.6 Recommendations for future research and development

The final goal of electrotherapeutic interventions, such as tsDCS, is a controlled change in neural behavior. To achieve this, future research should focus on a target oriented intervention development, based on viable models or theories of the underlying chain of action.

Specific questions that need to be targeted are the subject specific variability in intervention response, as well as the relationship between acute and long-term neural effects. Especially for the latter, not much research exists and should be investigated thoroughly for better intervention outcome control.

To handle the high complexity of the underlying mechanisms, future research should focus on improving the existing modeling frameworks to predict electrotherapeutic outcomes in a subject specific manner. Possibly including multiple factors such as subject specific anatomy, genetics or other necessary variables, these models should predict long term plasticity changes based on the generated electric field, the polarization effects on the targeted neural structures as well as the ongoing neural activity during stimulation. Generally, model development should be conducted

in parallel to rigorous experimental validation to develop a reliable and generalizable predictor of electrotherapeutic neuromodulation outcomes.

Since this approach can be resource and time intensive, intensifying the coordination across research groups may be useful to increase the common scientific benefit. This could be achieved via the exchange of hypotheses and modeling techniques, their implementation in easy to handle modelling pipelines and the coordination of mutually beneficial research plans. Studies could be designed with a clear theoretical component based on state of the art modeling results, while reporting initial hypotheses about the possible mechanism of action. For example, when designing a neurostimulation procedure for the modulation of the descending corticospinal motor pathways, the stimulation protocol should be based on an initial model that contains the expected neural signal flow in the CNS, as well as an approximation of the targeted neural morphologies (e.g. neuron locations, fiber orientations) and generated electric field in the CNS. Too much of the current research in electrotherapy design is conducted in an empirical, trial-and-error fashion. Hypothesis-driven, model-based research is necessary to improve intervention control and knowledge transfer.

6.7 Conclusion

The final goal of this dissertation, was the investigation of tsDCS to be employed for the use of spinal cord injury rehabilitation. This mainly included the necessary knowledge for a target oriented intervention design, while aiming to induce lasting functional modulation tin the lumbar- and cortico-spinal motor circuitry. This was investigated with a combination of experimental as well as computational methods.

An initial, computational study supplied necessary knowledge about electric field distribution in the spinal cord for different electrode configurations as well as the induced polarization on the targeted motoneurons and axon terminals in the lumbar spinal cord. Furthermore, a comparative connection between the simulated acute-, and experimentally observed long term effects was established. This can be regarded as a first prediction model for the effects of tsDCS, based on the axon terminal polarization for the two main, voluntary and reflexive incoming pathways. It can subsequently act as an initial basis for a more thorough analysis and understanding of the relationship between tsDCS acute and long-term effects.

The experimental studies that followed, were subsequently able to shed light on protocol specific variables and their effect on the intervention outcome. This included the effect of different electric field directions, as well as paired neural activity on tsDCS modulatory effects. However, these studies also raised major questions about repeatability and inter-subject variability, which are both important topics to be dealt with in future.

In a final computational study, the safety of tsDCS in combination with the presence of metallic spinal implants was investigated. This is relevant since 1) metallic spinal implants are prevalent in people with a spinal cord injury, and 2) the presence of metallic objects is still considered a safety hazard in combination with electrical stimulation interventions. Nonetheless, these widespread concerns could not be enforced by the work presented here, which implies that people with a metallic spinal implant may be able to benefit from possible electrotherapeutic rehabilitation

regimes in the future. The work presented here, therefore represents a meaningful contribution for the understanding and further development of tsDCS, while also extending to the application to other electrotherapeutic protocol variations.

References

[1] Rampersad S M, Janssen A M, Lucka F, Aydin Ü, Lanfer B, Lew S, Wolters C H, Stegeman D F and Oostendorp T F 2014 Simulating transcranial direct current stimulation with a detailed anisotropic human head model. *IEEE Trans. Neural Syst. Rehabil. Eng.* **22** 441–52

[2] Wagner S, Rampersad S M, Aydin Ü, Vorwerk J, Oostendorp T F, Neuling T, Herrmann C S, Stegeman D F and Wolters C H 2014 Investigation of tDCS volume conduction effects in a highly realistic head model. *J. Neural Eng.* **11** 16002

[3] Kuck A, Stegeman D and van Asseldonk E 2017 Modeling trans-spinal direct current stimulation for the modulation of the lumbar spinal motor pathways *J. Neural Eng.* **14** 56014

[4] Dmochowski J P, Datta A, Bikson M, Su Y and Parra L C 2011 Optimized multi-electrode stimulation increases focality and intensity at target. *J. Neural Eng.* **8** 46011

[5] Lamy J-C, Ho C, Badel A, Arrigo R T and Boakye M 2012 Modulation of soleus H reflex by spinal DC stimulation in humans. *J. Neurophysiol.* **108** 906–14

[6] Cogiamanian F, Ardolino G, Vergari M, Ferrucci R, Ciocca M, Scelzo E, Barbieri S and Priori A 2012 Transcutaneous Spinal Direct Current Stimulation *Front. Psychiatry* **3**

[7] Rahman A, Reato D, Arlotti M, Gasca F, Datta A, Parra L C and Bikson M 2013 Cellular effects of acute direct current stimulation: somatic and synaptic terminal effects. *J. Physiol.* **591** 2563–78

[8] Matsunaga K, Nitsche M A, Tsuji S and Rothwell J C 2004 Effect of transcranial DC sensorimotor cortex stimulation on somatosensory evoked potentials in humans *Clin. Neurophysiol.* **115** 456–60

[9] Dieckhöfer A, Waberski T D, Nitsche M, Paulus W, Buchner H and Gobbelé R 2006 Transcranial direct current stimulation applied over the somatosensory cortex - differential effect on low and high frequency SEPs. *Clin. Neurophysiol.* **117** 2221–7

[10] Lamy J-C and Boakye M 2013 BDNF Val66Met polymorphism alters spinal DC stimulation-induced plasticity in humans. *J. Neurophysiol.* **110** 109–16

[11] Fritsch B, Reis J, Martinowich K, Schambra H M, Ji Y, Cohen L G and Lu B 2010 Direct current stimulation promotes BDNF-dependent synaptic plasticity: Potential implications for motor learning *Neuron* **66** 198–204

[12] Chhabra H, Shivakumar V, Agarwal S M, Bose A, Venugopal D, Rajasekaran A, Subbanna M, Kalmady S V, Narayanaswamy J C, Debnath M and Venkatasubramanian G 2015 Transcranial direct current stimulation and neuroplasticity genes: implications for psychiatric disorders *Acta Neuropsychiatr* 1–10

[13] Wiegand A, Nieratschker V and Plewnia C 2016 Genetic Modulation of Transcranial Direct Current Stimulation Effects on Cognition *Front. Hum. Neurosci.* **10**

[14] Bikson M and Rahman A 2013 Origins of specificity during tDCS: anatomical, activity-selective, and input-bias mechanisms. *Front. Hum. Neurosci.* **7** 688

[15] Kronberg G, Bridi M, Abel T, Bikson M and Parra L C 2016 Direct Current Stimulation Modulates LTP and LTD: Activity Dependence and Dendritic Effects *Brain Stimul.* **10** 51–8

[16] Reato D, Rahman A, Bikson M and Parra L C 2010 Low-Intensity Electrical Stimulation Affects Network Dynamics by Modulating Population Rate and Spike Timing *J. Neurosci.* **30** 15067–79

[17] Fröhlich F and McCormick D A 2010 Endogenous electric fields may guide neocortical network activity *Neuron* **67** 129–43

[18] Fricke K, Seeber A A, Thirugnanasambandam N, Paulus W, Nitsche M A and Rothwell J C 2011 Time course of the induction of homeostatic plasticity generated by repeated transcranial direct current stimulation of the human motor cortex *J. Neurophysiol.* **105** 1141–9

[19] Sköld C, Levi R and Seiger Å 1999 Spasticity after traumatic spinal cord injury: Nature, severity, and location *Arch. Phys. Med. Rehabil.* **80** 1548–57

[20] Pierrot-Deseilligny E and Burke D 2012 The Circuitry of the Human Spinal Cord of Movement: Spinal and Corticospinal Mechanisms of Movement - Back Matter *The Circuitry of the Human Spinal Cord of Movement: Spinal and Corticospinal Mechanisms of Movement* pp 33–5

[21] Gill J, Shah-Basak P P and Hamilton R 2015 It's the thought that counts: Examining the task-dependent effects of transcranial direct current stimulation on executive function *Brain Stimul.* **8** 253–9

[22] Ahmed Z 2013 Electrophysiological characterization of spino-sciatic and cortico-sciatic associative plasticity: modulation by trans-spinal direct current and effects on recovery after spinal cord injury in mice. *J. Neurosci.* **33** 4935–46

[23] Ahmed Z 2011 Trans-spinal direct current stimulation modulates motor cortex-induced muscle contraction in mice. *J. Appl. Physiol.* **110** 1414–24

[24] Lapenta O M, Minati L, Fregni F and Boggio P S 2013 Je pense donc je fais: transcranial direct current stimulation modulates brain oscillations associated with motor imagery and movement observation. *Front. Hum. Neurosci.* **7** 256

[25] Radman T, Su Y, An J H, Parra L C and Bikson M 2007 Spike Timing Amplifies the Effect of Electric Fields on Neurons: Implications for Endogenous Field Effects *J. Neurosci.* **27** 3030–6

[26] Kim G W and Ko M H 2013 Facilitation of corticospinal tract excitability by transcranial direct current stimulation combined with voluntary grip exercise *Neurosci. Lett.* **548** 181–4

[27] Arlotti M, Rahman A, Minhas P and Bikson M 2012 Axon terminal polarization induced by weak uniform DC electric fields: a modeling study. *Conf. Proc. IEEE Eng. Med. Biol. Soc.* **2012** 4575–8

[28] Horvath J C, Vogrin S J, Carter O, Cook M J and Forte J D 2016 Effects of a common transcranial direct current stimulation (tDCS) protocol on motor evoked potentials found to be highly variable within individuals over 9 testing sessions *Exp. Brain Res.* **234** 2629–42

[29] Chew T, Ho K-A and Loo C K 2015 Inter- and Intra-individual Variability in Response to Transcranial Direct Current Stimulation (tDCS) at Varying Current Intensities *Brain Stimul.* **8** 1130–7

[30] López-Alonso V, Fernández-del-Olmo M, Costantini A, Gonzalez-Henriquez J J and Cheeran B 2015 Intra-individual variability in the response to anodal transcranial direct current stimulation *Clin. Neurophysiol.* **126** 2342–7

[31] Horvath J C, Forte J D and Carter O 2015 Evidence that transcranial direct current stimulation (tDCS) generates little-to-no reliable neurophysiologic effect beyond MEP amplitude modulation in healthy human subjects: A systematic review *Neuropsychologia* **66** 213–36

[32] Vannorsdall T D, van Steenburgh J J, Schretlen D J, Jayatillake R, Skolasky R L and Gordon B 2016 Reproducibility of tDCS Results in a Randomized Trial *Cogn. Behav. Neurol.* **29** 11–7

[33] Kameyama O, Hayes K C and Wolfe D 1989 Methodological considerations contributing to the variability of the quadriceps H-reflex *Am. J. Phys. Med. Rehabil.* **68** 277–82

[34] Kiers L, Cros D, Chiappa K H and Fang J 1993 Variability of motor potentials evoked by transcranial magnetic stimulation *Electroencephalogr. Clin. Neurophysiol. Evoked Potentials* **89** 415–23

[35] Wiethoff S, Hamada M and Rothwell J C 2014 Variability in response to transcranial direct current stimulation of the motor cortex *Brain Stimul.* **7** 468–75

[36] Wenger N, Moraud E M, Gandar J, Musienko P, Capogrosso M, Baud L, Le Goff C G, Barraud Q, Pavlova N, Dominici N, Minev I R, Asboth L, Hirsch A, Duis S, Kreider J, Mortera A, Haverbeck O, Kraus S, Schmitz F, DiGiovanna J, van den Brand R, Bloch J, Detemple P, Lacour S P, Bézard E, Micera S and Courtine G 2016 Spatiotemporal neuromodulation therapies engaging muscle synergies improve motor control after spinal cord injury *Nat. Med.* **22** 138–45

[37] van den Brand R, Heutschi J, Barraud Q, DiGiovanna J, Bartholdi K, Huerlimann M, Friedli L, Vollenweider I, Moraud E M, Duis S, Dominici N, Micera S, Musienko P and Courtine G 2012 Restoring voluntary control of locomotion after paralyzing spinal cord injury. *Science* **336** 1182–5

[38] Gerasimenko Y, Gorodnichev R, Moshonkina T, Sayenko D, Gad P and Reggie Edgerton V 2015 Transcutaneous electrical spinal-cord stimulation in humans *Ann. Phys. Rehabil. Med.* **58** 225–31

[39] Merrill D R, Bikson M and Jefferys J G R 2005 Electrical stimulation of excitable tissue: Design of efficacious and safe protocols *J. Neurosci. Methods* **141** 171–98

[40] Parazzini M, Fiocchi S, Liorni I, Rossi E, Cogiamanian F, Vergari M, Priori A and Ravazzani P 2014 Modeling the current density generated by transcutaneous spinal direct current stimulation (tsDCS) *Clin. Neurophysiol.* **125** 2260–70

[41] Bikson M, Grossman P, Thomas C, Zannou A L, Jiang J, Adnan T, Mourdoukoutas A P, Kronberg G, Truong D, Boggio P, Brunoni A R, Charvet L, Fregni F, Fritsch B, Gillick B, Hamilton R H, Hampstead B M, Jankord R, Kirton A, Knotkova H, Liebetanz D, Liu A, Loo C, Nitsche M A, Reis J, Richardson J D, Rotenberg A, Turkeltaub P E and Woods A J 2016 Safety of Transcranial Direct Current Stimulation: Evidence Based Update 2016 *Brain Stimul.* **9** 641–61

[42] Liebetanz D, Koch R, Mayenfels S, König F, Paulus W and Nitsche M A 2009 Safety limits of cathodal transcranial direct current stimulation in rats *Clin. Neurophysiol.* **120** 1161–7

[43] Nitsche M A, Liebetanz D, Lang N, Antal A, Tergau F and Paulus W 2013 Safety criteria for transcranial direct current stimulation (tDCS) in humans. *Clin. Neurophysiol.* **133** 285

[44] Datta A, Bikson M and Fregni F 2010 Transcranial direct current stimulation in patients with skull defects and skull plates: high-resolution computational FEM study of factors altering cortical current flow. *Neuroimage* **52** 1268–78

[45] Theeuwen M M H J, Gootzen T H J M and Stegeman D F 1993 Muscle electric activity I: A model study on the effect of needle electrodes on single fiber action potentials *Ann. Biomed. Eng.* **21** 377–89

[46] Gad P, Choe J, Shah P, Garcia-Alias G, Rath M, Gerasimenko Y, Zhong H, Roy R R and Edgerton V 2013 Sub-threshold spinal cord stimulation facilitates spontaneous motor activity in spinal rats *J. Neuroeng. Rehabil.* **10** 108

[47] Harkema S, Gerasimenko Y, Hodes J, Burdick J, Angeli C, Chen Y, Ferreira C, Willhite A, Rejc E, Grossman R G and Edgerton V R 2011 Effect of epidural stimulation of the lumbosacral spinal cord on voluntary movement, standing, and assisted stepping after motor complete paraplegia: a case study. *Lancet* **377** 1938–47

[48] Gerasimenko Y, Lu D, Modaber M, Zdunowski S, Gad P, Sayenko D, Morikawa E, Haakana P, Ferguson A R, Roy R R and Edgerton V R 2015 Noninvasive Reactivation of Motor Descending Control after Paralysis. *J. Neurotrauma* **13** 1–13

[49] Lu D C, Edgerton V R, Modaber M, AuYong N, Morikawa E, Zdunowski S, Sarino M E, Sarrafzadeh M, Nuwer M R, Roy R R and Gerasimenko Y 2016 Engaging Cervical Spinal Cord Networks to Reenable Volitional Control of Hand Function in Tetraplegic Patients *Neurorehabil. Neural Repair* **30** 951–62

[50] Ievins A and Moritz C T 2017 Therapeutic Stimulation for Restoration of Function After Spinal Cord Injury *Physiology* **32** 391–8

[51] Bocci T, Marceglia S, Vergari M, Cognetto V, Cogiamanian F, Sartucci F and Priori A 2015 Transcutaneous Spinal Direct Current Stimulation (tsDCS) Modulates Human Corticospinal System Excitability *J. Neurophysiol.* jn.00490.2014

[52] Gabriel C 1996 Compilation of the Dielectric Properties of Body Tissues at RF and Microwave Frequencies. *Environ. Heal.* **Report No.** 21

Acknowledgements

Firstly, I would like to express my deepest gratitude to my advisors and promotors: Dr. Edwin van Asseldonk, Prof. Dick Stegeman and Prof. Herman van der Kooij. I was blessed to have had the opportunity to be taught, advised, corrected, encouraged and inspired by you. Thank you for believing in me, giving me the personal and academic freedom to develop my own ideas as well as offering your guidance and encouragement when things seemed to be too fierce and challenging.

In addition to that, I would like to thank Prof. Peter Veltink and Dr. Jan Buitenweg for their additional guidance on my academic quest at the University of Twente, which lasted over 6 years. Your doors were always open to me and the advice and insights you offered were truly valuable and influential. Also, I want to thank my former advisor and colleague Dr. Ard Westerveld, with whom I had the pleasure to start my journey at the University of Twente as a Bachelor and Master student. Thank you for your trust, guidance, the countless lab hours we spent together and your friendship.

Furthermore, I want to thank Simone Fricke and Magali Hanot, whom I had the pleasure to work with as a daily supervisor during their respective master projects. Thank you for your hard and excellent work as well as your dedication. I was lucky to have been able to work with you.

I also want to mention all of our collaborators at the Roessingh Rehabilitation Center and Roessingh Research and Development. Our project was experimentally complex and organizationally challenging. I therefore want to thank you for all your efforts, scientific input and the great collaboration, all of which were essential for this work as well as the overall project.

Importantly, I want to send a big thank you to my paranymphs and friends, Arvid Keemink and Jan de Jong, whose personal and professional input was vital during the course of my PhD and in the completion of this thesis. Thank you guys for everything!

To all my friends and colleagues at the Lab, the University and the surrounding outskirts (the Netherlands and the rest of the World): Thank you for a truly amazing time, for your friendship and sharing your wisdom, over long hours in the lab, local pubs, house parties and Italian restaurants. While, at this point in time, I am especially known for moving to far and remote places, I hope our paths will cross again on a personal and/or professional level.

Naturally, I would not be here today without the support of my parents, my sister and the rest of my family. Thank you for raising me, allowing me to be as ambitious as I wanted, fostering my curiosity and supporting me, no matter where the wind would carry me.

Last, but most importantly, my deepest thanks and appreciation goes to my wife Dounia. Your unwavering love, selfless and limitless support have undoubtedly been the foundation upon which this work and our life has been able to flourish. Thank you for keeping me sane and being there during the good times and the bad times. This PhD is for both of us. I love you.

Biography

Alexander Kuck was born on the 23rd of December 1985 in Kircheim unter Teck, Germany. He started his professional education by pursuing a Bachelor's degree in Biomedical Engineering at the Hochschule Ulm, Ulm, Germany, after which he obtained a corresponding Master's degree at the University of Twente, Enschede, NL. During this time, he was also able to work and study at the Miller Laboratory of Limb Motor Control, Northwestern University, Chicago, USA as well as at the Courtine -Lab, EPFL, Lausanne, CH.

In 2013 he started his PhD, under the supervision of Dr. Edwin H.F. van Asseldonk, Prof. dr. ir. Herman van der Kooij and Prof. dr. ir. Dick F. Stegeman.

His main professional interests are focusing on neurotechnology and neurorehabilitation of the central nervous system as well as central motor control.

Dissemination

Scan or click for full Scopus search

Scopus author ID: 55516769400